



**Mauritius Research and Innovation Council**  
INNOVATION FOR TECHNOLOGY

**TOWARDS LOW COST NOWCASTING  
OF FLASH FLOODS IN MAURITIUS:  
ASSESSING THE EFFECTIVENESS OF  
A COMBINED APPROACH INVOLVIING  
WIRELESS SENSOR NETWORK AND  
MACHINE LEARNING**

**Final Report**

*December 2019*

**Mauritius Research and Innovation Council**

*Address:*  
Level 6, Ebene Heights  
34, Cybercity  
Ebene

Telephone: (230) 465 1235  
Fax: (230) 465 1239  
E-mail: [contact@mrhc.mu](mailto:contact@mrhc.mu)  
Website: [www.mrhc.mu](http://www.mrhc.mu)

**This report is based on work supported by the Mauritius Research and Innovation Council under award number MRC/RUN-1708. Any opinions, findings, recommendations and conclusions expressed herein are the author's and do not necessarily reflect those of the Council.**



# TOWARDS LOW COST NOWCASTING OF FLASH FLOODS IN MAURITIUS:

*Assessing the Effectiveness of a Combined Approach Involving  
Wireless Sensor Network and Machine Learning*

## **Report**

Date: December 2019

A Research Report By:

1. **Dr. Geerish Suddul (Principal Investigator)**  
*University of Technology, Mauritius*
2. **Dr. Girish Bekaroo (Co-Investigator)**  
*Middlesex University Mauritius*
3. **Dr. Kumar Dookhitram (Co-Investigator)**  
*University of Technology, Mauritius*
4. **Mr. Nikhilesh Shankhur (Research Assistant)**  
*University of Technology, Mauritius*

## Executive Summary

Flash floods are rapidly occurring events usually associated with very intense rainfall. Their fast manifestation considerably restricts the possibilities for the issuing of warnings. They are considered as one of the most hazardous natural events, which are frequently responsible for the loss of lives and severe damage to infrastructure and the environment. During recent years, Mauritius has witnessed different occurrences of flash flood. The two most significant episodes happened in March 2008 and 2013, causing a total of 15 reported death cases, over 300 vehicle damages and more than 2000 requests for assistance received by the Fire Services. As is the case worldwide, with climate change, this natural phenomenon has the tendency of increasing in frequency as well as magnitude. Furthermore, with increased urbanisation, more areas are prone to flooding. In an attempt to cope with flash floods, there is the need for a nowcasting system.

This study aims at assessing the effectiveness of a low-cost prototype to nowcast flash floods in the Mauritian context. A system based on simulation, using Wireless Sensor Network and modern Machine Learning techniques has been designed and implemented for the prediction of flash floods. The Wireless Sensor Network component reads and collects different features from river flow and rainfall monitoring. It has been tested through simulation and is estimated to have a relatively low unit cost. The Machine Learning component of the system is based on a deep learning approach with the implementation of the Recurrent Neural Network (RNN), and has been trained and tested using simulated datasets. The efficiency of the model has been further optimised with the application of Genetic Algorithm, and experiments demonstrate a relatively low error in predictions. The results achieved in this study cannot be generalized for the Mauritian context at large, but serve as an approach for the development of an automated flash flood nowcasting system based on rainfall and water flow monitoring in rivers/canals.

## Acknowledgements

We wish to express our appreciation to the Mauritius Research Council for the financial assistance provided. The successful completion of the research project would not have been possible without the support of University of Technology, Mauritius (UTM), and that of the Middlesex University (Mauritius Branch Campus).

Our Research Assistant, Mr. Nikhilesh Shankhur has contributed towards the realization of this project in every step, and we are grateful for his dedication and commitment.

Finally, a special note of appreciation for the Mauritius Meteorological Services and the Water Resources Unit for all the information provided.

## Table of Contents

Executive Summary.....	i
Acknowledgements.....	ii
Chapter 1 – Introduction .....	1
1.1 Background of Study .....	1
1.2 Problem Statement.....	1
1.3 Aim and Objectives of Project.....	2
Chapter 2 - Flash Floods and Associated Impacts.....	3
2.1 The Growing Climate Change Concerns for Mauritius.....	3
2.2 Flash Floods and Associated Negative impacts .....	4
2.2.1 26th March 2008.....	4
2.2.2 30th March 2013.....	4
2.2.3 Torrential Rainfall & Cyclone Berguita.....	6
2.3 Reducing the Impacts of Flash Flood .....	7
2.3.1 Flash Flood Forecasting in Northern Austria.....	7
2.3.2 Flash Flood Forecasting in Australia.....	7
2.3.3 The European Flood/Flash Flood Forecasting System (EFFS) .....	8
2.4 Critical Analysis .....	9
Chapter 3 - ICT Driven Flash Flood Nowcasting.....	10
3.1 Technology Driven Flash Flood Nowcasting .....	10
3.2 WSN & Machine Learning Based Flash Flood Prediction.....	11
3.2.1 Combining wireless sensor networks and machine learning for flash flood nowcasting... 11	
3.2.2 Model-based monitoring for early warning flood detection .....	11
3.2.3 Merging multiple precipitation sources for flash flood .....	12
3.2.4 Watershed rainfall forecasting using neuro-fuzzy networks with the assimilation of multi-sensor information.....	12
3.2.5 Artificial Neural Network based algorithms in forecasting flood .....	13
3.2.6 Forecasting Rainfall based on Computational Intelligent Techniques.....	14
3.2.7 Flash floods forecasting without rainfall forecasts by recurrent neural networks. Case study on the Mialet basin (Southern France) .....	15
3.2.8 Flash flood forecasting using Support Vector Regression: An event clustering based approach 16	

3.2.9	Wireless Smart Sensor Networks for Real-Time Warning System of Flash Floods and Torrents in KSA.....	17
3.3	Comparative Analysis of Different Techniques.....	18
3.4	Chapter Summary .....	21
Chapter 4	– A Review of Environmental Parameters for Flash Flood Nowcasting.....	23
4.1	Variables Behind Flash Flood Nowcasting .....	23
4.2	Parameters involved in Flash Flood Forecasting/Nowcasting .....	26
4.3	Measuring the Flash Flood Nowcasting Parameters .....	27
4.4	Parameters Specific to Mauritius.....	28
4.5	Comparative Analysis of Neural Network based Machine Learning Techniques .....	30
4.5.1	Introduction .....	30
4.5.2	Experiments .....	31
4.5.3	Experimental Setup.....	32
4.5.4	Data Preparation.....	33
4.5.5	Experiment 1 – Regression.....	33
4.5.6	Result .....	34
4.5.7	Experiment 2 – Classification .....	35
4.6	Chapter Summary .....	36
Chapter 5	- Design of a Low-Cost Flash Flood Nowcasting Solution .....	37
5.1	Proposed Solution.....	37
5.2	Architecture of the Proposed Solution .....	38
5.2.1	System Architecture.....	38
5.2.2	Logical Architecture for WSN.....	39
5.3	Proposed Flash Flood Nowcasting Approach.....	40
5.4	Requirement Specification.....	40
5.4.1	Functional Requirement .....	40
5.4.2	Non-functional Requirements .....	41
5.5	Use Case Diagram and Scenarios .....	42
5.6	Class Diagram .....	43
5.7	Database Design.....	44
5.8	User Interface Design.....	45
5.8.1	Mobile Interface (User).....	45
5.8.2	Web Interface (Admin) .....	46
5.9	Chapter Summary .....	46

Chapter 6 – Implementation and Testing.....	47
6.1 Wireless Sensor Network Prototype.....	47
6.1.1 System Cost.....	48
6.1.2 WSN System Implementation Challenges.....	51
6.1.3 WSN Prototype .....	52
6.2 Machine Learning Engine.....	53
6.3 Web Application User Interface Implementation.....	56
6.4 Test Strategies.....	59
6.5 Chapter Summary .....	62
Chapter 7 – Experimental Results & Evaluation .....	63
7.1 Evaluation Method.....	63
7.1.1 Data Set Information.....	63
7.1.2 Experimental results and analysis.....	65
7.1.3 Performance Analysis.....	70
7.2 RNN-GA Evaluation .....	70
7.2.1 Dataset Creation .....	71
7.2.2 Simulation results .....	72
7.3 General Discussion.....	72
Chapter 8 – Conclusion & Future Works.....	74
8.1 Research Summary .....	74
8.2 Research Limitations.....	75
8.3 Future Works .....	75
References .....	76
Appendix A.....	79
List of Known Flood Prone Areas .....	79
Director of Public Prosecutions office .....	84
Flood Damages.....	89
Flash Flood Forecasting/Nowcasting Algorithms.....	90
A.4.1 Basha (2008) flood prediction linear regression algorithm. ....	90
A.4.2 Wu & Chau (2006) Artificial Intelligence flood forecasting algorithms.....	91
A.4.3 Chaing et al. (2007) Recurrent Neural Network QPE and QPF .....	92
A.4.4 Abdul-Kader et al. (2018) Forecasting Rainfall based on Computational Intelligent Techniques .....	94
Installation Procedures .....	101

## Table of Figures

Figure 2.1: Death from flash floods trends (DesInventar) .....	5
Figure 2.2: Houses Destroyed/Damaged from flash floods Trends (DesInventar) .....	6
Figure 2.3: Houses Destroyed/Damaged from torrential rain trends (DesInventar).....	6
Figure 3.1: Flowchart of model .....	13
Figure 3.2: Comparison of not assimilated and assimilated ANFIS model performance .....	13
Figure 3.3: Performance comparison in terms of absolute errors for different algorithms .....	14
Figure 3.4: MLP linear and non-linear.....	16
Figure 3.5: Guesmi WSN architecture.....	17
Figure 4.1: Sensors Placed Upstream and Downstream.....	32
Figure 4.2: WRU Water Flow Data: .....	33
Figure 4.3: Water Flow and Rainfall Data .....	34
Figure 4.4: Synthetic data .....	34
Figure 4.5: Water Flow Data in Gfurquim format.....	35
Figure 4.6: Results Gfurquim format .....	35
Figure 4.7: Results Confusion Matrix.....	36
Figure 5.1: WSN Setup .....	37
Figure 5.2: System Architecture.....	38
Figure 5.3: WSN Logical Architecture .....	39
Figure 5.4: WSN Architecture .....	39
Figure 5.5: Use Case Diagram .....	42
Figure 5.6: Class Diagram.....	43
Figure 5.7: Database ERD.....	44
Figure 5.8: Mobile Interface-main .....	45
Figure 5.9: Web Interface-main .....	46
Figure 6.1: Proposed WSN Implementation Architecture .....	47
Figure 6.2: Main Screen .....	57
Figure 6.3: Graph .....	57
Figure 6.4: Buttons.....	58
Figure 6.5: System Logs.....	58
Figure 6.6: Error Logs.....	58
Figure 6.7: Live+Predicted data .....	59
Figure 7.1: WHWFR graph.....	64
Figure 7.2: WHWFRD graph .....	65
Figure 7.3: HPT graph.....	65
Figure 7.4: MLP result (scenario 1) .....	66
Figure 7.5: RNN result (scenario 1) .....	66
Figure 7.6: RNN-GA results (scenario 2) .....	67
Figure 7.7: MLP result (scenario 3) .....	68
Figure 7.8: RNN result (scenario 3) .....	68
Figure 7.9: RNN-GA result (scenario 4) .....	69
Figure 7.10: Normal .....	71
Figure 7.11: Drought .....	71

Figure 7.12: Extreme .....	71
Figure A.1: Canal Dayot.....	89
Figure A.2: Poste-de-Flacq .....	89
Figure A.3: Montagne Blanche.....	89
Figure A.4: Music Instruments Shop, La Louise, Quatre-Bornes .....	89
Figure A.5: La Louise, Quatre-Bornes.....	89
Figure A.6: Albion.....	89
Figure A.7: Baie-du-Tombeau .....	90
Figure A.8: River in Vacoas.....	90
Figure A.9: RNN architecture .....	92
<i>Figure A.10: ANN flowchart .....</i>	<i>95</i>

## Table of Tables

Table 2.1: Observed impacts of climate change in Mauritius.....	3
Table 2.2: Projected impacts of climate change in Mauritius .....	4
Table 3.1: Performance comparison for different models in flood prediction.....	14
Table 5.2: Non-functional Requirements.....	41
Table 6.1: Estimated Cost of Base Station .....	49
Table 6.4: Estimated Cost of Power Source .....	51
Table 7.1: Models Comparison of Scenario 1 .....	66
Table 7.2: GA parameters (scenario 2) .....	67
Table 7.3: Models Comparison of Scenario 2 .....	67
Table 7.4: Models Comparison of Scenario 3 .....	68
Table 7.5: GA parameters (scenario 4) .....	69
Table 7.6: Models Comparison of Scenario 4 .....	69
Table 7.7: Performance Comparison of Experiments .....	70
Table 7.8: Evaluation.....	72
Table A.2: Communication Hardware.....	97
Table A.4: Base Station .....	98
Table A.5: Communication Hardware.....	99
Table A.6: Sensors.....	100

## Table of Equations

<i>Equation 1: Basha Linear Regression Algorithm</i> .....	91
<i>Equation 2: Genetic optimisation Algorithm</i> .....	91
<i>Equation 3: ANFIS</i> .....	92

## List of Acronyms

ACR - Average Cumulative Rainfall

ALADIN - Aire Limitée Adaptation dynamique Développement InterNational

ANFIS – Adaptive Network-Based Fuzzy Inference System

ANN - Artificial Neural Network

ANN-GA - Genetic Algorithm-Based Artificial Neural Network

BPNN - Back Propagation Neural Network

Bays Net – Bayesian Network

BoM - Australia Bureau of Meteorology

CC – Correlation Coefficient

DIMP - Distributed Model Intercomparison Project

ECMWF - European Centre for Medium Range Weather Forecasts

EFFS - European Flood/Flash Flood Forecasting System

GA – Genetic Algorithm

GHG – Global Greenhouse Gasses

LM - Levenberg-Marquardt

LR- Linear Regression

LQE - Linear Quadratic Estimation

MAE - Mean Absolute Error

MLP - Multilayer Perception

MMS - Mauritius Meteorological Services

MRWFEPS - Medium Range Weather Forecasting Ensembled Solution

NDOCC - National Disaster Operations and Coordination Centre

NRMSE - Normalized Root Mean Square Error

NWP - Numerical Weather Prediction

PERSIANN-CCS - Precipitation Estimation from Remotely Sensed Information using Artificial Neural Networks-Cloud Classification System

PPD – Percentage of Peak Discharge

QPESUMS - Quantitative Precipitation Estimation and Segregation Using Multiple Sensors

RBF - Radial Basis Function

RMSE - Root Mean Square Error

RNN - Recurrent Neural Network

RNN – Recurrent Neural Network

SIDS – Small Island Developing State

SMF - Special Mobile Force

SPPD – Synchronous Percentage of Peak Discharge

SVR – Support Vector Regression

WRU - Water Resource Unit

WSN - Wireless Sensor Network

ZAMG - Austrian Meteorological Office

# Chapter 1 – Introduction

## 1.1 Background of Study

Studies have shown that climate change does not only alter the average temperatures in different regions around the globe, but also increases the occurrence of certain types of natural disasters (European Parliament, 2006; Houghton, et al., 2001). Flood is one among these natural disasters, and its magnitude and frequency has increased over the years, making its impact even more significant (Guha-Sapir, et al., 2012). It is even considered among the most catastrophic natural disasters affecting human lives and causing economic damage (Easterling, et al., 2000). In the U.S., it is estimated that flood causes the loss of around 100 lives and damages above \$2 billion over a year (Sharif, et al., 2006). Similarly, torrential rains and flood related fatalities have dramatically increased in Africa over the past half century with countries including Burkina Faso, Senegal, Ghana and Niger were the worst hit (Di Baldassarre, et al., 2010).

In Mauritius, this issue is becoming of significant importance due to the dire consequences of torrential rain and flash floods in March 2008 and 2013. During both episodes, 15 cases of death were reported in addition to over 300 vehicle damages and more than 2000 requests for assistance were received by the Fire Services (Cabinet Decision, 2008; PQ Written Answers, 2013). In March 2013 particularly, around 152 millimetres of rain was recorded in less than an hour by the local meteorological service (Disaster Report, 2013) and this contributed to the rapid rise of water level in rivers that flows from the central plateau down to the sea. The city of Port Louis, which hosts the only harbour of the island, was mostly affected as water rapidly accumulated around the waterfront, affecting road networks, pedestrian underpass and surrounding domestic habitats (lexpress, 2018). Several other regions, such as Bois Rouge, Cottage, Piton, Mapou, Fond du Sac are also frequently affected by sever flash flood occurrences (Week-End, 2016). Several inhabitants in these regions often have to leave their flooded houses to seek assistance for basic needs, provided by relatives, other inhabitants, government and Non-Governmental Organisations (NGOs).

## 1.2 Problem Statement

Based on the preliminary literature survey, it is apparent that not enough consideration has been given to the problem of flash flood in Mauritius and few technological-based solutions have been proposed. Additionally, existing weather monitoring technologies and emergency warning systems in Mauritius have not been very effective. It has been noted that a flood prediction and mitigation map for Mauritius has been developed, focusing on parameters including maximum surface water depth, street water depth, flow velocity and hazard level (Mauritius Research Council, 2016). Although this model has been projected as a vital tool to identify flood prone regions, it does not automatically predict flash floods occurrences. Nowcasting this phenomenon is critical in order to take early actions to reduce damage and loss of lives.

Also, existing systems usually require expert hydrologists to monitor real-time data 24 hours a day and run sophisticated computational models (Furquim, et al., 2014). Although data mining approaches have been applied to hydrological data, no specific and effective algorithms have been derived using machine learning approaches.

While warning systems exist in developed countries, these cannot be readily applied to the local context due to the different environmental variables involved and are often very costly. As such, a low-cost system that can automatically make predictions based on a Machine Learning approach is necessary.

### 1.3 Aim and Objectives of Project

This project proposes to investigate, design, develop and evaluate a low-cost automated flood warning prototype system taking into consideration the constraints and requirements of the Mauritian context. The system consists of a Wireless Sensor Network (WSN) for monitoring water level in rivers and the collected data are automatically analysed through Machine Learning models for nowcasting. The proposed system therefore does not directly depend on the availability of local experts to predict the probability of an imminent flood. Although the role of a subject expert is important for data analysis, they might not be available in all specific high-risk regions of the island all day round. Such a system has the potential to provide early warning for decision makers within reasonable time such that timely actions could be taken by key stakeholders so as to reduce damages. The aim and objectives of the project are described as follows.

The aim of this study is to investigate, design, develop and assess the effectiveness of a low-cost prototype system to nowcast flash floods using a combined approach based on wireless sensor networks and machine learning techniques. The objectives of this project are:

- Obj1: To investigate parameters involved in nowcasting of flash floods within the Mauritian context,
- Obj2: To critically review and assess the relevance of existing models pertaining to nowcasting of flash floods within Mauritius,
- Obj3: To assess the availability of data in Mauritius to use machine learning in nowcasting flash floods within the island,
- Obj4: To design and develop a low-cost prototype for sensing and collecting environmental data pertaining to flash flood detection,
- Obj5: To assess the accuracy of machine learning techniques, and propose an efficient algorithm to assist in flash flood nowcasting in Mauritius,
- Obj6: To evaluate the prototype using available data and provide recommendations on the combined approach.

## Chapter 2 - Flash Floods and Associated Impacts

### 2.1 The Growing Climate Change Concerns for Mauritius

Climate change is the result of global warming, which refers to the rise of average surface temperatures on earth, primarily due to the use of fossil fuels which releases greenhouse gases in the atmosphere (Climate NASA, 2018). According to the same source, a range of effects have been noticed on the ecosystem, including rising sea levels, droughts, heat waves, changes in precipitation patterns and severe weather events. Higher temperature causes greater evaporation which increases the water vapour content in the atmosphere (Trenberth, 2011). Hence, extratropical and tropical rain, tropical cyclones and snow storms are higher producing more intense events, increasing the risk of flooding.

On a worldwide scale from 1980 to 2009, flood has caused more than 500,000 deaths and affected more than 2.8 billion people (Doocy, et al., 2013). In the U.S, flood accounts for more than 4000 deaths from 1959 to 2005 and costs about 8 billion US Dollars per year over 1981 to 2011 (U.S Global Change Research Program, 2014). As per (U.S Global Change Research Program, 2014), heavy downpours increased by 30% on average over the year 1901-1960. Even in Mauritius, flash floods have had various negative impacts.

Mauritius, as a Small Island Developing State (SIDS), is highly vulnerable to the effects of climate change and its negative impacts on socio-economic development and it has been reported that SIDS contribute to only 1% of the global GHG emission, are the ones to suffer most from the impacts of climate change (Ministry of Environment and Sustainable Development Division, 2015). According to the World Risk Report (2014), Mauritius is ranked as the 14<sup>th</sup> country with the highest disaster risk and ranked 7<sup>th</sup> on the list of countries most exposed to natural disasters. Mauritius is highly vulnerable to the adverse impacts of climate change, manifesting itself in several ways, including intense cyclones, abnormal tidal surges, prolonged droughts, flash floods, increase of sea surface temperature among others (INDC, 2015). Meteorological observations have confirmed a change in the climate parameters of Mauritius. An average temperature rise of 0.74 degrees Celsius over mainland and 1.1 degrees Celsius over Agaléga have been recorded, precipitation has decreased by 8% between 1950 and 2008 but the frequency of extreme climatic events is on the rise as well as the extent of damage to infrastructure and toll on human life. The intensification of cyclones and heavy precipitations in shorter periods of time has also been observed (Ministry of Environment and Sustainable Development Division, 2015).

Table 2.1 shows some of the main observed impacts of climate change since 1950 to 2017 and Table 2.2 shows prediction impacts of climate change in Mauritius. The data shows that although there is a decrease in annual rainfall and more hot days, more torrential rainfall and cyclones are expected in shorter amount of time, representing high risks of flash floods.

<b>YEAR</b>	<b>OBSERVED EFFECTS</b>
SINCE 1950	Decrease in annual rainfall around 8%
1998 - 2007	Mean rise sea level of 2.1mm – 3.8mm per year.
2008 AND 2013	Flash floods resulting in loss of lives and infrastructure.
1999 AND 2011	Worst drought.
2008	Rise of temperature by 0.74 degrees Celsius compared to 1961-90 mean. Increase in the annual number of hot days and warm nights.
2017	Increase frequency of extreme weather events, torrential rainfall and cyclones.

*Table 2.1: Observed impacts of climate change in Mauritius*

YEAR	PROJECTED IMPACTS
AS FROM 2008	More frequent and longer heat waves in summer.
AS FROM 2017	Increase in number of intense tropical cyclones. Increase in heavy precipitation with increased risk of flash flood.
BY 2050	Decreasing trend of 8% in annual rainfall. Decrease up to 13% water resources.
BY 2100	Live corals to be reduced by 80-100% in the event of 3.28 degrees Celsius rise in temperature

*Table 2.2: Projected impacts of climate change in Mauritius*

Due to climate change flash floods have been a major threat to Mauritius resulting in victims and infrastructural damages. Torrential rain causing flash floods in March 2008 and 2013 reported 15 cases of death, over 300 vehicle damages and more than 2000 requests for assistance received by the Fire Services (Cabinet Decision, 2008; PQ Written Answers, 2013). Appendix A provides a list of flood prone areas within Mauritius. (NDRRMC, 2017)

## 2.2 Flash Floods and Associated Negative impacts

During recent years, different major flash floods occurred and these are described as follows: flash flood is a phenomenon which occurs suddenly due to heavy rain over a short period of time. It is often accompanied by other hazards like landslides and mud flows which causes damage to infrastructure and may also result in loss of lives (Collier, 2007). In Mauritius, torrential rain alert is set when 100 millimetres of widespread rain falls in less than 12 hours and is likely to continue for several hours (Mauritius Meteorological Services, 2018). Flash floods are caused by heavy rainfall or torrential rain during a short lapse of time generally between three to six hours. In urban areas, flash floods are more severe as water does not infiltrate the impermeable ground and rivers as well as water canals overflows on land. People are usually caught off-guard with the rapid rise of water level.

### 2.2.1 26th March 2008

On 26<sup>th</sup> of March 2008, torrential rain was caused by the trail of clouds from cyclone Lola (2014). The soil was already saturated with previous precipitation of the cyclone, an unexpected change in directory of cyclone Lola towards North East of Mauritius caused heavy rainfall and flash floods. The torrential rain warning was activated at 11.00 a.m. on reaching 100 mm of rainfall in 13 hours and the soil permeability was not taken into account.

As impacts, four persons lost their lives following the torrential rainfall and flash floods mainly in the North, East and South. A student age 13 and a woman age 58 were swiped away by torrents of muddy water at Mon Gout. A body was found in his house drowned by a nearby overflowing river in Saint Remi, Flacq. The fourth victim age 18 was found drowned in Bel Air.

### 2.2.2 30th March 2013

On 30<sup>th</sup> of March 2013, more than 136mm of rain fell within two hours that is between 13h00 and 16h00. Members of the public were taken by surprise by the sudden downpour. The Port Louis area between the Caudan Flyover and the Place D'Armes was drained by four main water courses namely the Deviation Canal which runs along Signal Mountain Road, the drain along Volcy Pougnet Street, Le Pouce Stream which passes behind Cinema Majestic and Le Pouce Canal which passes in front of the Museum and Shoprite Supermarket. These main water courses are completely flooded. The cumulative effect of the

deficient drainage system and the surface run-off generated with the urban area has contributed to the flooding.

During the flooding, the police and Fire Services faced communication problems due to clogged telephone network. People were not able to reach the emergency services.

- The Fire Services do not have sufficient manpower to deal with the situation.
- The National Disaster Operations and Coordination Centre (NDOCC).
- The Cyclone and Other Natural Disaster Scheme 2012-2013 are not equipped to deal with the situation and do not make any provision for flash floods as it is a new phenomenon.

The lack of coordination of the authorities and concerned parties lead to a poor handling of the situation.

The special bulletin of the Mauritius Meteorological Services (MMS) came late after several places was already flooded. The MMS is not equipped in terms of knowledge, skills and equipment to forecast or nowcast flash floods. Also, the Water Resource Unit (WRU) lacks the required expertise to predict flash floods.

As impact, following the heavy flooding in Port-Louis, ten people lost their lives. Six human bodies were retrieved from the Caudan underpass, two were retrieved from the underground parking of Harbourfront Building. One body was found in the Company Garden and the last near KFC outlet of Chaussée Street. Figure 2.1 show an increase in death due to flash floods in the period of 1975 to 2013. In addition, serious damage was caused to not less than 300 vehicles, homes, and the level of muddy water has also affected commercial buildings and stocks of goods, while debris, stones and mud were transported for miles. Figure 2.2 shows an increase in houses damaged/destroyed from flash floods in the period of 1975 to 2013. According to economist Eric Ng the estimate cost of damages caused is between Rs 400-500 Million (Ng, 2013).

This natural disaster has revealed the flaws in our system of drains, which implies a significant investment in the short-term remedy. According to records from national parliament, a sum of Rs 500 million were disbursed after the flash flood for the construction of drains across the country. An SMS alert system was also announced, as well as better equipment for the Mauritius Meteorological Service.r (Defi Media Group, 2013).

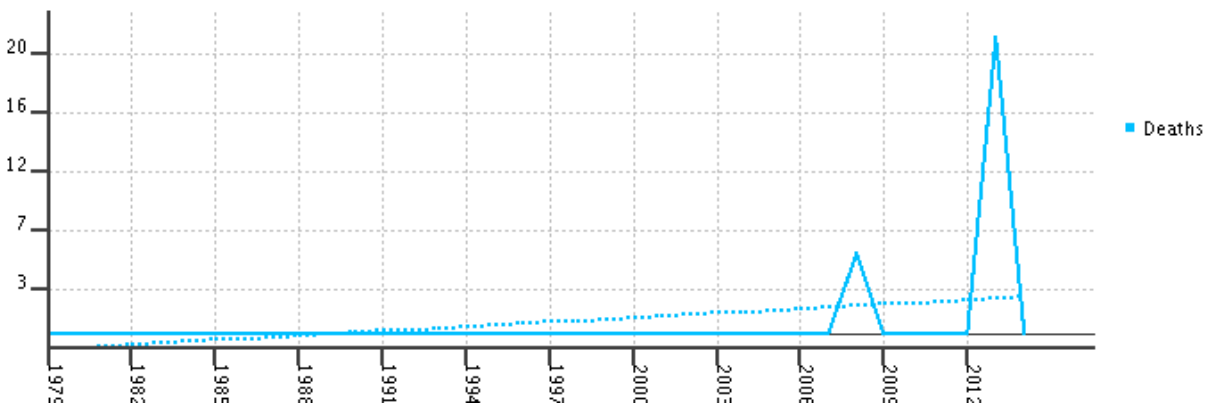


Figure 2.1: Death from flash floods trends (DesInventar)

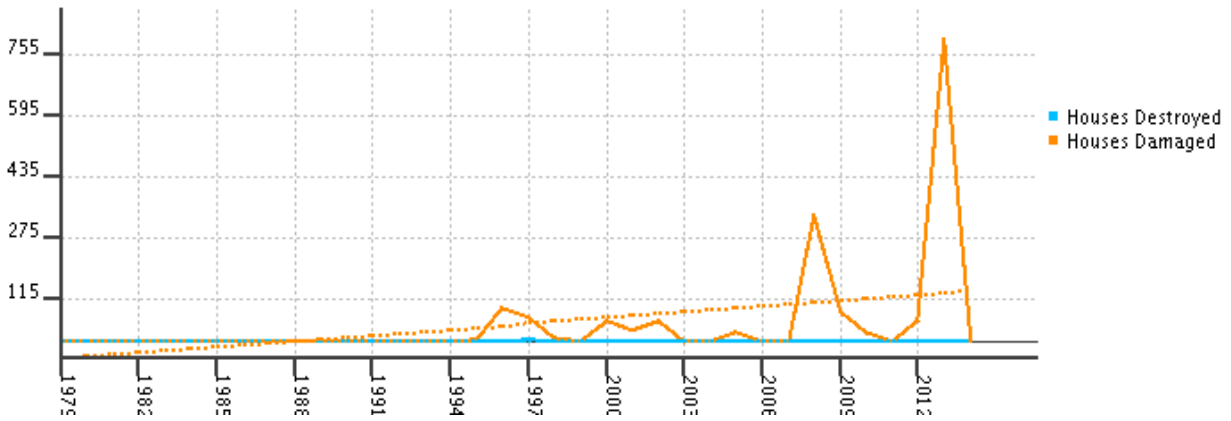


Figure 2.2: Houses Destroyed/Damaged from flash floods Trends (DesInventar)

### 2.2.3 Torrential Rainfall & Cyclone Berguita

In January 2018, the country faced huge rainfall events. These events led to many cases of floods, landslides, river overflow and obstructed drains due to high water flow carrying debris. In the period of 4<sup>th</sup> to 8<sup>th</sup> January 2018, heavy rainfall and cyclone Berguita caused floods and water accumulation in various regions. The water level at Canal Dayot, was at the maximum which posing a potential threat to the locality. Montagne Blanche and Poste-De-Flacq were also affected by floods.

Torrential rainfall on the 25<sup>th</sup> January 2018, caused flash floods in the region of Quatre-Bornes, Albion, Baie-du-Tombeau and Point-aux-Sables. La Louise in Quatre-Bornes businesses suffered loss with goods and electronic appliances being damaged by muddy water. Drains and water canals were flooded. In Albion, a road flooded by a river restricting access. In Baie-du-Tombeau, houses, yards and roads were flooded due to obstructed water canal.

From January 3<sup>rd</sup> to 11<sup>th</sup> 2018, the fire brigade received 705 calls on their emergency line and they responded 420 times including 214 homes being flooded (Deputy Chief Fire Officer). On the 23<sup>rd</sup> February of 2018, heavy rainfall and flooded river caused a flash flood at Réunion Road, Vacoas. The quick rise of water flooded two schools (Sai Satya School and Quinze-Cantons School). Children and staff members had to take refuge in the upper floors of the building until they were rescued by the Special Mobile Force (SMF) officers. Figure 2.3 shows an increase in houses damaged/destroyed from torrential in the period of 1975 to 2013, no statistical data is available beyond 2013. Figure A.1 to Figure A.8 (See appendix A, Flood Damages) shows some flooded photos of regions in the period of events in January.

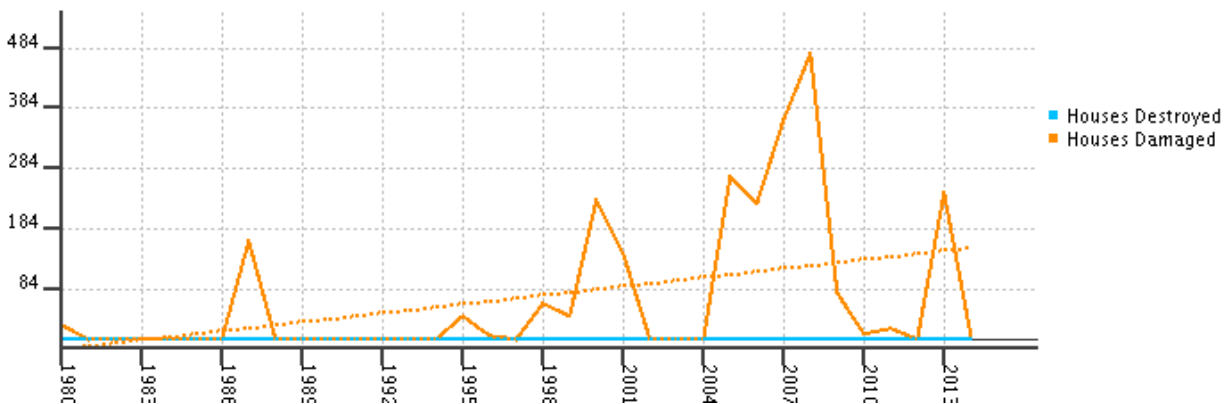


Figure 2.3: Houses Destroyed/Damaged from torrential rain trends (DesInventar)

## 2.3 Reducing the Impacts of Flash Flood

It is apparent from the previous section that flash floods can be very destructive, causing damage to properties, loss of life and having an impact on the economy. It is mainly caused by a combination of the: obstructed drains, overflowing of drains and rivers, water saturated soil from prolonged rainfall, primarily due to torrential rainfall and heavy rainfall during a short lapse of time. In the following section, investigation on how other countries deal with flash flood forecasting is conducted.

### 2.3.1 Flash Flood Forecasting in Northern Austria

A spatially distributed model for flash flood forecasting is in operational use in Northern Austria since 2006 (Blöschl, et al., 2007). The model uses a grid based of 1 km square over 1550 km square Kamp catchment. The model is able to simulate snow processes, soil moisture processes and hill slope scale routing. Each grid cell uses a total of 21 parameters for the simulations, which includes 5 snow model parameters, 5 soil moisture accounting parameters, and 11 hillslope scale routing parameters. As input, 35 rain gauges are used with 19 of them registering data at 15 minutes interval and the remaining works on a daily level. The precipitation forecasts are made by the Austrian Meteorological Office (ZAMG). The forecasts are at 15 minutes temporal resolution over a lead time of 48 hours and are estimated as two components. The first component is an observation-based extrapolation or nowcasting of the interpolated precipitation field using motion vectors determined from consecutive fields. The second component is a weighted mean of the forecast fields of the ALADIN (Aire Limitée Adaptation dynamique Développement InterNational) and ECMWF (European Centre for Medium Range Weather Forecasts) numerical weather prediction (NWP) models by Wang, et al (2006). The two components are weighted together by another weighting function to provide better predictions and reduce precipitation error by 20-30%. The weighing function gives full weight to the nowcast during the 2 hours and decreases linearly to zero at 6 hours, remains at zero for larger lead times. Air temperature from eight stations are added to the 1 km grid. Precipitation and air temperature parameters are used to estimate state variables such as soil moisture, soil and groundwater reservoir storage and snow water at each time step. Kalman Filter function<sup>1</sup> is used to update the model states variables based on observed runoff. Existing data of 12 stream gauges are used from 1990 to 2005. All the parameters and state variables are then used for flash flood forecasts over the lead time of 48 hours. Two algorithms have been implemented that use runoff in real time. The first algorithm adjusts the catchment soil moisture state by the Ensemble Kalman Filter and the second algorithm exploits the autocorrelation of the forecast error and consist of an additive error model that updates runoff directly. The average forecast errors range from 10 to 30% for 4 to 24 hours lead time, respectively. Comprehensive model test and simulation results accuracy indicated that the methodology used is feasible and performs well for a range of hydrological situations and a range of temporal scales. However, the performance of the model diminished on the accuracy of the rainfall data, biases in rainfall is translated into biases in soil moisture and hence lowering forecast accuracies.

### 2.3.2 Flash Flood Forecasting in Australia

The Bureau of Meteorology (BoM) operates a real-time flood forecasting and warning system (Hapuarachchi & Wang, 2008). In 1987 an automated flash flood warning system called ALERT was introduced in local agencies to alert officials. The system can be used on small catchment areas and large river basins to detect floods and issue alerts It uses radio signals to transfer real time data of rainfall and

---

<sup>1</sup> Kalman filtering, also known as linear quadratic estimation (LQE), is an algorithm that uses a series of measurements observed over time, containing statistical noise and other inaccuracies, and produces estimates of unknown variables

water level to a station where the data are analysed. In some cases, data are directly input to the model to assess the magnitude and timing of flood events. Flooding can be assessed using manual look-up tables provided by the BoM. An alert is sent if the criteria of rainfall intensity or stream level is exceeded.

Similarly, like ALERT, a low-cost flash flood warning system, using sensors, was developed by MacGeorge in Hobart, Tasmania in 1997. When water reaches the predefined level, the system issues a warning via telephone with a played synthesized voice alerting the recipient of the river location and level.

### 2.3.3 The European Flood/Flash Flood Forecasting System (EFFS)

The EFFS provides daily information on potential floods for large rivers, and flash floods in small catchments. The system consists of four basic components (De Roo, et al., 2003):

- 1 global numerical weather prediction models,
- 2 optional downscaling of global precipitation using a regional Numerical Weather Prediction model,
- 3 a catchment hydrology model comprising a soil water balance model with daily time step and a flood simulation model with hourly time step,
- 4 a high-resolution flood inundation model.

All the components are integrated within a generic modelling framework linked to a central database. The system uses large scale weather forecast derived from the European Center for Medium Range Weather Forecasting Ensembled Solution (MRWFEPS). MRWFEPS forecast weather variables for each cell of 40-80 km horizontal resolution every 6h for up to 10 days lead time.

A higher spatial and temporal resolution provides more realistic weather predictions. To increase the forecast spatial and temporal resolution of the output of MRWFEPS, two regional NWP models are used: the DMI-HIRLAM model and the DWD-LM model. The DMI-HIRLAM model is a hydrostatic grid-based model that produces hourly output for the whole of Europe for lead times of up to 72h at approximately 11 km horizontal resolution. The DWD-LM uses a non-hydrostatic representation of the atmosphere for a grid covering Western Europe only at a horizontal resolution approximately 7 km and produces outputs in the range of 6 to 48 hours.

The output from DMI-HIRLAM and DWD-LM models are re-formatted and used in the raster-based distributed rainfall-runoff modelling suite, LISFLOOD (De Roo, et al., 2000; 2001). The LISFLOOD-FF simulates river flow and flooding at hourly time steps and 1 km square grid resolution with topography, precipitation amounts and intensities, antecedent soil moisture content, land-use types, and soil types as variables. A two-dimensional hydraulic module, LISFLOOD-FP is used to model the overbank flows and inundation areas.

The performance of EFFS system was tested using data from the Meuse River flood. The results were encouraging and the system produced flood peaks with acceptable accuracy. The EFFS simulation driven by the deterministic forecasts of rainfall can capture the flood peaks 5 days ahead, but thereafter failed to capture the main body of the flood. The inundation model (LISFLOOD-FP) was run using the observed flow and compared to observed inundation extent derived from oblique aerial photography. The model was run at 50m resolution with a 5 sec time step and correctly classified inundation extent in 85% of model grid cells.

## 2.4 Critical Analysis

Since flash floods are relatively new weather phenomena in Mauritius, all previous occurrences have not been properly predicted and in some cases not predicted at all. Prem Saddul, Geomorphologist (lexpress.mu, 2018), confirmed that new regions are likely to be at risk of flooding. Commercial centres with large asphalt parking and new urban areas where concrete reduces the rate of water infiltration in the soil. Since pores in the earth are saturated with water and earth surface area has been reduced, the water tends to stay on the surface for longer periods even after a short rainfall period. As the island topology indicates a slope of eight degrees going to the sea, the flow of water volume is high with fast velocity. Water arriving near a small bridge or a partially blocked passage, is susceptible to overflow and cause flash floods. It therefore, is essential to study existing methodologies and parameters involved in flash flood forecasting and nowcasting for Mauritius.

We have seen an increase in extreme weather conditions that are caused by the rise of average surface temperatures as a result of climate change. Amongst others, intensification of cyclones and heavy precipitations have been observed in Mauritius, causing frequent accumulations of water and flash floods, resulting in dramatic impact of human loss and infrastructural damages. Little work has been done at national level to mitigate and alert the population in case of an upcoming flash flood, while several solutions exist at international level. In Northern Austria a spatially distributed model for flash flood forecasting uses a grid based of 1 km square over 1550 km square Kamp catchment and is able to simulate snow processes, soil moisture processes, hillslope scale routing and forecast flash flood at a temporal resolution of 15 minutes over a lead time of 48 hours. In 1987, Australia Bureau of Meteorology (BoM) introduced real-time a flash flood warning system called ALERT which is able to send alerts to officials if the rainfall intensity of stream water level is exceeded. Flood is assessed using manual look-up tables provided by BoM. To forecast flash flood the EFFS combined several models: MRWFEPS(weather forecasting), DMI-HIRLAM(hydrostatic grid base model), DWD-LM(non-hydrostatic representation of the atmosphere), LISFLOOD-FF(simulates river flow and flooding) and LISFLOOD-FP(model overbank flows and inundation areas). While most of the mentioned models are functional, they are not currently applicable in Mauritius as their complexity requires high resolution radar and satellite data. In the next chapter we investigate on rainfall and flash flood forecasting and nowcasting models that make use of machine learning techniques and wireless sensor network for prediction.

## Chapter 3 - ICT Driven Flash Flood Nowcasting

### 3.1 Technology Driven Flash Flood Nowcasting

During recent years, different studies have attempted to investigate the parameters that are involved in forecasting of flash floods (Doswell III, et al., 1996; Collier, 2007; Blöschl, et al., 2008). Based on the identified parameters, different models have also been proposed to forecast flash floods although their effectiveness remain questionable. As such, effective flash flood forecasting remains one of the most challenging areas in hydrology due to the uncertainties associated with rainfall forecasts (Hapuarachchi, et al., 2011). This also led to a change in flash flood research direction from forecasting to nowcasting. Nowcasts refer to short-time and space-specific forecasts of periods less than a few hours, and may include storm initiation, growth, dissipation, and storm features such as wind speeds and direction and precipitation rates (Sharif, et al., 2006). As the need for reliable flash flood forecasting has increased in recent years, different works have been undertaken within different regions to nowcast this phenomenon. A spatially distributed flash flood forecasting model was conceptualised and evaluated for the region of northern Austria (Blöschl, et al., 2008). Similar work was undertaken for the mountainous Mediterranean basin (Dolcine, et al., 2001) and Slovenia (Grillakis, et al., 2010), among others. However, in addition to nowcasting models, recent research focus has shifted towards technology driven flash-flood nowcasting.

Abdul-Kader, et al., 2018 propose an evaluation of two Artificial Neural Network (ANN) training models consisting of 4 nodes in the input layer, 20 nodes in one hidden layer and 1 node in the output layer against Radial Basis Function (RBF) and four input weather variables were used. Wu & Chau, 2006 evaluate two ANN training algorithms, namely the Genetic Algorithm-Based Artificial Neural Network (ANN-GA) and Adaptive-Neuro-Fuzzy Inference System (ANFIS) against linear regression for forecasting flood. Basha, et al., 2008 and Guesmi, 2017 propose a wireless sensor network (WSN) to monitor and predict flash floods events by the use of sensors nodes capturing weather and river parameters in real-time. The data collected are processed by a flood prediction algorithm. Chiang, et al., 2007 and Chang, et al., 2014 propose an ANN model to merge multiple rainfall sources and rainfall forecast for better flash flood forecasting by assimilation of satellite-derived and radar-derived precipitation forecasts provided by PERSIANN-CSS and QPESUMS combined with rain gauges parameters as input. Furquim, et al., 2014 evaluate the flood nowcasting accuracy of seven machine learning classification techniques with the input data type used and window sizes. Artigue, et al., 2011 present a recurrent neural network (RNN) model for flash flood forecasting without considering rainfall forecasts nor previous discharge. Levenberg-Marquardt (LM) algorithm is used to train the multilayer perceptron (MLP) model and two models with different criteria are tested and performance compared. Boukharouba, et al., 2013 present support vector regression machine learning approach to flash flood forecasting without rainfall forecasts, based on agglomerative hierarchical clustering of flood events. Two models are tested and evaluated, global model and specific model both with different criteria.

A key technology for common flash flood warning systems is the wireless sensor networks (WSN) and to a small extent machine learning. WSN provides the flexibility of having small computing devices with sensors and communication capabilities for monitoring purposes without direct human intervention. Systems based on WSN for monitoring water levels in rivers have been studied and proposed for various locations around the world (Basha, et al., 2008; Furquim, et al., 2014; Guesmi, 2017). On the other hand, an early warning system named RAPIDS, based on Machine Learning, focuses on the utilization of rainfall data to predict flooding in urban areas using Artificial Neural Network. Furquim et al. (2014) present a

combination of WSN and 7 Machine Learning techniques for flash flood nowcasting in Sao Carlos, Brazil. Additionally, a low-cost automated sensor network has been proposed that runs prediction software which measures and computes in real time in order to address changing conditions during a flood (Basha, et al., 2008). These technology-driven flash-flood nowcasting solutions are described in the next section.

## 3.2 WSN & Machine Learning Based Flash Flood Prediction

### 3.2.1 Combining wireless sensor networks and machine learning for flash flood nowcasting

Furquim et al. (2014) discuss the evaluation of seven machine learning techniques. The results indicate that different approaches are required to improve the accuracy of each technique, such as using the vector of an attribute as opposed to raw data. The following ML techniques have been tested with two window sizes ( $w=2$  and  $w=10$  hours) which is the number of previous readings used:

- Decision Trees: J48, Random Forest, Random Tree, BFTree, Simple Cart
- ANN: Multi-Layer Perceptron – MLP
- Bays Net: Bayesian Learning

The result of all the techniques have been compared to find the most performant one. Wireless Sensor Network (WSN) of 3 sensors provides water level data and snapshots from rivers and hydrographic basins. Multi-Layer Perceptron (MLP) and BFTree ML Techniques have proved to be more efficient. The forecasting for 3 minutes yields an accuracy of 66%. The window size of 5 and 10 vary slightly. However better accuracy can be achieved by taking data from all sensors and adding more environmental parameters to the prediction algorithms.

### 3.2.2 Model-based monitoring for early warning flood detection

Basha (2008) created a statistical linear regression algorithm to predict flash flood, see Appendix A.4.1 for detailed algorithm description. The algorithm uses data from the node sensor network in real-time. The model can self-calibrate and adapt itself to the latest seasonal changes in weather condition. Inputs of past flow, air temperature and rainfall data taken at given time intervals are processed by the algorithm to produce a prediction. The model has been tested with 7 years of existing data from the Blue River in Oklahoma. The criteria for evaluating the algorithm quality are: the modified correlation coefficient, the false positive rate of prediction, and the false negative rate of prediction. To find the proper training window, the model run several times with windows of 3, 6, 9, 12 months covering all seasons. The model computes prediction of 1 hour and 24 hours. The autocorrelation of the model of 1 hour is near 1 and decreases to 0.627 at 24 hours. The prediction performs equally well for all window sizes using last flow, temperature and rainfall value. Better results have been obtained when using errors associated with the latest result. The developed model performed better than DMIP (Distributed Model Intercomparison Project), persistence and climatology models at 1 and 24 hours. A calibrated DMIP model outperforms the developed model by 3% with DMIP predicting only at 1 hour. The flood prediction algorithm has been implemented in a large scale WSN system in real environmental conditions using multiple sensing sensors and communication devices. The Multiple linear regression algorithm provides accurate predictions and fast computation is required if computation is done on low power nodes. However, more powerful and computation intensive algorithm is needed to better predict flash flood with more parameters such as soil moisture, land slope and air humidity.

To be able to monitor and predict floods events, a WSN consisting of nine nodes were built at the Aguan River Basin in Honduras. The long-range nodes consist of sensing nodes and communicate over a distance

of 25 km at 144 MHz radio and uses higher power to operate, which implies more online time for computation. The sensing nodes communicate at 900 MHz using low power. To save power transmission of data occurs every 10 minutes and measurement every 5 minutes. The nodes (3.7 V) are powered with lithium polymer batteries along with photovoltaic panels for charging. Transmitting 144 MHz signal uses 25W, occurring 6 times every hour for 15 seconds. The radio system uses a 12V lead-acid battery along with 6W photovoltaic panel. Antennas are located 5 m up, requiring antenna towers. The sensing nodes log raw data, compute data statistics over each hour and inter-transmission time period, and analyse data for indication of potential sensor failures. These nodes transmit regularly at 900 MHz creating mini sensors network. The water level sensor system is developed in an external box and communicates via RS485 with the sensing node. The box consists of a LPC2148 microcontroller, RS485 interface, Honeywell 24PCDFA6A, and instrumentation amplifier. Computation nodes connect to mini-network of sensors and perform distributed computation of prediction. Data arriving from nearby sensors and other computation nodes are recorded and evaluated for correctness. Eventually, the data goes through the model which computes the uncertainty of the prediction, and request additional data from sensing nodes to reduce the uncertainty. Computation nodes communicate to sensing nodes via 900 MHz and to each other via 144 MHz. The work of Basha et al. provides a very interesting WSN efficient architecture at a relatively low cost. Sensors used are simple and readily available or can be substituted for similar sensor.

### 3.2.3 Merging multiple precipitation sources for flash flood

Chiang et al. (2007) propose a Recurrent Neural Network (RNN) model to merge multiple precipitation sources for flash flood forecasting with lead time up to three hours, see Appendix A.4.3 for detailed algorithm description. The effectiveness of combining gauge observation and satellite-derived precipitation on flood prediction has been investigated. Satellite-based rainfall forecast is provided by the PERSIANN CCS (Honga, et al., 2004) with the spatial and temporal resolution of 4 km grid and hourly, respectively. The optimal merging parameters in both calibration datasets showed that the satellite-derived precipitation has limited contribution (5%) to merging procedures. However, the merged precipitation helped to improve the flood forecasting with improvement of root mean square error (RMSE) for about 2–14%. The contribution from gauged precipitation to the merged procedure depends greatly on the number of gauges and the quality of data. Despite improvements, the system is site specific as satellite derived data is not available everywhere.

### 3.2.4 Watershed rainfall forecasting using neuro-fuzzy networks with the assimilation of multi-sensor information

Chang, et al. (2014) propose the use of neuro-fuzzy or ANFIS (Adaptive Network-Based Fuzzy Inference System) networks with the assimilation of multi-sensor rainfall sources (gauge measurement, and radar and satellite products) for watershed rainfall forecasting of 1 to 2 hours lead time. Back Propagation Neural Network (BPNN) was used for bias correction of both radar and satellite precipitation products generated through the Quantitative Precipitation Estimation and Segregation Using Multiple Sensors (QPESUMS) and the Precipitation Estimation from Remotely Sensed Information using Artificial Neural Networks-Cloud Classification System (PERSIANN-CCS), respectively. Genetic Algorithm (GA) was used after bias correction for finding the optimal weighting factor in merging the different sources of precipitation data including gauge measurements. Figure 3.1 shows a flowchart of the model. Two scenarios were defined to test the ANFIS rainfall forecasting model. Scenario 1 used rain gauge, corrected PERSIAN-CSS and QPESUMS precipitation products as input. Scenario 2 used assimilated precipitation product as input. Ways of evaluating the model performance are: correlation coefficient (CC), root mean square error (RMSE), normalized root mean square error (NRMSE), and mean absolute error (MAE). Figure

3.2 shows that ANFIS model with assimilated inputs from scenario 2 proved to be more accurate and stable to forecast rainfall in comparison to scenario 1 with 25% and 19% improvement for one and two hours ahead in terms of RMSE. This model also uses satellite derived data, the same disadvantage as 3.2.3 applies for this model.

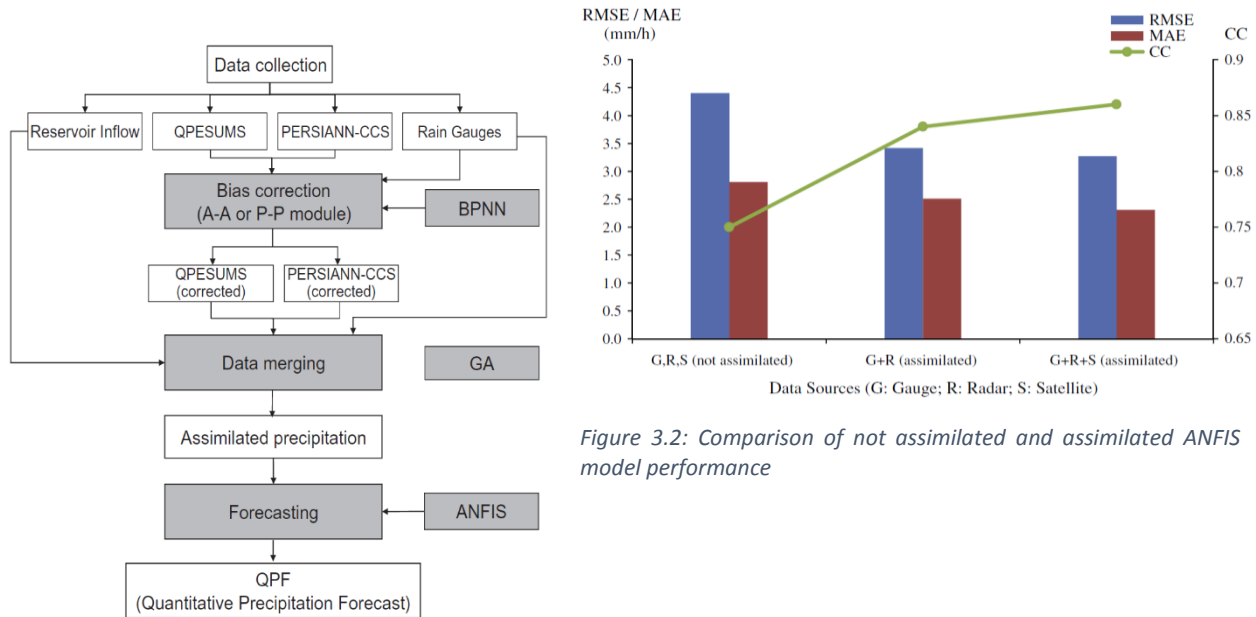


Figure 3.1: Flowchart of model

Figure 3.2: Comparison of not assimilated and assimilated ANFIS model performance

### 3.2.5 Artificial Neural Network based algorithms in forecasting flood

Wu and Chau (2006) demonstrate an evaluation of Genetic Algorithm-Based Artificial Neural Network (ANN-GA) and Adaptive-Network-Based Fuzzy Inference System (ANFIS) against linear regression in forecasting flood, see Appendix A.4.2 for detailed algorithm description. A hybrid integration of ANN and GA may be able to increase solution stability and improve performance of an ANN model. ANFIS model is able to enhance the intelligence when working in uncertain, imprecise, and noisy environments and to accomplish faster convergence. It possesses the characteristics of both the neural networks, including learning abilities, optimization abilities, connectionist structures, and fuzzy control systems, including human like “if-then” rule thinking and ease of incorporating expert knowledge. In this system, the parameters defining the shape of the membership functions and the consequent parameters for each rule are determined by the back-propagation learning algorithm and the least-squares method, respectively. For ANN-GA model, a three-layer network is adopted with three input nodes and one output node with data normalised to between 0 and 1. It is found that having 3 nodes in the hidden layer is optimal. For ANFIS model, more categories yield higher accuracy, but have the disadvantages of larger rule bases and higher computation cost. The optimal number of hidden nodes is 3, obtained by trial and error. The comparison of three models on a 24h lead time shows that the absolute error is largest for the LR model and smallest with the ANFIS model, as shown in Figure 3.3. The ANFIS model gets the highest accuracy and requires less training time than ANN-GA model. However, ANFIS model requires more parameters than the other two models, as shown in Table 3. The approach of using LR model for comparison is interesting as it set a baseline for the other models. However, the ANN-GA and ANFIS algorithms are not well described and there is no mention of the number of training examples used.

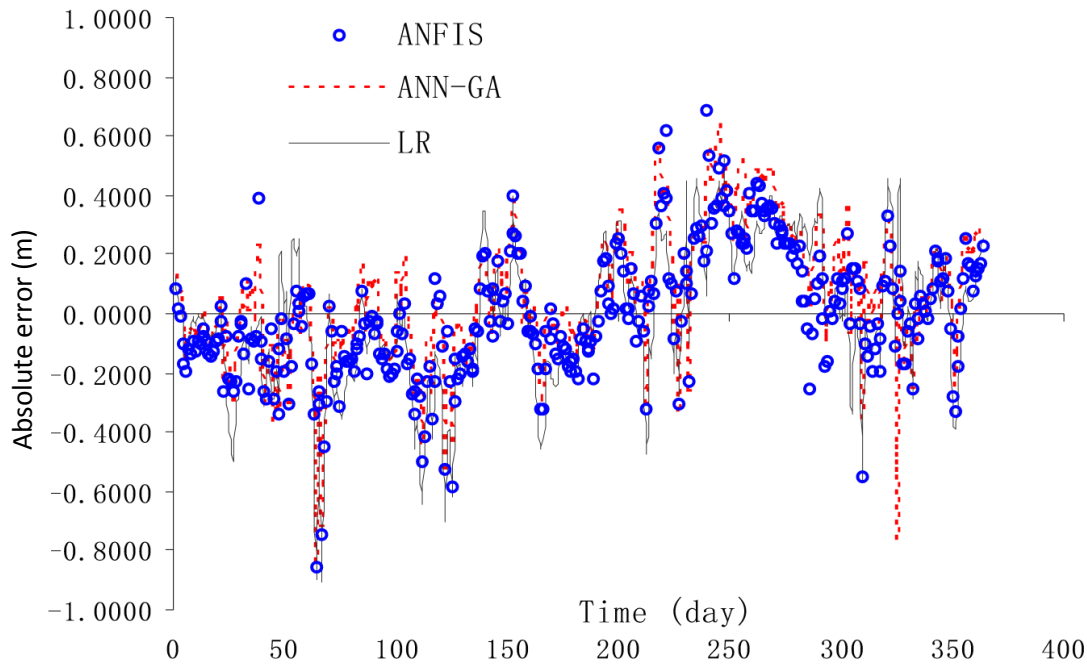


Figure 3.3: Performance comparison in terms of absolute errors for different algorithms

Models	RMSE_training (m)	RMSE_validation (m)	Training time (s)	Number of parameters
LR	0.238	0.237	Nil	4
ANN-GA	0.213	0.226	135	16
ANFIS	0.204	0.214	49	135

Table 3.1: Performance comparison for different models in flood prediction

### 3.2.6 Forecasting Rainfall based on Computational Intelligent Techniques

Abdul-Kader, et al. (2018) compared two Artificial Neural Network (ANN) training models, Partial Swarm Optimisation (PSO) and Levenberg-Marquardt (LM) Back Propagation (BP) based on Multi-Layer Perceptron (MLP) against Radial Basis Function (RBF) for rainfall forecasting. MLP is known as a supervised neural network, it requires parameters of historical data as input. MLP consist of input layer, one or several hidden layers and an output layer. Outputs with several hidden layers are more accurate but requires more time to train. BP algorithm is popularly used to train MLP. LM algorithm is used to train MLP for nonlinear problems and is more powerful than gradient descent algorithm but does not always reach a global minimum. RBF consist of three layers, the input layer, the output layer and one hidden layer. PSO is a stochastic algorithm that mimic the behaviours of animals as fish schools or flock of bird where there is always a bird that has optimistic position to the food source and others attempt to follow. In this algorithm, each particle works on finding the global minimum by changing velocity and position accordingly. The proposed technique for forecasting rainfall consists an ANN that has 4 nodes in the input layer, 20 nodes in one hidden layer and 1 node in the output layer which are trained by PSO and LM

algorithms and was compared to RBF model. Weather data of Cario City, (2009) were used to train (90%) and test (10%) the models with low temperature, high temperature, humidity and wind speed as input parameters. The three algorithms were compared using statistical method RMSE. Training and testing proved MLP-PSO to be the most efficient model with least error compared to MLP-LM and RBF, as shown in Table 3.2. However, it is worth noting that PSO complex hence requiring more computational power. This might not be the best solution for low power computation device.

Technique	Training RMSE	Testing RMSE
<b>MLP-PSO</b>	0.12	0.14
<b>MLP-LM</b>	0.15	0.18
<b>RBF</b>	0.35	0.44

Table 3.2: Comparison of three models

### 3.2.7 Flash floods forecasting without rainfall forecasts by recurrent neural networks. Case study on the Mialet basin (Southern France)

Artigue, et al. (2011) presents a recurrent neural network (RNN) model for flash flood forecasting without rainfall forecasts nor previous discharge considered. 58 events with detection threshold of 100 millimetres during 48 hours are selected from 17 years of rainfall and discharge data of Mialet basin in France. Levenberg-Marquardt algorithm is used to train and minimise the mean squared error of the multilayer perceptron model and regularisation method is used to minimize the number of parameters of the model. Two models is tested; first a linear and second a non-linear model. The first model is a standard multilayer perceptron and the second model network contain a superposition of a multilayer perceptron and of a linear model as shown in Figure 3.4, where  $w_1-w_5$ ,  $w_2-w_6$ ,  $w_3-w_7$  are rain gauges of *Mialet*, *Saint-Roman-de-Tousque* and *Barre-des-Cévennes* for linear and non-linear respectively.  $W_8$  is the average cumulative rainfall (ACR) and  $N_c$  for non-linear model as shown in Figure 3.4: MLP linear and non-linear. Four criteria are used to quantify the quality of the forecasts. Nash criteria is used to determine the coefficient predicted and the observed discharge, percentage of the peak discharge (PPD) compares the ratio of the forecast and the observed maximum peak discharges, synchronous percentage of peak discharge (SPPD) is used to compare the ratio of the estimated discharge at the instant of the maximum observed peak discharge, the time delay between the maximum of the observed peak discharge and the forecast one. Table 3. shows the criteria obtained for each prediction with the standard multilayer perceptron. Table shows the criteria obtained for each prediction with the non-linear multilayer perceptron. The results show that ANN can be used to perform flash flood prediction without rainfall forecast nor previous discharge information. The developed models are well evaluated using multiple criteria.

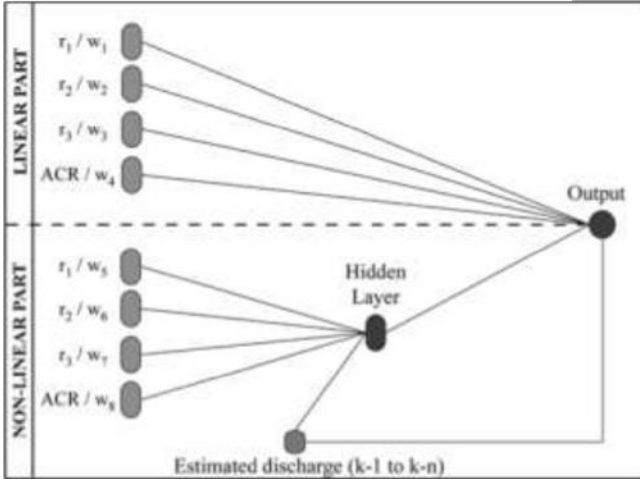


Figure 3.4: MLP linear and non-linear

Criterion	Nash	PPD	SPPD	Delay
$k+1$	0.76	67%	63%	30min
$k+2$	0.74	62%	61%	60min
$k+3$	0.73	58%	56%	30min
$k+4$	0.83	60%	59%	30min

Table 3.3: Linear performance criteria

Criterion	Nash	PPD	SPPD	Delay
$k+1$	0.92	72%	72%	0 min
$k+2$	0.93	84%	75%	60 min
$k+3$	0.91	77%	75%	90 min
$k+4$	0.92	77%	76%	30 min

Table 3.4: Non-linear performance criteria

### 3.2.8 Flash flood forecasting using Support Vector Regression: An event clustering based approach

Boukharouba, et al. (2013) presents a support vector regression machine learning approach to flash flood forecasting without rainfall forecasts, based on agglomerative hierarchical clustering of flood events. Rainfall and water level data collected from 1993 to 2008 in the watershed of Gardon d'Anduze in south-east of France contains 23 main flood events of 30 minutes sampling period data which is used for training and testing of the model. The rain gauge data and water level data were normalised to have a maximum value of 0.9 in each input vector. The six rain gauge data was reduced to a single weighted average precipitation variable by the Thiessen polygon. Support vector regression (SVR) is a kernel-based method with a built-in regularization mechanism, similar to that of support vector machine classifiers. The approach consists of clustering the events of the training database for each cluster containing events whose model have a similar behaviour. A specific SVR model is designed from each non-singleton cluster of events and a global SVR model was designed from all flood events. Cross-validation with grid search was used to find the SVR hyperparameters and the rainfall window length. The quality of the model is assessed by Nash coefficient and persistence. The specific model except for 30mm forecast yields better on test events and got better accuracy of the estimated water level peak than the global model which tends to be more linear.

### 3.2.9 Wireless Smart Sensor Networks for Real-Time Warning System of Flash Floods and Torrents in KSA

Guesmi (2017) proposed a wireless sensor networks for real-time flood monitoring and warning system. The research aims to set up an early warning system for the event of flash floods and torrents in the Kingdom of Saudi Arabia (KSA). The model analysis uses hydrological data such as water level, water velocity, precipitation combined with remote measurement images and geographic models to analyse and simulate flood events. The simulation identifies vulnerable zones and the potential of flood danger degree. The proposed WSN architecture consists of groups nodes communicating over short distances to reduce transmission power and some nodes capable of long-range communication. The model uses a hybrid model composed of centralized and distributed model to combine advantages and cancel out the disadvantages of both models.

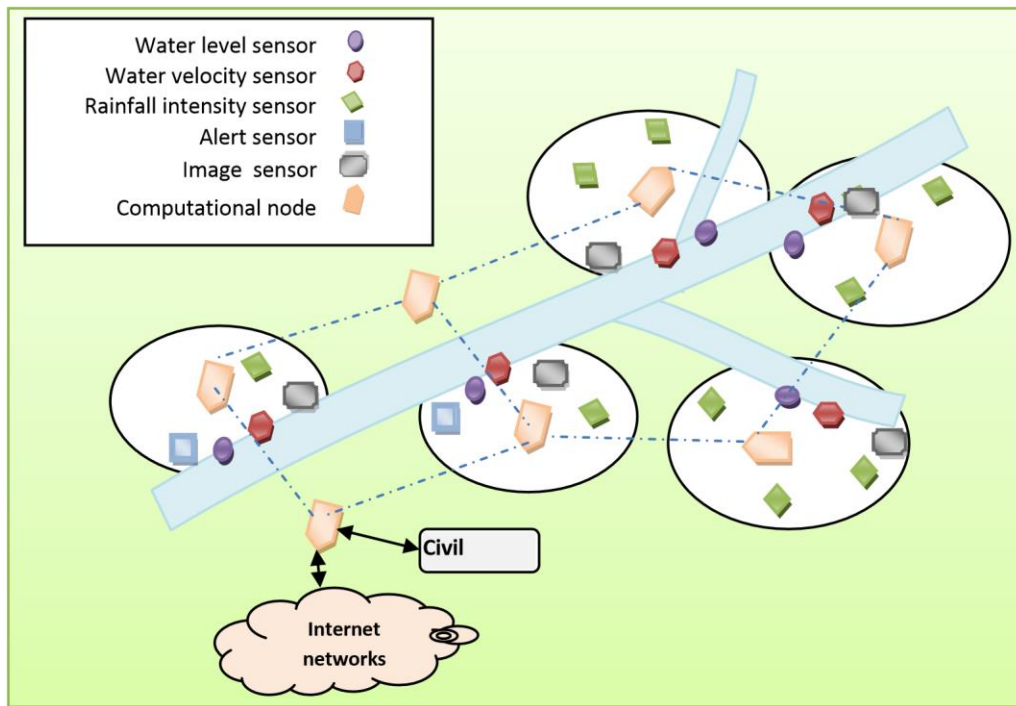


Figure 3.5: Guesmi WSN architecture

The above Figure 3.5 consists of sensor nodes and computational nodes. The sensor nodes collect data of rainfall, water level and water velocity. Computational nodes have large processing powers and implement the distributed prediction algorithm. A computational node act as a manned central monitoring office. This node verifies the results with the available online information and implements a centralized version of the prediction algorithm as a redundancy mechanism, issues alerts and initiates evacuation procedures. At each group of nodes, the sensor nodes send collected data to its computational node where the prediction take place. Then, the computational nodes send the data to the central (office) node and among themselves and can also send detect and send information of malfunctioning nodes. Results show that the model can efficiently prioritize the high risk flooded areas and provide detailed information for assessing further needs. The downside of this system is that the sensors, computation nodes, and software used are very expensive and requires special training to use these devices.

### 3.3 Comparative Analysis of Different Techniques

Table 3.5 shows different models and algorithms that were used in literature review to forecast rainfall, floods and flash floods. Basha’s model makes use of WSN to collect data from gauges and other sensors and LR is used to compute data collected and make flood prediction. While Basha’s model is more aligned to our objective to make a low cost WSN and machine learning for prediction, other more powerful machine learning and Artificial intelligence is worth investigating. ANN based algorithms showed to perform better than LR but at the cost of more computation time and more power.

	Tools 1	Tools 2	Tools 3	Tools 4	Tools 5	Tools 6
Region	Honduras	-	-	-	France	France
Technology	Sensors	-	-	-	-	-
Purpose	Flood Forecast	Flood Forecast	Precipitation Forecast	Precipitation Forecast	Flash Flood Forecasting	Flash Flood Forecasting
Model Implemented by	(Basha, et al., 2008)	(Wu & Chau, 2006)	(Chiang, et al., 2007)	(Abdul-Kader, et al., 2018)	(Boukharouba, et al., 2013)	(Artigue, et al., 2011)
Underlying ICT concept	ML, WSN	ANN	RNN	ANN	Clustering Events	RNN
Algorithm	LR	ANN-GA, ANFIS, LR	RTRL, PERSIAN-CSS	RBF, PSO, LM	SVR	LM
RMSE	0.58(Modified Correlation Coefficient)	0.226, 0.214, 0.237	0.43	0.44 ,0.14, 0.18	0.99(Nash Coefficient)	0.76(Nash Coefficient)

Table 3.5: Different tools comparison

Table 3.6 shows is a list of studies models with features, forecast lead-time (time between the issuance of a forecast and occurrence of the event), and advantages and disadvantages of the method used.

Reference (ID)	Model	Method	Forecast lead-time	Advantages & Disadvantages
4.6	Forecasting Rainfall based on Computational Intelligent Techniques (Abdul-Kader, et al., 2018)	Comparing two training algorithms, MLP-LM and MLP-PSO for Artificial Neural Network and RBF model find the most efficient model for forecasting rainfall.	2h	MLP based PSO proved to be more efficient as the algorithm does not fall in a local minimum thus getting more accuracy.

4.9	Wireless Smart Sensor Networks for Real-Time Warning System of Flash Floods and Torrents in KSA (Guesmi, 2017)	Identifies vulnerable zones and the potential of flood danger degree. The model uses a hybrid model composed of centralized and distributed model. Sensor nodes collect data of rainfall, water level and water velocity.	2h	The model can efficiently prioritize the high risk flooded areas and provide detailed information.
4.1	Combining wireless sensor networks and machine learning for flash flood nowcasting (Furquim, et al., 2014)	The ML techniques employed consist of five types of Decision Trees J48, Random Forest, Random Tree, BFTree, Simple Cart, one type of Artificial Neural Networks (Multi-Layer Perceptron – MLP) and one type of Bayesian Learning (Bays Net). Each tested with two window size (i) w=5 and (ii) w=10. The results of all the techniques were compared to find the most performant one. ML environment used: WEKA (Waikato Environment for Knowledge Analysis – free software GNU)	Nowcast	The best results were obtained with Multi-Layer Perceptron (MLP) and BFTree ML Techniques. The research uses only one parameter type. It does not demonstrate the use of two or more weather variables.
4.4	Watershed rainfall forecasting using neuro-fuzzy networks with the assimilation of multi-sensor information (Chang, et al., 2014)	Merging gauge measurements, radar, and satellite products rainfall sources for rainfall forecasting. Using BPNN for bias correction of QPESUMS and PERSIANN-CCS. GA is used to merge precipitation products of QPESUMS, PERSIANN-CCS and rain gauge sources. ANFIS is then used to forecast rainfall using the assimilated precipitation product as input.	1-2h	CC, RMSE, NRMSE, MAE was used to evaluate the performance of the model. Bias correction improved the QPESUMS model by 38% and PERSIANN-CCS by 4%. The methodology used requires rainfall gauge measurements, radar and satellite derived precipitation data.
4.7	Flash floods forecasting without rainfalls forecasts by	Flash flood forecasting without using rainfall forecast nor previous discharge as input but 17 years rainfall data and discharge data. LM algorithm was used to train	0-1.5h	Neural network is able to forecast flash flood without rainfall forecast nor previous discharge information. The model needs to be validated

	<p>recurrent neural networks. Case study on the Mialet basin (Southern France) (Artigue, et al., 2011)</p>	<p>and minimise the mean squared error of the multilayer perceptron network model. Nash coefficient, PPD, SPPD and time delay between the maximum of the peak discharge and the forecast was used to quantify the quality of the forecast. Two models were tested and compared; a linear and non-linear multilayer perceptron model</p>		<p>against another model with the same parameter.</p>
4.2	<p>Model-based monitoring for early warning flood detection (Basha, et al., 2008)</p>	<p>Statistical linear regression algorithm to predict flash flood. Inputs of past flow, air temperature and rainfall are collected with sensors in real time. Modified correlation coefficient, the false positive rate of prediction, and the false negative rate of prediction were used to evaluate the algorithm performance.</p>	1-16h	<p>The algorithm is simple and yet yields good accuracy. The algorithm uses little computation power compared hydrology models. The prediction algorithm will be distributed on the computation nodes on the WSN.</p>
4.3	<p>Merging multiple precipitation sources for flash flood (Chiang, et al., 2007)</p>	<p>The RNN model utilizes gauged rainfall and satellite-derived rainfall for flash flood forecasting. The two rainfall inputs are merged using weights in the RNN model. The contribution from satellite-based rainfall to the forecasts is limited (5%).</p>	3h	<p>An improvement of 2-14% has been observed from the merged precipitation. However, in this setup the accuracy of the forecast depends greatly on the quality of the existing gauges data.</p>
2.1	<p>A Spatially distributed flash flood forecasting model (Blöschl, et al., 2007)</p>	<p>Grid bases of 1 km square with 21 parameters for each cell. Simulates Snow processes, soil moisture and hillslope scale routing. 15 minutes temporal resolution. Observation-based extrapolation or nowcast of the interpolated precipitation field and NWP model prediction are weighted together to provide better prediction and reduce error by 20-30%. Kalman Filter function is used to update the model states</p>	48h	<p>Robust system capable of forecasting flash flood with good level of accuracy. However, the performance of the model hinges on the accuracy of the rainfall data, and biases in rainfall may translate into biases in soil moisture and hence diminished forecast accuracies.</p>

		variables based on observed runoff.		
2.2	ALERT BoM Australia	Input data are fed into a hydrological model to assess the magnitude and timing of a flood event. Sometimes the likely severity of flooding is assessed using simple manual guides look-up tables	Nowcast	The system can send warning to officials via telephone. More advance and robust system is now available.
4.5	Evaluation of Several Algorithms in Forecasting Flood (Wu & Chau, 2006)	Two hybrid models (ANN-GA and ANFIS) were evaluated against Linear Regression. ANFIS yields better results but requires more parameters	24h	Both ANN-GA and ANFIS models got better accuracy than LR model but at the cost of higher computing power.
2.3	Development of a European flood forecasting system (De Roo, et al., 2003)	The system uses MRWFEPS forecast weather variables for each cell of 40-80 km horizontal resolution every 6h for up to 10 days lead time. DMI-HIRLAM model and DWD-LM model are used to increase forecast spatial and temporal resolution of MRWFEPS. The LISFLOOD's models simulates river flow and flooding at hourly time steps and 1 km square grid resolution and model the overbank flows and inundation areas.	72h	The EFFS system got acceptable level of accuracy. The model could forecast at 5 days ahead but failed to capture the main body of the flood.

Table 3.6: Flood forecasting/nowcasting models summary

### 3.4 Chapter Summary

Flood and rainfall prediction techniques have been investigated. We notice that in the work of Furquim that the best results were obtained with MLP and BFTree ML techniques for flood nowcasting at an accuracy of 66% over 3 minutes nowcast. Basha created a WSN and a linear regression prediction algorithm. The WSN is low-cost and able to withstand extreme weather conditions. The model outperforms a calibrated DMIP model by 3% with an autocorrelation of 1 at 1 hour forecast and decreases to 0.0627 at 24 hours. Chiang and Chang have proposed an ANN model to merge and evaluate the effectiveness of satellite and radar derived precipitation forecast and gauged data. The proposed models have shown better results than satellite and radar precipitation products alone with 2-14% RMSE

improvement for Chiang model and 19-25% improvement for Chang model for a lead time of 1 to 3 hours. C.L. Wu and K.W. Chau evaluated the ANN-GA and ANFIS against LR for flood forecasting at a lead time of 24 hours. They conclude that ANFIS model gets the highest accuracy and requires less training time than ANN-GA but with more parameters than the other two models. Artigue presented an RNN model, where it was noticed that ANN can be used to perform flash flood prediction without rainfall forecast nor previous discharge considered. Boukharouba presented an SVR ML model for flash flood forecasting without rainfall forecast. Two models were created and evaluated by Nash coefficient and persistence. Abdul-Kader compared several A.I training techniques, training. It was noticed that MLP-PSO is the most efficient model with least error compared to MLP-LM and RBF. Guesmi proposed a WSN hybrid architecture composed of both centralized and distributed model for combined advantages. Hardware and software used are expensive and not readily available in Mauritius.

From the literature review it is noted that there are many techniques to forecast flash floods but little has been done on flash flood nowcasting. As flash floods are unexpected weather phenomenon that occurs in a short amount of time and is region specific in Mauritius, it is important to be able to use real-time data in flash flood risk regions and produce a prediction (nowcast) for a few hours ahead of time. Further investigation is needed to find the best approach to effectively nowcast flash floods in Mauritius. Due to the nature of environment and weather conditions, and the limited availability of meteorological data for Mauritius, WSN can be considered to capture real-time data of rivers and weather variables at a low cost. The results of all the Machine Learning techniques reviewed are not directly applicable to the Mauritian contexts the input parameters can differ. As such, there is a need to further identify the different parameters which can be considered for a Machine Learning Algorithm.

## Chapter 4 – A Review of Environmental Parameters for Flash Flood Nowcasting

### 4.1 Variables Behind Flash Flood Nowcasting

To be able to effectively nowcast flash floods, it is very important to gather and use appropriate weather variables specific to Mauritius. The table below identifies and maps several parameters and variables involved in flood prediction used by the models and frameworks from Chapter 3. The relevance of the parameters used by each model is investigated and critical analysed.

Model	Rainfall	Water Level	Water Flow	Temperature	Soil Moisture	Land Topology	Humidity	Wind Speed	Satellite	Radar
A Spatially distributed flash flood forecasting model (Blöschl, et al., 2007)	✓			✓	✓	✓				
ALERT BoM Australia	✓	✓								
Development of a European flood forecasting system (De Roo, et al., 2003)	✓		✓		✓	✓				
Combining wireless sensor networks and machine learning for flash flood nowcasting		✓								

(Furquim, et al., 2014)										
Model-based monitoring for early warning flood detection (Basha, et al., 2008)	✓	✓		✓	✓					
Merging multiple precipitation sources for flash flood (Chiang, et al., 2007)	✓					✓			✓	✓
Wireless Smart Sensor Networks for Real-Time Warning System of Flash Floods and Torrents in KSA (Guesmi, 2017)	✓	✓	✓	✓						
Evaluation of Several Algorithms in Forecasting Flood (Wu & Chau, 2006)	✓	✓								

Watershed rainfall forecasting using neuro-fuzzy networks with the assimilation of multi-sensor information (Chang, et al., 2014)	✓		✓						✓	✓
Forecasting Rainfall based on Computational Intelligent Techniques (Abdul-Kader, et al., 2018)				Low & High temperature			✓	✓		
Flash floods forecasting without rainfalls forecasts by recurrent neural networks. Case study on the Mialet basin (Southern France) (Artigue, et al., 2011)	✓		✓							
Flash flood forecasting using Support Vector	✓	✓								

Regression: An event clustering based approach (Boukharouba, et al., 2013)										
---	--	--	--	--	--	--	--	--	--	--

Table 4.1: Parameters unit of measure and techniques

## 4.2 Parameters involved in Flash Flood Forecasting/Nowcasting

### Rainfall

Rainfall driven floods occur when the soil is no longer able to absorb water (Basha, et al., 2008) and the magnitude of the rainfall affect dramatically the water runoff because of the saturated soil moisture (Blöschl, et al., 2007). The quality of any flood forecast/nowcast depends heavily on the quality of the rainfall input. An efficient wide rain gauge network in the entire flood prone region properly calibrated is necessary. Nevertheless, rainfall data alone is not enough to provide proper flood forecast (Yang & Su, 2015).

### River/Canal water level

Rainfall and water level are correlated. River water level can be predicted by determining the rainfall surface runoff and soil ability to absorb water. Water level data can give an indication for potential risk of river or canal overflow, by calculating in real-time the rate in rise of water level together with rainfall data.

### River/Canal water flow

The velocity or flow rate of water is important to determine the severity of a flash flood event. Water flow is dependent on land topology and land slopes (Guesmi, 2017). A high-water velocity can overflow a river or canal in a relatively small period of time and the result can be devastating to the surrounding locality. Water flow is highly correlated with land slope and rainfall intensity.

### Air temperature

Air temperature is related to seasonal weather conditions, tornados or blizzard for high and low temperatures, respectively (Basha, et al., 2008). In Mauritius, floods and flash floods mainly occur during the summer season. Air temperature data can be used as an indication of the season, as well as to assess the rate of evaporation, among others and combined in the prediction algorithm.

### Soil moisture

Soil moisture is highly correlated with rainfall and water level. A prolonged episode of rainfall renders the soil saturated and unable to absorb water which causes water accumulation and rainfall runoff causing drains and rivers to overflow rapidly resulting in flash floods. Soil moisture can be used estimate river level.

### Land topology

Land topology or land slope can be used to determine the flow direction of surface runoff water and to determine water velocity in a river or water canal (Blöschl, et al., 2007).

### Satellite and Radar

Satellite and radar are powerful tools when it comes to rainfall forecasting they provide information on the formation of clouds and their direction. Chiang and Chang (2007; 2014) used satellite and radar derived rainfall sources combined with rain gauges for flash flood forecasting. Wind drift can also be used in precipitation estimation by meteorological radar.

### 4.3 Measuring the Flash Flood Nowcasting Parameters

While flash floods depend heavily on rainfall quantity and intensity, other correlated parameters such as river water level, water flow, temperature, soil moisture, satellite, radar and land topology can be used by a model to forecast/nowcast flash floods with greater accuracy.

A sensor-based flood forecasting/nowcasting model is much simpler than hydrology model which requires expensive tools, equipment and trained hydrology personal to operate and interpret data. Machine learning and artificial intelligence models can be used to interpret sensed data and provide accurate nowcast.

Parameters	Unit of Measure	Measuring Apparatus	Sensor	Technique
Rainfall	Millimetre (1mm = 1L/m <sup>2</sup> )	Rain gauge	Reed switch	Water is funnelled into a bucket. When the correct amount of water is present, a swing activates a reed switch. Each swing is registered as one count.
Water level	Centimetres or metre	Vertical pipe with scale	Air pressure sensor	A hose is connected to the pressure sensor and the other end runs in the river. As water level rises air pressure in the hose rises. Air pressure is recorded and converted into centimetres.
Water flow	Litres/sec or Cubic metres/sec	Bucket method, Float method, weirs	Pygmy meter	A wheel is rotated by water flow and the rate of the rotation signifies the water velocity.
Air temperature	Degrees Celsius	Thermometer	DHT22	Digital temperature and air humidity sensor.
Soil moisture	Percentage	Soil moisture meter		Can be measured by electric conductivity

<b>Land topology</b>	Percentage or angle	Inclinometer	Accelerometer or gyroscope	Accelerometer: Tilt can be measured by this equation $\theta = \sin^{-1}$ (Measured Acceleration / Gravity Acceleration). Gyroscope is used to measure the angular velocity.
<b>Satellite and Radar</b>	Imagery	Satellite and Radar		Computational  Satellite: Photos taken by satellite  Radar: Sending radio pulses and listening for return signals to detect clouds.

Table 4.2: Parameters unit of measure and techniques

#### 4.4 Parameters Specific to Mauritius

Satellite based or radar-based forecasting may not be feasible using a low-cost approach. Also, high resolution and real time images are necessary for flood nowcasting. Water flow and flash floods depends heavily on rainfall intensity and duration. Rainfall parameters alone cannot be used for prediction as water flow is required. The MMS provides rainfall data collected from different stations for every 3 hours. A more elaborated set of weather parameters, i.e. (Rainfall-Temperature (Min,Max), Temperature(dry bulb, wet bulb, dew point), relative humidity, wind speed, sunshine radiation, evaporation, atmospheric pressure, vapour pressure), are available from only two stations, Vacoas and Plaisance station. The price for one parameter is Rs1500 per month or Rs18000 per year. Using data available from MMS makes it quite complex to determine possible events of flash floods, especially that region specific data is coarse grained. Other sources of data have been identified and presented in Table 4.3. Some of the sources uses data from MMS.

Link	Description	Parameters	Price
<a href="#">Mauritius Meteorological Services</a>	50 years of climate data distributed spatially over the island stations.	Rainfall-Temperature (Min,Max), Temperature(dry bulb, wet bulb, due point), relative humidity, wind speed, sunshine radiation, evaporation, atmospheric pressure, vapour pressure	Rs1500/M per parameter Or Rs18000/Y per parameter
<a href="#">meteoblue.com</a>	30 years hourly weather data for Mauritius.  Available in CVS format.	Temperature, Relative humidity, Precipitation amount, Wind speed and direction	Last 2 week free.  \$115, 30+ years of historical data
<a href="#">World Meteorological Organization</a>	6 days MMS daily forecast for Vacoas, Port-Louis, Plaisance.  Available in JSON format.	Weather (e.g. Partly cloudy, isolated Showers, etc), Minimum temperature, Maximum temperature.	Free
<a href="#">wunderground.com</a>	Hourly & daily data for 4 stations.  Historical data view only.	Temperature (mean, max, min), dew point, humidity (avg, max, min), precipitation, sea level pressure, max wind & gust speed, visibility	n/a
<a href="#">World Weather Online</a>	Hourly data.  Historical data in xml format.  All data are forecast only (not actual)	Temperature (mean, max, min), dew point, humidity (avg, max, min), precipitation, sea level pressure, max wind & gust speed, visibility	Trial 500 calls free.  \$105 monthly 500 calls per day.

Table 4.3: Parameters Available in Mauritius

Water level from rivers are monitored by another institution, The Water Resources Unit (WRU). It has been established in May 1993 and is responsible for the assessment, development, management and conservation of water resources in the Republic of Mauritius. The WRU collects monthly water flow data for several rivers across the island. From the list data available from WRU, it has been noted water flow is available in readable format for very few rivers and only for a period year from 2006 to 2010.

## 4.5 Comparative Analysis of Neural Network based Machine Learning Techniques

### 4.5.1 Introduction

As per our literature review, various ML techniques have been used in different contexts. Given the case of Mauritius, we first investigate different Neural Network techniques through experimentation. The main aim is to define which techniques are more appropriate as well as the attributes of the data required for effective nowcasting.

#### **Artificial Neural Network (ANN)**

ANNs are machine learning algorithms developed to teach computers to recognize patterns and think like humans. An ANN emulates the human brain consisting of an input layer, hidden layers and an output layer. Each layer consists of nodes (neurons) connected by weighted edges (synapses).

Feed-forward propagation is the process by which data are fed in from input to output. Back propagation is the learning process by which the output error of the network is propagated backwards through the network and weights are adjusted.

#### **Deep Neural Network (DNN)**

While a simple ANN have 2-3 layers, a DNN or MLP can have several hidden layers use to compute more complex solutions.

#### **Dropout**

A common problem that occurs in neural network training is overfitting (Ashiquzzaman, et al., 2018). This happens when the network learns to fit too closely the data points and pick up noise in the training data. As a result, performance is negatively impacted as the model has not generalized enough to fit new data.

One way prevent overfitting is adding dropout in the network architecture. Dropout refers to ignoring a percentage of nodes (neurons) at random in one or many layers. Dropped nodes is not considered during a forward and backward pass. By doing so nodes are hindered from co-adapting too well and all nodes are given the chance to learn equally. This in turn reduces the possibility of overfitting (Ashiquzzaman, et al., 2018).

#### **Kernel Regularization**

Another way to reduce overfitting is to implement a kernel regularization technique by reducing the weights complexity. It implies filtering out the weight of false or fake features. Thus, there is an increase in accuracy mainly based on the extraction of the appropriate (good) features.

#### **Early Stopping**

It is used to avoid overfitting. Early stopping provides guidance as to how many iterations can be run before the model begins to over-fit.

### **Recurrent Neural Network (RNN)**

RNNs are mostly used for time series dataset where the previous, actual and future data inputs are related to each other. RNN can do better predictions by taking previous inputs sequences into account. RNN does this by persisting the previous information in the network with a loop.

Long-Short Term Memory (LSTM) network is an extension for RNN which enables RNN to recall previous inputs over a long period of time.

### **Genetic Algorithm (GA)**

GAs are used to optimize any type of ANN to produce the best results out of them. They are inspired by the natural selection process where the fittest individuals are selected for reproduction in order to produce offspring of the next generation. The network parameters for the offspring are inherited from the fittest parent network in the previous generation.

#### 4.5.2 Experiments

To assess the effectiveness of using WSN to capture real-time data for flash flood nowcasting. MMS rainfall data and WRU water flow data for the period of year 2006-2010 are used to generate synthetic rainfall and water flow data to simulate an operational WSN. AS per the NDRRMC identified Riviere du Poste to have flooded during the 2013 episode. Therefore, data for the same river has been combined with data from the MMS, and water flow peaks from year 2006 to 2010 have been extracted. A 389 days' worth of water flow data has been constructed. In order to use the water flow data in machine learning regression, we need to pre-process the daily data in to 3-hourly data to match MMS rainfall data intervals.

Two experiments has to be carried out, based on regression and classification. The following steps for the first experiment are as follows: 1. To assess MMS data necessity, synthetic rainfall data based on the water flow levels are created and evaluated. 2. To simulate a WSN setup to increase predictions accuracy. Rainfall and water flow data are created that simulates the river level upstream. 3. Arrange the upstream data by moving the records 3 hour earlier to the original water flow. The figure below shows how the WSN data collection is simulated. Upstream collected data together with downstream data should be able to predict next 3-hours downstream data. Figure below shows sensors upstream and downstream at flooded area.

The second experiment consists of: 1. arranging the pre-processed 3-hourly water flow data in sequential. 2. Labelling the data form 0 High decrease to 4 High increase for classification in the same format as Gfurquim approach.

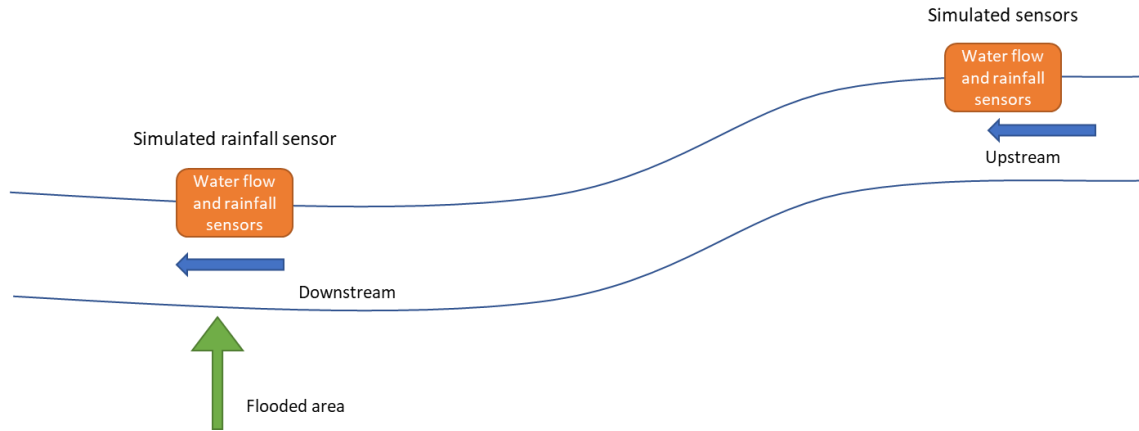


Figure 4.1: Sensors Placed Upstream and Downstream

### 4.5.3 Experimental Setup

We developed and test our models using various Python packages, see appendix A for installation procedures. The table below shows the three main Python packages.

Package/ Description	Use
Scikit-Learn/ Free ML library, data mining and analysis tools for Python.	Read and split dataset for training and testing, Scale values, Design and run ML algorithms, Calculate accuracy.
TensorFlow/ Open source ML framework such as neural network. Can use GPU computational power for faster computations.	Design AI models, Train and run AI models, Calculate accuracy.
Keras/ High-level neural network API, written in python running on top of TensorFlow.	Allows for easy and fast prototyping, Run on CPU and GPU.

Table 4.4: Python Packages Used

We ran our experiments on the machine listed in Table 4..

Type	Laptop
CPU	Intel Core i7-7700HQ @ 3.80 GHz with 4 cores and 4 threads
GPU/ MEM	NVIDIA GTX 1050, 768 CUDA cores @ 1645 MHz/ 4GB GDDR5
RAM	8GB DDR4
Storage	SSD

Table 4.5: Experiments Hardware Configuration

#### 4.5.4 Data Preparation

##### Initial data

Data from WRU: Riviere du Poste

Data period daily water flow (Total records: 389):

Feb-Apr 2006 (89 days)

Jan-Mar 2007 (90 days)

Feb-May 2008 (120 days)

Jan-Mar 2010 (90 days)

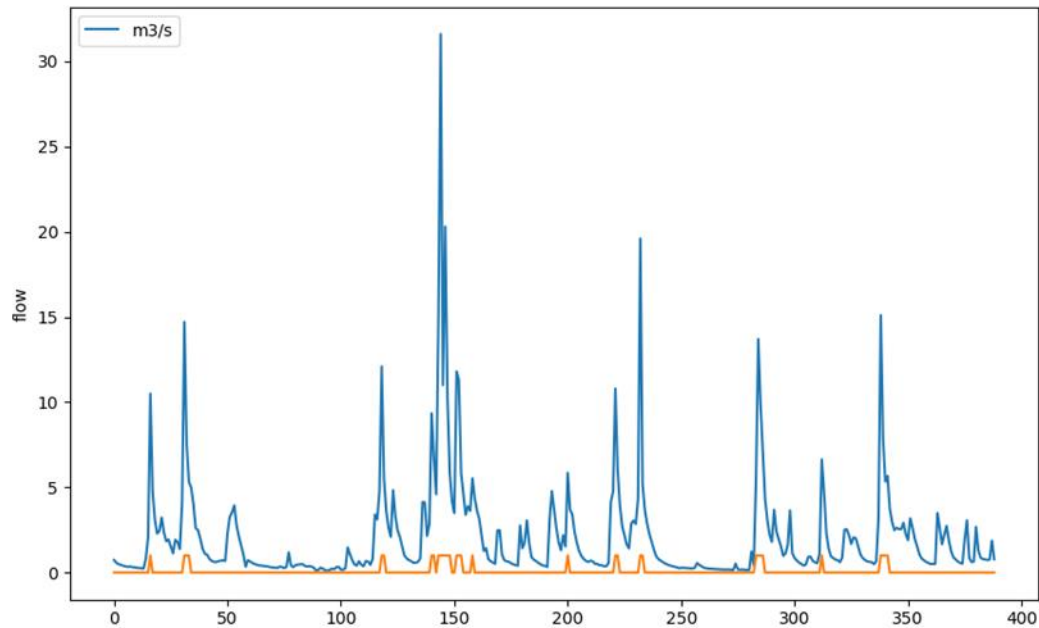


Figure 4.2: WRU Water Flow Data:

##### Convert to 3-hourly data

Data is converted from daily to 3-hourly by splitting each record into 8 and adding 0-15% to the number at random.

Calculation:  $\text{Next} - \text{previous} / \text{by } 8 + \text{a random percentage of } 0\text{-}15\%$  to the number to make it less-linear.

Total records: 2717 (or hours of data)

#### 4.5.5 Experiment 1 – Regression

##### Create a synthetic rainfall dataset

The 3-hourly flow data us converted to rainfall data.

Calculation:  $\text{Dataset flow peak} / 200\text{mm} * \text{flow} = \text{rain}$ . Rain + random -15% to 15%.

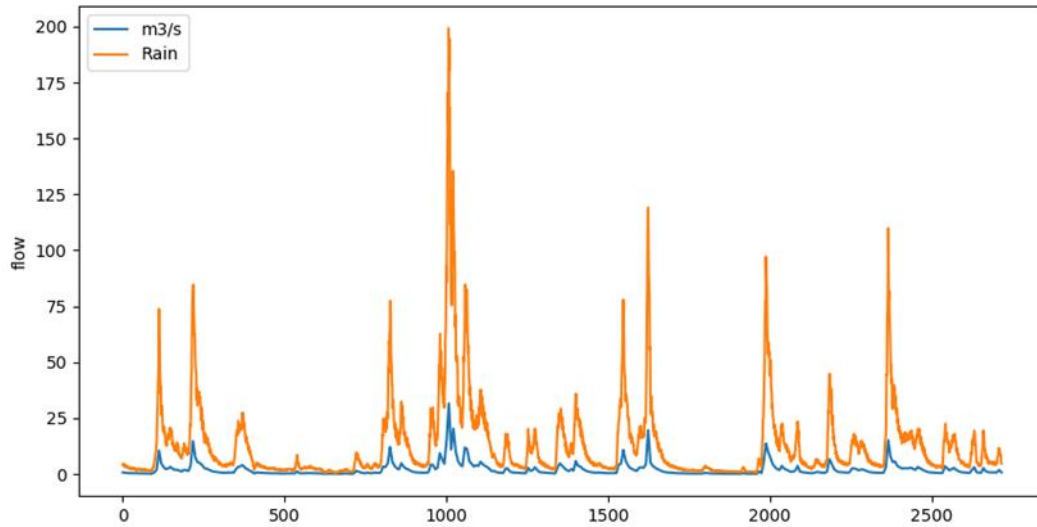


Figure 4.3: Water Flow and Rainfall Data

### Create synthetic flow and rainfall dataset

Create an additional flow and rainfall dataset to simulate flow and rainfall at another point of the river upstream.

Calculation: Divide all rainfall and flow by 2 and add -20 to 20% of the number to them randomly.

Add lag by moving all new records 3 steps up.

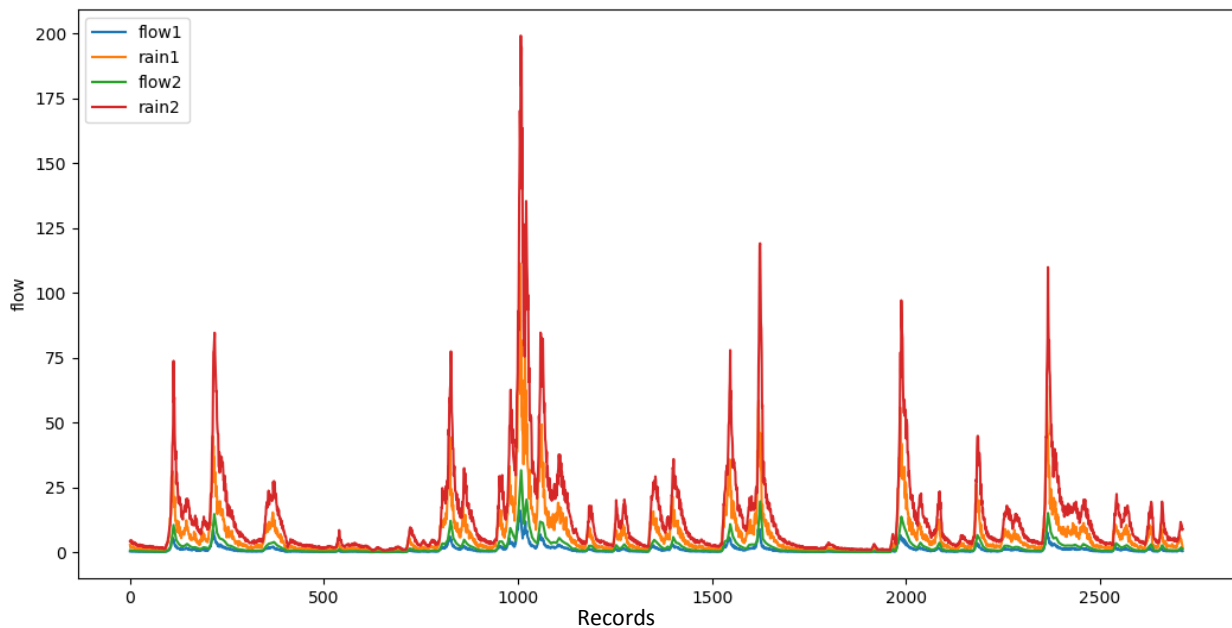


Figure 4.4: Synthetic data

### 4.5.6 Result

ANN RMSE: 0.137

RNN RMSE: 0.146

#### 4.5.7 Experiment 2 – Classification

Using the same 3-hourly flow data as above.

The data is then formatted in Gfurquim dataset format.

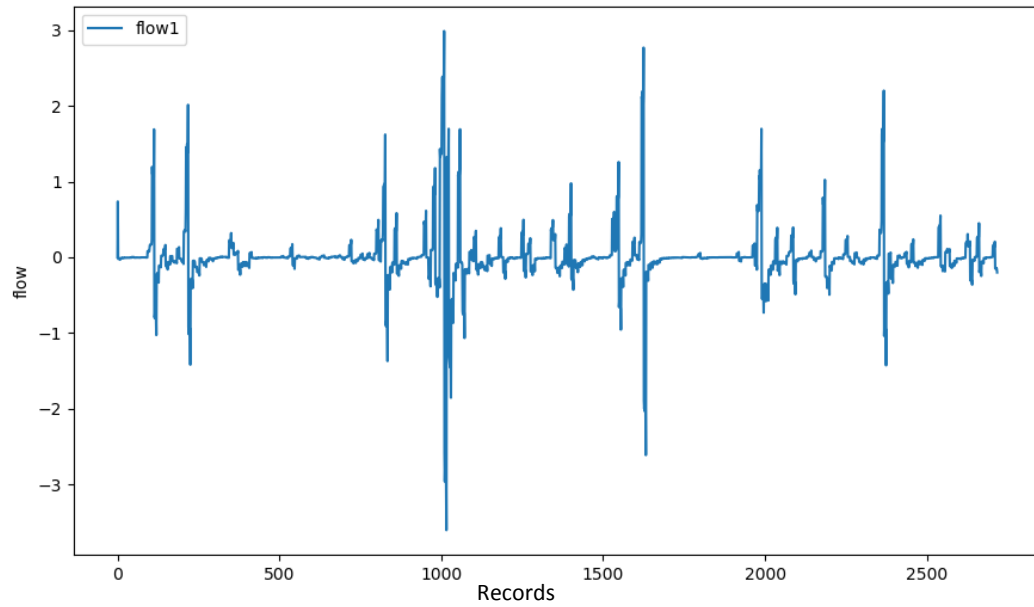


Figure 4.5: Water Flow Data in Gfurquim format

The data is then converted to a sequence of flow data:

flow < -2 = class 0 (High decrease)

flow < -0.5 = class 1 (Low decrease)

flow > -0.5 and flow < 0.5 = class 2 (stable)

flow > 0.5 = class 3 (Low increase)

flow >= 2 = class 4 (High increase)

#### Results

```
Duration (seconds): 47.945
Accuracy on train set (%): 82.13
Accuracy on test set (%): 84.68
Recall (%): [86. 29. 99. 46. 87.]
Precision (%): [100. 83. 84. 79. 96.]
F1 (%): [92. 42. 91. 58. 91.]
```

Figure 4.6: Results Gfurquim format

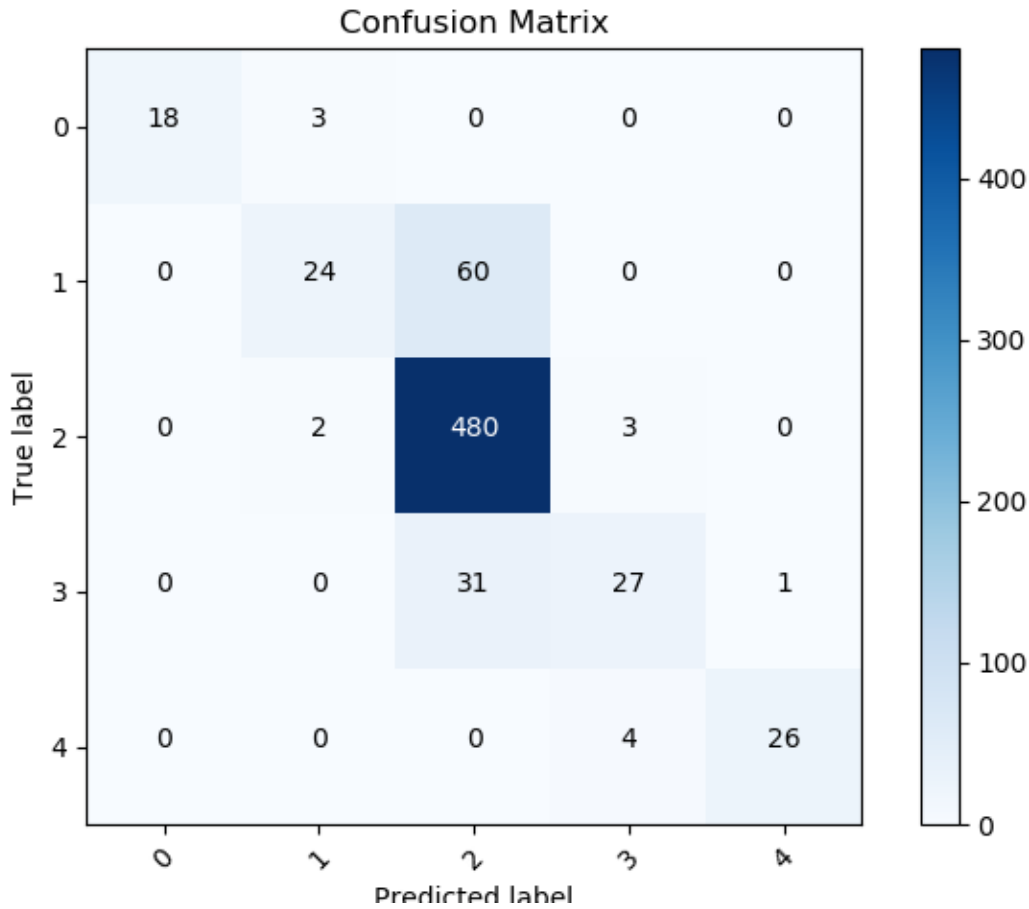


Figure 4.7: Results Confusion Matrix

#### 4.6 Chapter Summary

This chapter firstly provides an overview of existing forecasting methods and techniques as well as their parameters. They have been discussed in the Mauritian context and it is to be noted that none of the techniques have been applied in the same conditions. Most of the parameters used the techniques are considered as environmental variables that are essential for flood prediction. Also, combining parameters converge to more accurate predictions. Secondly, in an attempt to better understand the application of each model, a series of preliminary experiments have been conducted so as to understand their differences and assess their current applicability. It has not yet been decided which Machine Learning algorithm and or technique is most suitable, but two of them have been earmarked, the Artificial Neural Network and the Recurrent Neural Network. Further investigations in the form of experiments are required, and will be considered and described in the evaluation section (chapter 7).

## Chapter 5 - Design of a Low-Cost Flash Flood Nowcasting Solution

### 5.1 Proposed Solution

In order to nowcast flash-flood in Mauritius, a solution based on two main components is being proposed. The first component is the prediction engine based on Recurrent Neural Network (RNN) ML technique and the second component is Wireless Sensor Networks (WSN) which makes use of sensors to monitor rivers for water level and rainfall as shown in Figure 5.1. The squared orange rectangles 1,2,3 are groups of sensors that take measurements of water level and rainfall. As sensors are located in or near rivers, the risk of getting damaged is high. Therefore, each group consists of three sets of water level and rainfall sensors for redundancy purposes. When a sensor is offline or sends fake data to the base station, the system switches to another sensor. The local nodes station represented in yellow triangles are equipped with both short-range and long-range communication modules. The sensor nodes send data (water flow and rainfall) via the short distance module to its corresponding local nodes. The data is then relayed to the base station (green circle) via long distance module. The base station is a computer with enough computing power for data manipulation and needs an internet connection. It analyses data from sensors and detects if the sensors are working correctly, prepare error logs, and prepare and compress collected data. All data are then sent to a web server where the prediction and user intervention takes place. The proposed WSN solution is reliable in terms of redundancy as if a sensor node fails the system can continue to function. Noise can also be filtered out from the collected data. Collecting data from the river upstream proved to increase the prediction accuracy and the sum of node 1 and 2 can be used as node 3 data labels during training. The downside of this system is that it is costlier and complex in terms of infrastructures and prediction.

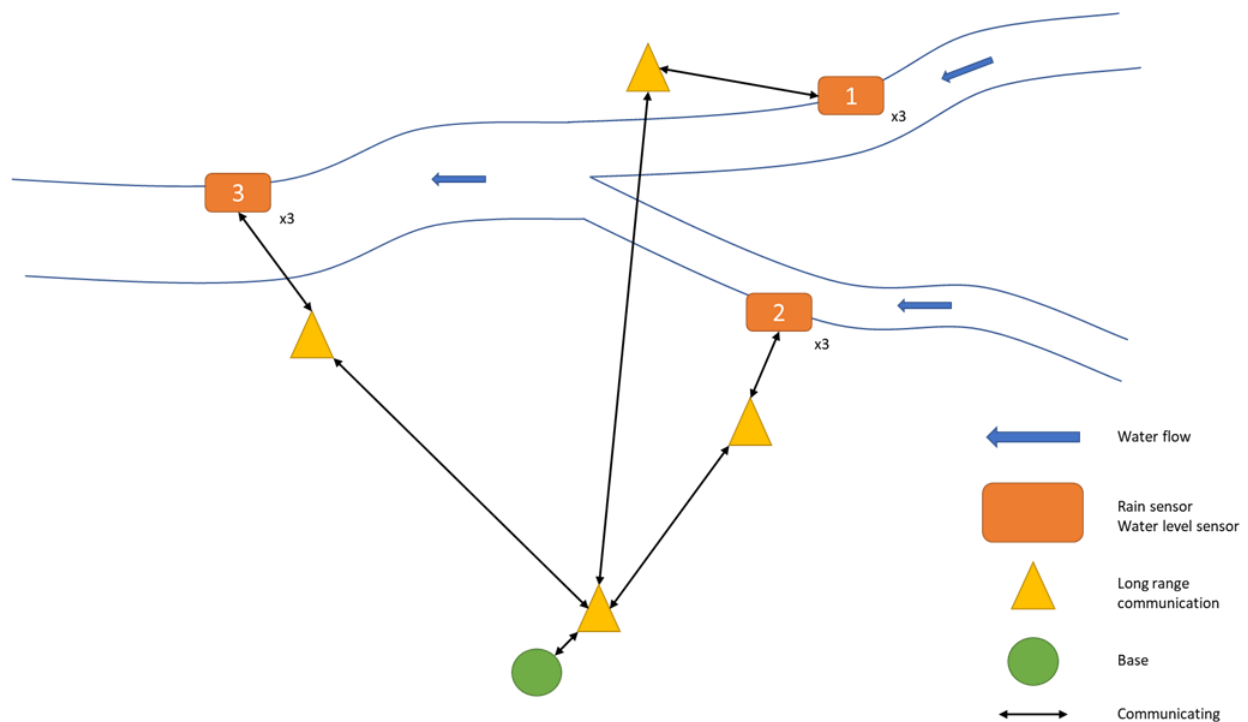


Figure 5.1: WSN Setup

## 5.2 Architecture of the Proposed Solution

This section describes in detail how the system is designed and how each component of the system works and interacts with each other. The system's logical architecture and hardware architecture are presented.

### 5.2.1 System Architecture

The system architecture consists of 3 major parts: WSN System, Software/Machine Learning and User interface. These parts are described as follows:

- WSN
  - The WSN is entirely located on a river site. It consists of the WSN system which collects river data continuously and send it to a server through an internet connection on a fix interval or on user demand.
- Software/ Machine Learning Engine
  - It consists of a server that collects data from the WSN, performs computations and makes predictions. It also contains a set of functions that can be called by the User Interface to interact with the WSN system.
- User Interface
  - The platform by which the user communicates with the system. The web application is the admin interface only where the user has full access to the system to view predictions, raw data, make predictions and is able to manage the power state of sensors. The mobile application is designed for a normal user, where the user can view the river data and predictions for the upcoming hours.

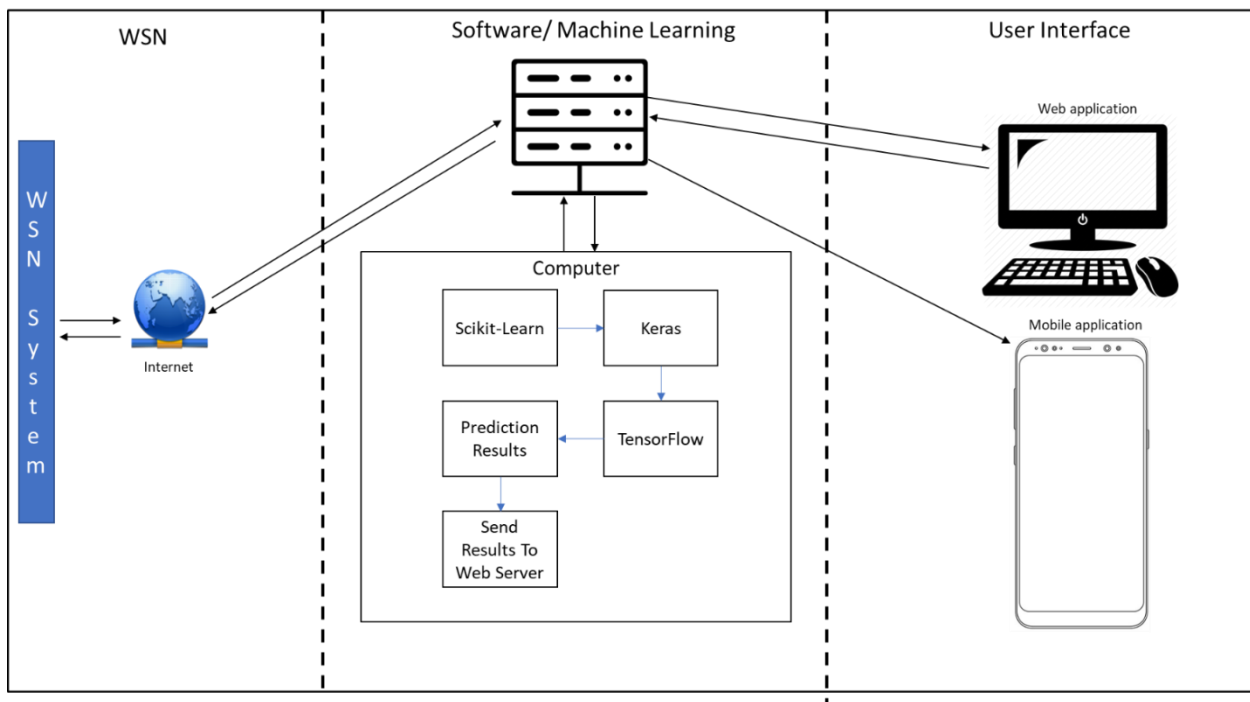


Figure 5.2: System Architecture

### 5.2.2 Logical Architecture for WSN

The Local Nodes Station and the Sensor Nodes have the same micro-controller, an Arduino Uno (Nano, Uno, Or Mega). The Sensor Nodes sense and collect data from weather sensors and power unit status. The collected data is then sent to its corresponding Local Nodes Station where the data is then relayed to a central Base Station. The Base Station is a micro-processor, a Raspberry PI3, capable of handling high workloads is used analyse and sort collected from all Local Nodes Stations and Sensor Nodes. The Base Station looks for faults or anomalies in the collected data and the data is cleansed before uploading it to the Web Server by the GSM Module. A report of faults is also uploaded to the web server where a decision about nodes management can be taken. Figure 5.3 and Figure 5.4 below gives an overview of the WSN system.

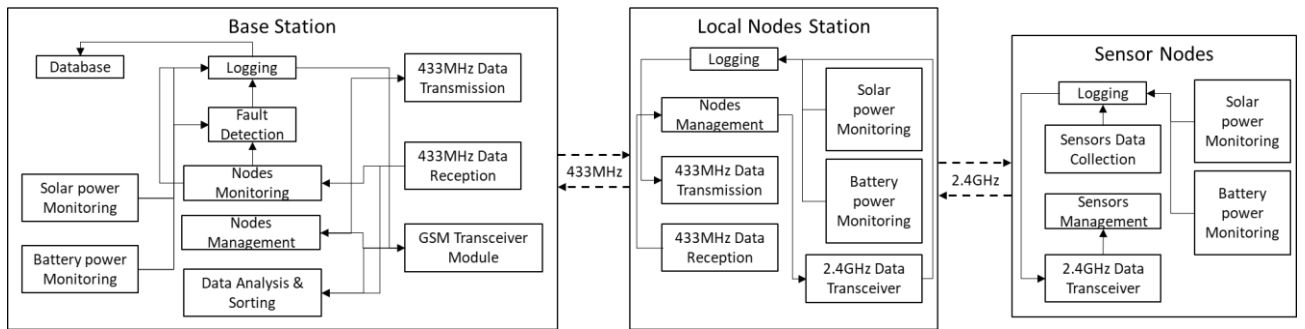


Figure 5.3: WSN Logical Architecture

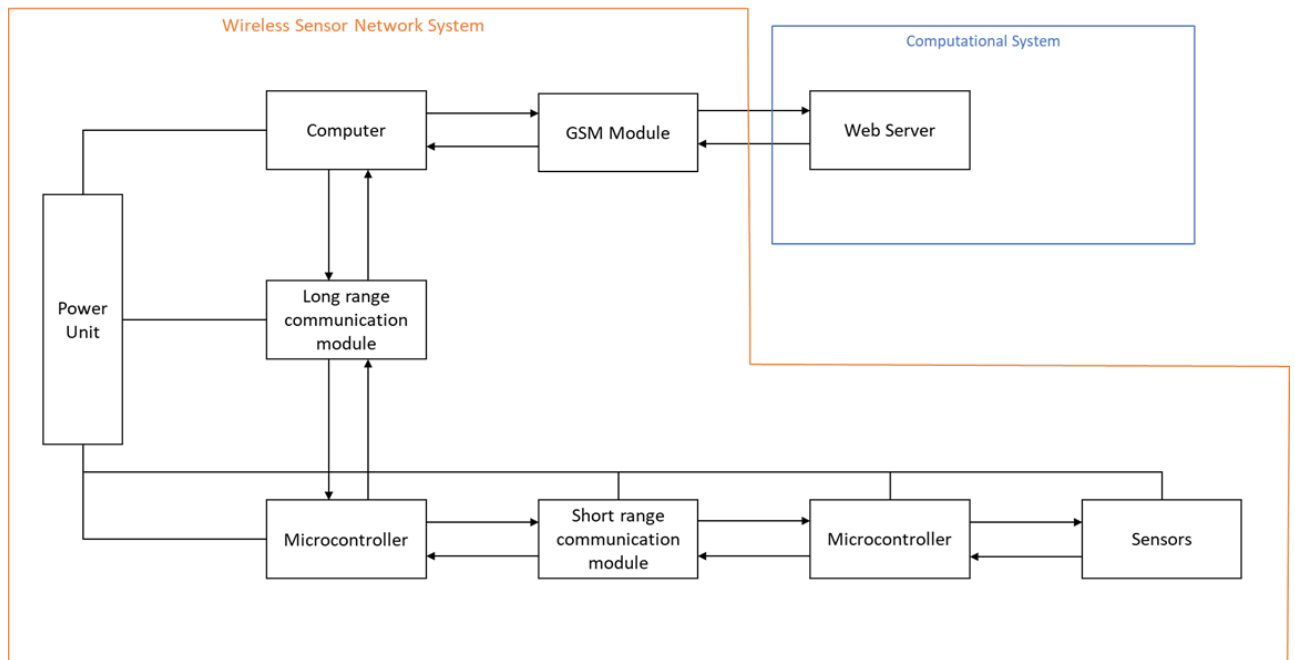


Figure 5.4: WSN Architecture

### 5.3 Proposed Flash Flood Nowcasting Approach

In this section, a comprehensive description of the proposed approach through which flash flood is nowcast. In section 4.5, ML experiments showed that better predictions are obtained when using collected water flow and rainfall data from two points in the river; the flooded area and the river upstream. The WSN should be able to withstand extreme weather conditions, using redundant sensors to ensure continuous data collection when primary sensors are down and able to monitor and manage sensors and power efficiently, and send collected data, error logs, and sensors data logs to the web server for processing. The web server processes all data and makes predictions where the administrators and users can access the results and manage system components. After the collected data are processed, the data are fed in the regression algorithm. RNN is used to make predictions to obtain water flow level in the next hour. The use of Genetic Algorithm (GA) to optimise RNN configuration parameters will be further considered for improving the prediction accuracy of the model.

### 5.4 Requirement Specification

In this section, functional and non-functional requirements of the proposed system are defined. Functional requirements are the main tasks that the system should be able to perform and functions that are provided to the user. Non-functional requirements are constraints on the functions provided by the systems in terms of security, reliability, performance and usability.

#### 5.4.1 Functional Requirement

**ID:** *The identification number of the functional requirements*

**Description:** *The functional requirement.*

**Explanation:** *An explanation of the requirement, and its purpose whenever needed.*

The functional requirements of the application are outlined in Table

ID	DESCRIPTION	EXPLANATION
F1	Users must be able to view real-time data	Normal users should be able to view processed real time data. Admin users should be able to view both raw and processed real-time data (data that are being collected) from each node and station.
F2	Users must be able to view flash flood-related predictions	Normal users (mobile version) should be able to view predictions for the next 3, 6, 9 hours real time. Admin users should be able to view predictions with previous predictions trends.
F3	Admin users must be able to download the latest raw collected data	As the WSN system transmits only processed data by default, there should be an option where the user can download the raw dataset
F4	Automated predictions	After each 5 minutes the system uses the collected data and make predictions for the following 3, 6, 9 hours
F5	Manual predictions	Admin users with a click of a button should be able to make predictions instantaneously

F6	The system must monitor sensors and log sensors activities	The system should be able to monitor all sensors activities including data transmission and power state
F7	The system must be able to detect errors in sensing nodes	The system has to collect data from sensors and redundant sensors and analyse the data to detect anomalies in the collected data
F8	The system must provide WSN components status	Admin users should be able to see connected sensors status; online, warning, offline. More details of the sensor's status can be found in the Local Nodes Station log file
F9	Power monitoring	The system should be able to calculate power usage, battery remaining current capacity and solar time. The system should also provide notification to the admin if a station is about to go offline in case of insufficient solar charging rate.
F10	Sensing nodes power control	Admin should be able to turn off redundant sensors in case of low battery alert to preserve power and damaged sensors
F11	The web and mobile version should have a search bar	The search bar will be used to search for river monitoring and predictions information.

Table 5.1: Functional Requirements

#### 5.4.2 Non-functional Requirements

**ID:** The identification number of the non-functional requirement

**Explanation:** An explanation of the requirement, and its purpose whenever needed.

The functional requirements of the application are outlined in Table 2.1

ID	DESCRIPTION	EXPLANATION
NF1	Scalability	The system should be designed in a way where the user can add new sensors and stations for other regions and able to perform every task separately for each region
NF2	Security	The web admin user should be prompted with a username and password to prevent unauthorised access
NF3	Performance	Both the WSN and web components should be very responsive. The user should not wait long to query critical information and operations
NF4	Usability	The screens should be designed in a way where the user can view data and perform operations quickly. The system should also provide useful information to the user in case of an error occurred in the system.

Table 4: Non-functional Requirements

## 5.5 Use Case Diagram and Scenarios

Figure 5.5 below represents a use case diagram outlining the interaction and relationship between the system and actors to achieve the required goal. The actors are individuals and sub-systems involved with the system defined according to their roles. In this case, the actors are represented by the users, web server and the WSN system.

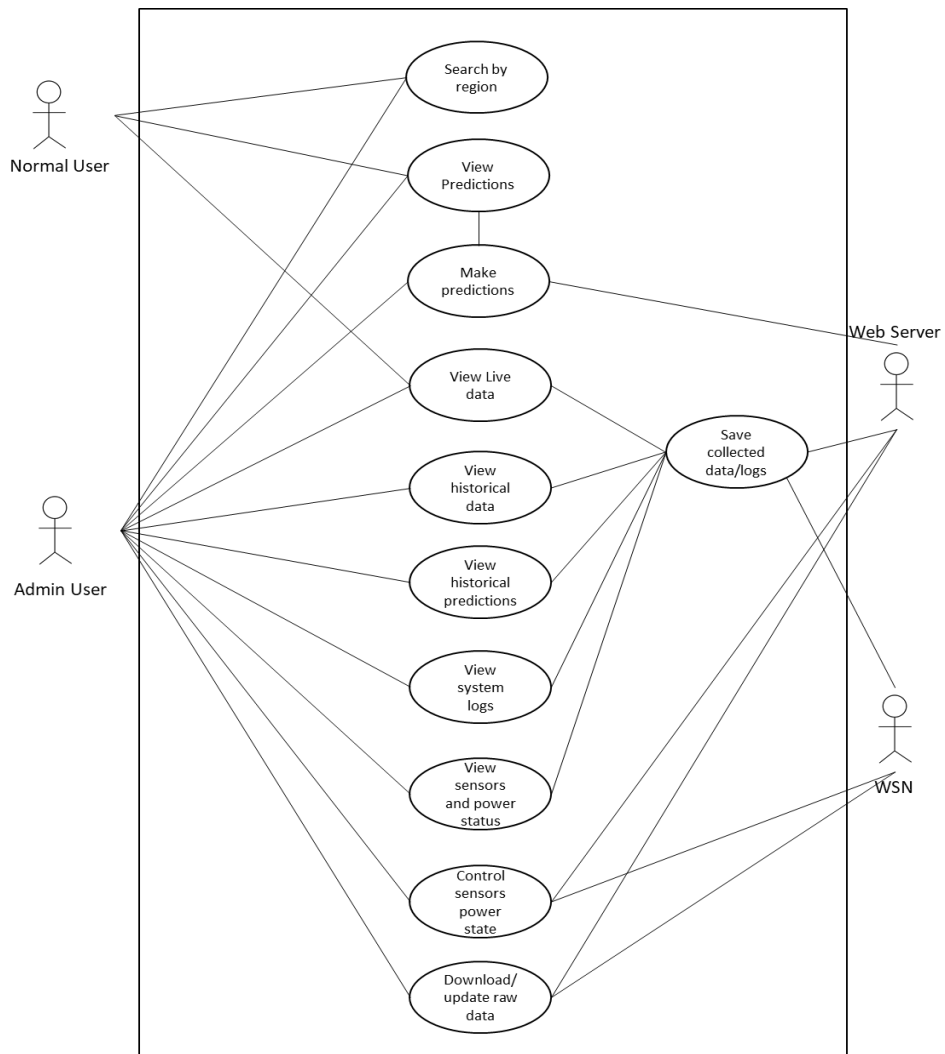


Figure 5.5: Use Case Diagram

## 5.6 Class Diagram

### Computational System and User System Class Diagram

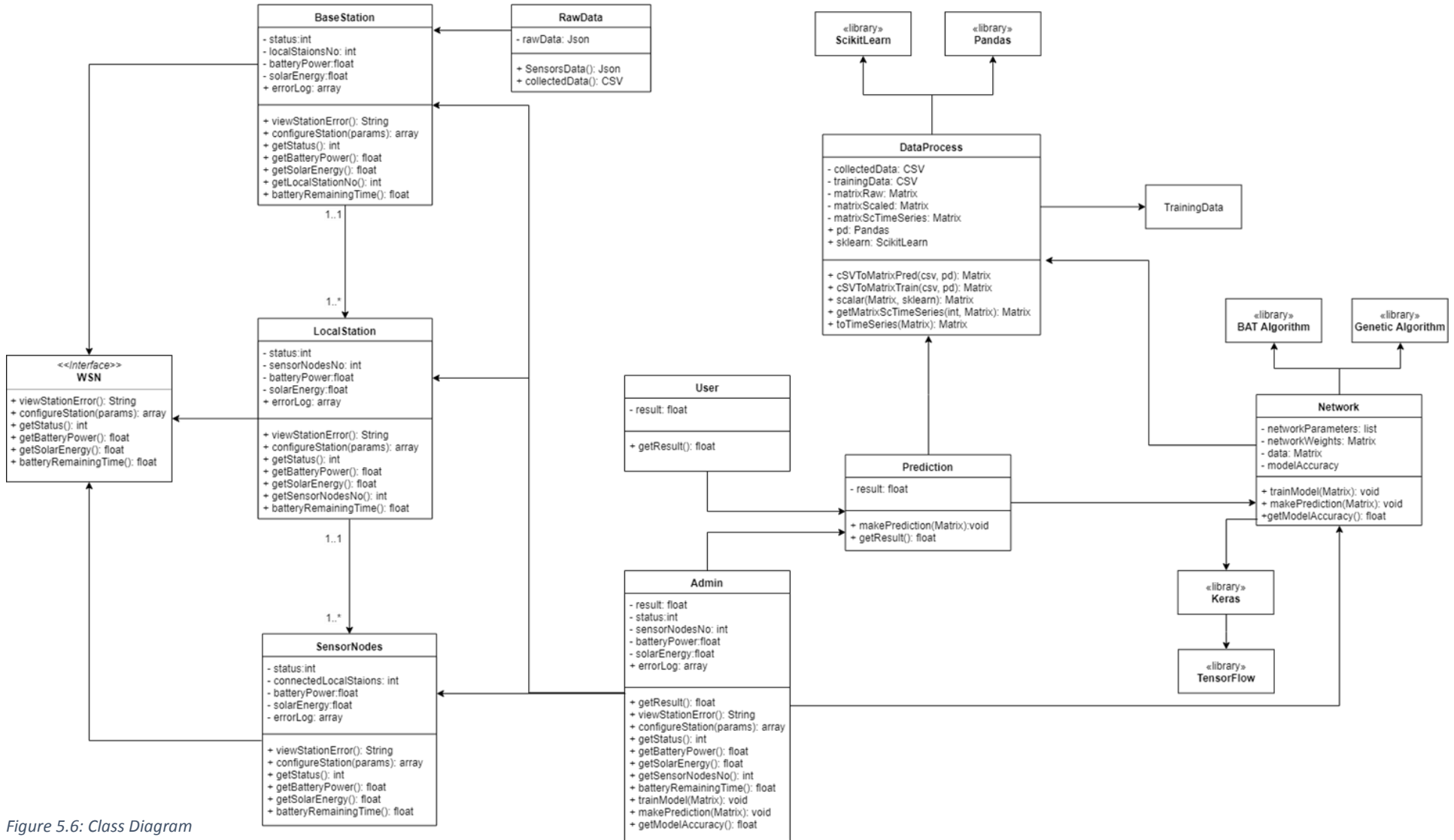


Figure 5.6: Class Diagram

## 5.7 Database Design

The system will be using a local database at the WSN system base station that stores collected data and sensors logs. The web server is also using the same local database to perform predictions and reduce latency lag from the WSN system. The ERD Figure 5.7 shows tables, attributes and relationship of the tables.

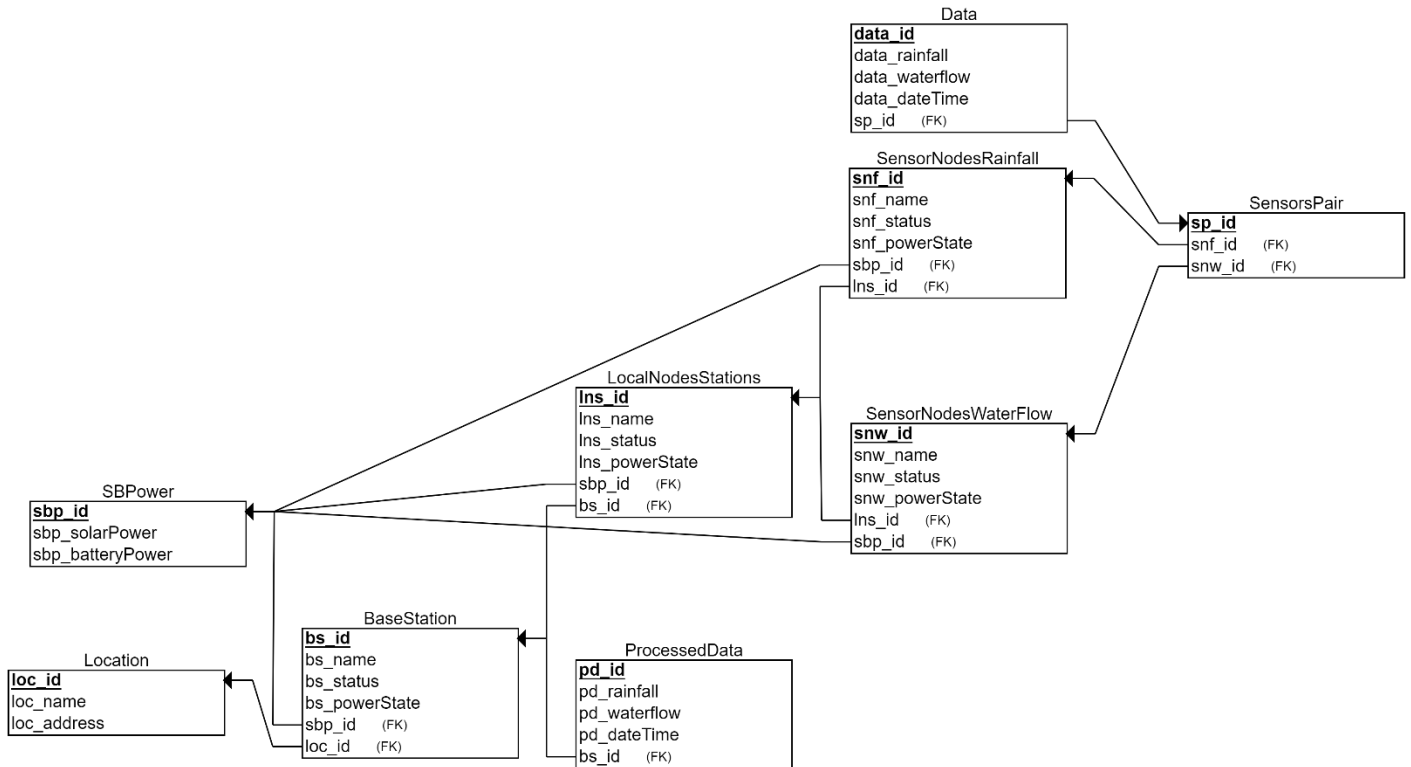


Figure 5.7: Database ERD

## 5.8 User Interface Design

In this section, the structure of the applications and layouts of the mobile application and web interface has been designed and explained.

### 5.8.1 Mobile Interface (User)

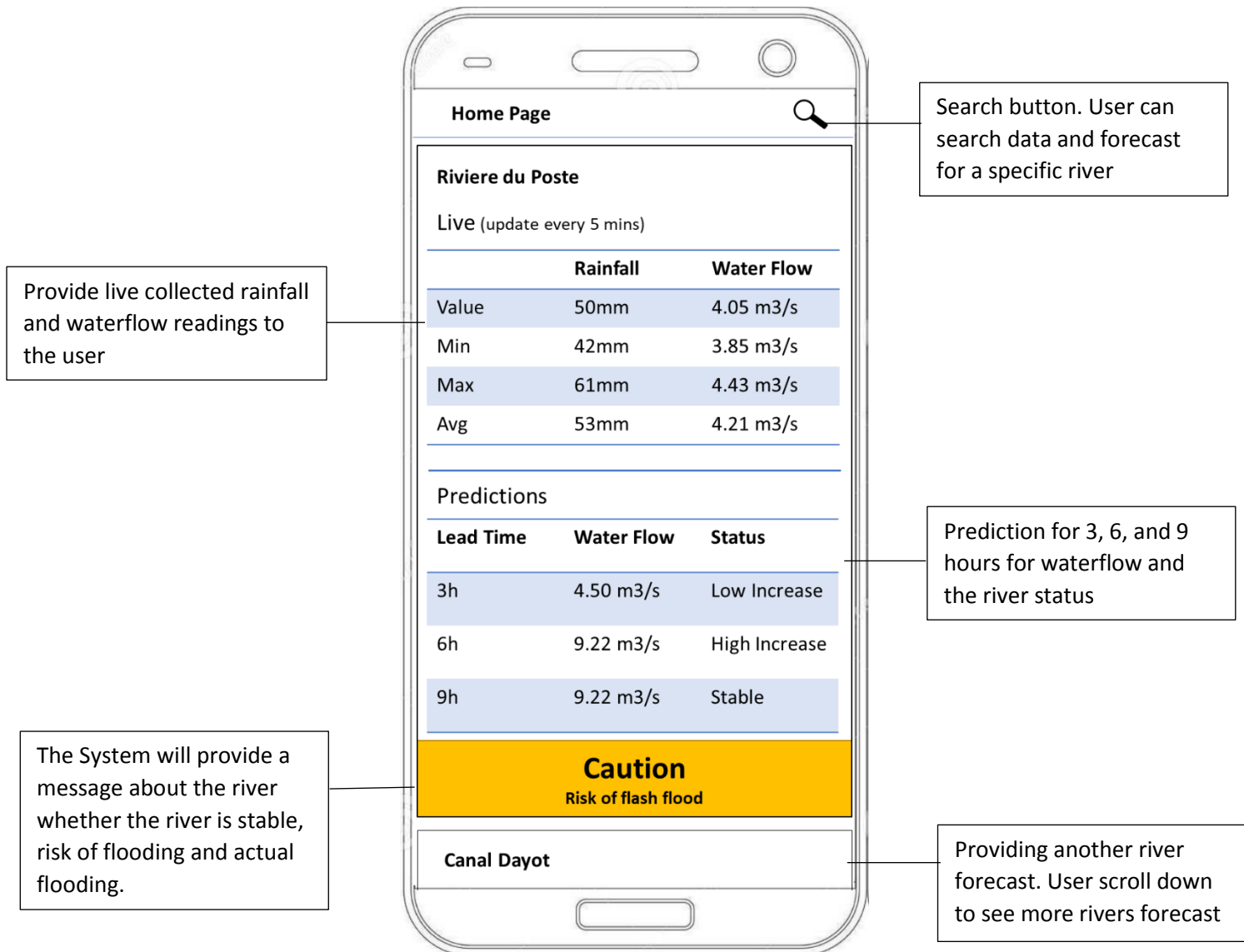


Figure 5.8: Mobile Interface-main

### 5.8.2 Web Interface (Admin)

In the web interface, the user has full access to the system. The search bar at the left top is used to search for a river system implementation, which in this case of the design is Riviere du Poste. Below the search bar is the selected river sensors controls. LS\_1 stands for Local Nodes Station number 1, the status indicates whether the nodes are functional, offline or warning if a problem occurred and requires user intervention. When the user clicks on the arrow a tab expands revealing controls for the sensors. The green dot indicates that the sensor is working normally, a yellow dot indicates the sensor is possibly damaged and transmitting false and bogus data, and a red dot indicates the sensor is not connected or data is not received. The view log provides details of sensors; online time, errors and user intervention. In the middle of the screen, the top line shows real time data for each Local Nodes Station. The below line chart shows water flow predictions for 3h, 6h and 9h at the flooded area. To the right of the screen, the logs button shows the whole system log information, the second button pulls the raw database from the WSN processing component (raspberry pi). The third button when click makes an instant prediction with the latest collected data.

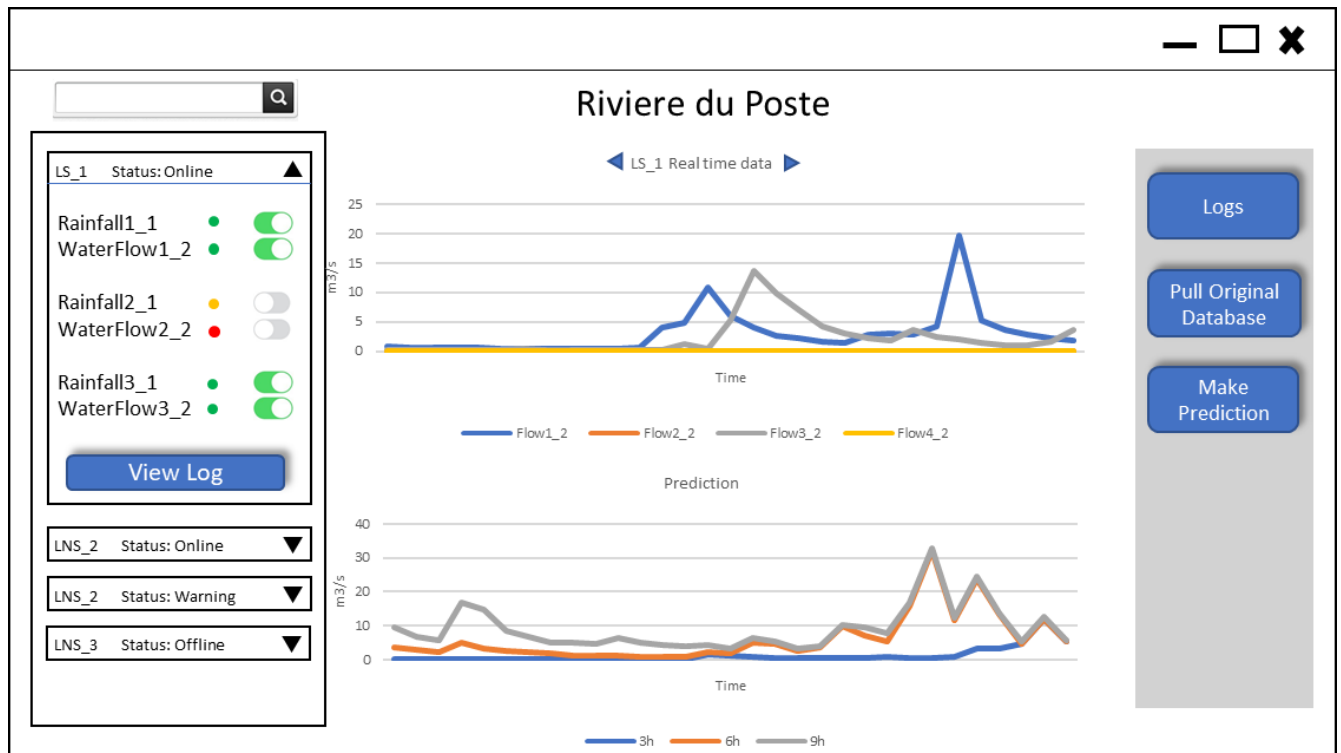


Figure 5.9: Web Interface-main

## 5.9 Chapter Summary

The system architecture follows a component-based approach consisting of a WSN System for the collection of data, which is fed into the Machine Learning Engine, which must be trained to predict possible occurrences of flash floods. Users can see the evolution and prediction of both the web and mobile interface.

## Chapter 6 – Implementation and Testing

Following the design phase, the implementation of the main components of the system are presented in this chapter. The implementation is described in three main sections: firstly, the Wireless Sensor Network, followed by the Machine Learning prediction Engine and finally the user interface application. Following the implementation, each component has been tested (with reasonable assumptions where necessary). The test results are also presented in this chapter.

### 6.1 Wireless Sensor Network Prototype

The WSN prototype consists of the sensor nodes connected to the Local Station. Each local station is further connected to the Base station for onward collection of information collected by the sensors. For a good and reliable WSN system, the sensors and other components should be functional, durable and low cost that is easily replaceable in case of damaged devices. The figure below shows how the different components are connected to each other.

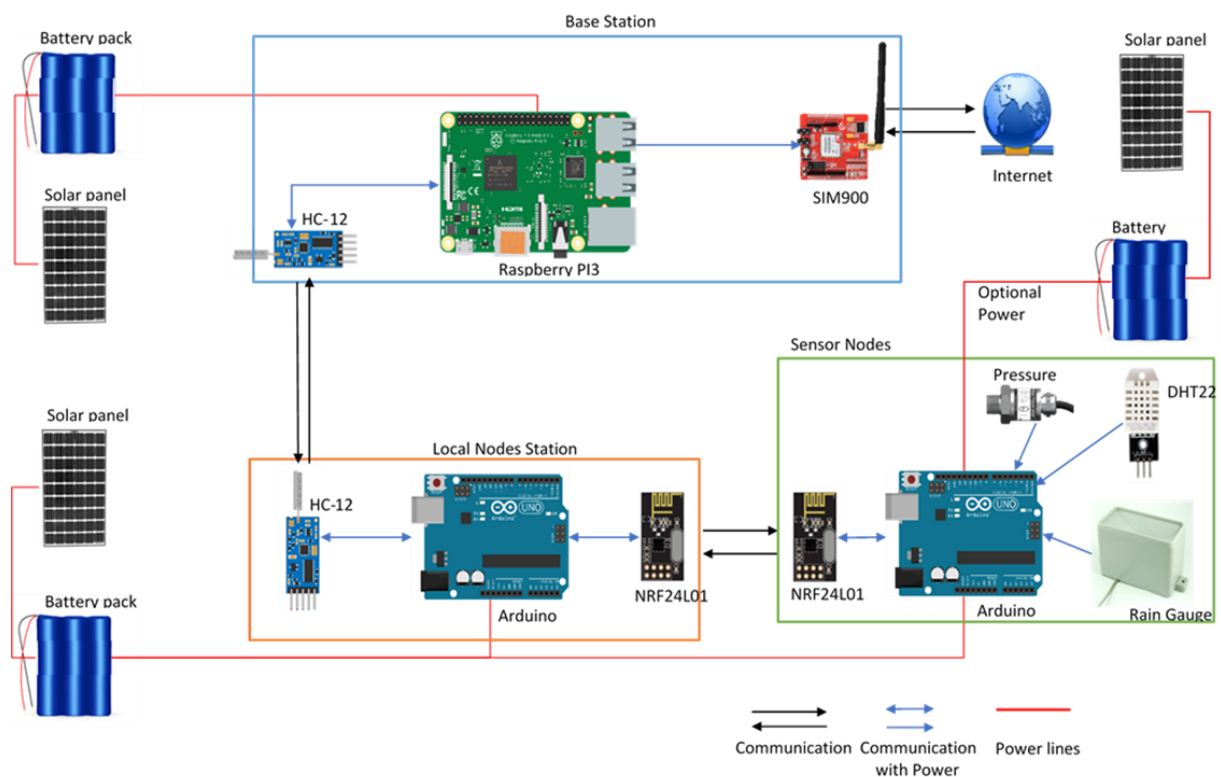


Figure 6.1: Proposed WSN Implementation Architecture

The main components of the WSN are described below:

**Power Source:** Each node may house their own power unit. The power unit consists of a battery pack and a solar panel. The solar panel will be used to charge the battery pack to keep the nodes functioning all the time. The battery should be large enough to provide enough current to the connected node and provide at least 1 to 2 days of power if ever the solar panel fails or didn't have enough sunlight during bad weather conditions.

**Base Station:** Highlighted in the blue rectangle, the base station is responsible for receiving data from local station nodes, process it and send the data to a web server over the internet. A Raspberry PI3 micro-processor is used as the main of the base station due to its credit card size, high performance and low power consumption of 1.2W. When connected to the internet the Raspberry PI is easily monitored and programmed wirelessly. Data gathered from local nodes can be processed and compressed to reduce the payload when uploading to the web server.

**Local Nodes Station:** Highlighted in orange rectangle, this node is responsible for relaying information from one or many groups of sensing nodes to the base station by using long range communication module. It consists of an Arduino UNO as mainboard and two communication modules, a long range to send data to the base station and a short range to collect data from sensing nodes. There can be many local nodes stations.

**Sensor Nodes:** Highlighted in green rectangle, powers and collects data from temperature, rain gauge and pressure sensor. An Arduino is used as baseboard. The Arduino collects sensed data and sends it to the local nodes station. The sensor nodes can be powered by the same power source as the local nodes station or by a dedicated power source.

**Communication:** SIM900 module is used to send data to the web server over the internet. It uses mobile GSM signal 850/900/1800/1900 MHz GPRS/GSM to connect to the internet. The SIM900 module consumes 1W to 2W while transmitting and 1.5mA in sleep mode. HC-12 module is used to make long range communication between the local nodes' stations to the base station. The module operates in the 433MHz band with a max range of 600m to 1800m. The transmitting power is 0.79 to 100mW. The NRF24L01 modules are used to send weather data from the sensing nodes to their respective local nodes station. The module operates in the 2.4GHz band with a range of 1000m line-of-sight and 270m in the forest region. The transmitting power is about 0.79-100mW.

### 6.1.1 System Cost

The total cost of a single unit set excluding infrastructure is around 303.18 USD (around Rs 10,611). The cost includes a single sensor node component estimated at around 139.20 USD per unit and in a configuration of redundancy, the costs is around 417.60 USD, to which the power source of 38.96 USD is required. These set of sensor nodes are further connected to a local station estimated at 93.30 USD (including the cost of a power source). Sub cost of each sensor node and its local station are therefore 549.86 USD (around Rs 19,245). Depending on the architecture, length of the rivers and the number of points which measurements are needed, the cost of the system will increase, as more sensors nodes and local station nodes will be required. Detailed costing for each single unit of the WSN is further presented.

## BASE STATION

link	Hardware	Description	Use	Price
<a href="#">Raspberry Pi3B</a>	Raspberry Pi 3B	Low cost, credit-card sized computer. Can connect to the internet, do complex computation. Have sensors I/O ports.	Acts as the network coordinator, responsible for configuring all distributed nodes, collecting measured data from all of them and sending the data to an online server.	\$42.75
<a href="#">433Mhz HC-12</a>	HC-12 Wireless Serial Port Module	433MHz band. Transmitting power: 0.79-100mW.  Max range: 600-1800m	Transfer data from 1 nodes to another close or long range in peer-to-peer.	\$14.20
<a href="#">GSM module</a>	SIM900 850/900/1800/1900 MHz GPRS/GSM	Class 4 (2 W @ 850 / 900 MHz)  Class 1 (1 W @ 1800 / 1900MHz)  Low power consumption - 1.5mA(sleep mode)  Embedded TCP/UDP stack - allows you to upload data to a web server.	Can be used to allow communication between very far apart nodes. Upload sensed data to server.	\$13.70
<b>TOTAL</b>				<b>\$70.65</b>

Table 6.15: Estimated Cost of Base Station

## LOCAL STATION NODE

link	Hardware	Description	Use	Price
<a href="#">Arduino MEGA</a>	Arduino MEGA	Microcontroller (base board)  Have more I/O ports than Arduino UNO	Operate sensors I/O. Do basic computation. 1 for each sensors' nodes	\$24.99
<a href="#">433Mhz HC-12</a>	HC-12 Wireless Serial Port Module	433MHz band. Transmitting power: 0.79-100mW.  Max range: 600-1800m	Can be used to transfer data from 1 nodes to another close or long range. Provides and peer-to-peer communication.	\$14.20

<a href="#">2.4G Wireless Transceiver module</a>	NRF24L01+PA+LNA SMA Antenna Wireless Transceiver module	2.4GHz band frequency. Max Current: 115mA.  Range: 1000m line-of-sight, 270m in forest.	Can be used to transfer data from 1 nodes to another. Provides and peer-to-peer communication.	\$15.18
<b>TOTAL</b>				<b>\$54.37</b>

Table 6.2: Estimated Cost of Base Stations

## SENSOR NODE

link	Hardware	Description	Use	Price
<a href="#">Arduino MEGA</a>	Arduino MEGA	Microcontroller (base board)  Have more I/O ports than Arduino UNO	Operate sensors I/O. Do basic computation. 1 for each sensors' nodes	\$24.99
<a href="#">2.4G Wireless Transceiver module</a>	NRF24L01+PA+LNA SMA Antenna Wireless Transceiver module	2.4GHz band frequency. Max Current: 115mA.  Range: 1000m line-of-sight, 270m in forest.	Can be used to transfer data from 1 nodes to another. Provides and peer-to-peer communication.	\$15.18
<a href="#">Pressure sensor</a>	Gravity: Analog Water Pressure Sensor	Water pressure is converted into water level.	Measure river water level	\$38.70
<a href="#">DHT22</a>	DHT22	Temperature and Humidity Sensor  Accuracy resolution:0.1.  Humidity range:0-100%RH.  Temperature range:-40~80°C.  Humidity measurement precision:±2%RH.	Temperature and Humidity	\$9.48

		Temperature measurement precision:±0.5°C		
<a href="#">WS-9004U Wireless Rain Center</a>	WS-9004U Wireless Rain Center with Self-Emptying Rain Bucket	Wireless Rain gauge. Transmission range 330 feet and the display unit updates every 4.5 seconds	Rain Gauge	\$50.85
<b>TOTAL</b>				<b>\$139.20</b>

Table 6.3: Estimated Cost of Sensor Nodes

link	Hardware	Description	Use	Price
<a href="#">Solar Cell</a>	Monocrystalline Solar cell	2 Watts peak output at 6 Volts. Monocrystalline cells	Power source	\$29.00
<a href="#">Rechargeable Battery</a>	18650 2400mAh 3.7V Li-ion Rechargeable Battery	Battery provides power to the board and sensors	Power source	\$4.95
<a href="#">Charging Module</a>	TP4056 5V 1A Lithium Battery Charging Module	Link between the solar cell and battery	Power source	\$1.80
<a href="#">Voltage booster</a>	5V Step-Up Breakout - NCP1402	Accept voltage inputs between 1 and 4 Volts and output a constant, low ripple 5V output capable of sourcing up to 200 mA.	Power source	\$3.21
<b>TOTAL</b>				<b>\$38.96</b>

Table 6: Estimated Cost of Power Source

### 6.1.2 WSN System Implementation Challenges

Fixing WSN nodes on existing rivers and/or canals requires specific metal or concrete support infrastructures to securely hold the devices. The WSN should also be able to capture real flash flood occurrences and get enough data to train the model. Given the time frame and scope of the study, getting permissions and building the necessary support infrastructure for the WSN nodes was not considered. Therefore, not much resources have been allocated to this activity and it has been decided that laboratory simulation techniques will be used instead.

### 6.1.3 WSN Prototype

The goal of this section is to demonstrate the connectivity capabilities of the WSN network and test the hardware used on a small-scale prototype based approach. The water flow and rainfall sensors are replaced with temperature and humidity sensors to simulate live data being transmitted to nodes and base stations. The figure below shows a picture of the actual test setup.

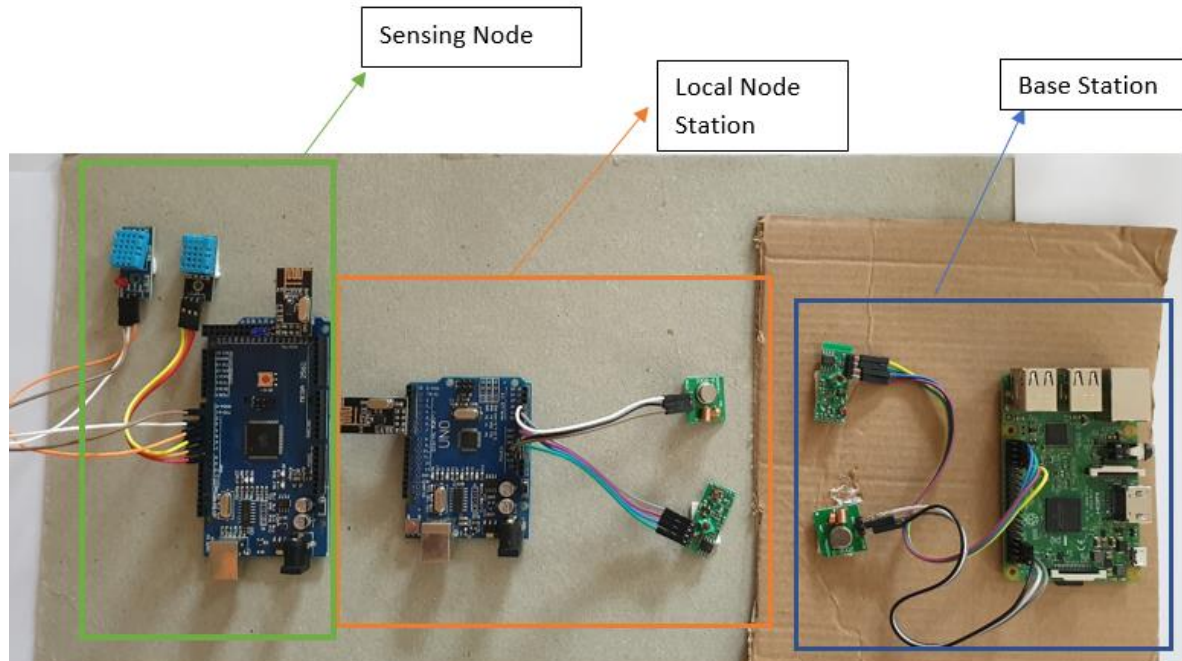


Figure 6.2: WSN Setup: Main Components

Figure 6.2, the highlighted blue rectangle is the base station, is responsible for receiving data from local station nodes. The Highlighted orange rectangle relays from the sensing nodes to the base station using wireless long-range module. The components in the highlighted green rectangle collect environmental data and send the data to the local node station by high frequency low range wireless module. (Referring to section 5.2.2, which describes the WSN architecture).

## 6.2 Machine Learning Engine

The Machine Learning Engine can be considered as a core component for the automatic prediction of flash flood occurrences. The Figure below describes our approach, where the data is received from the WSN System. The Machine Learning Engine is implemented in Python and follows a modular approach. The Machine Learning architecture used is called Recurrent Neural Networks - Long ShortTerm Memory (RNN-LSTM). The same will be further optimised for better forecast accuracy.

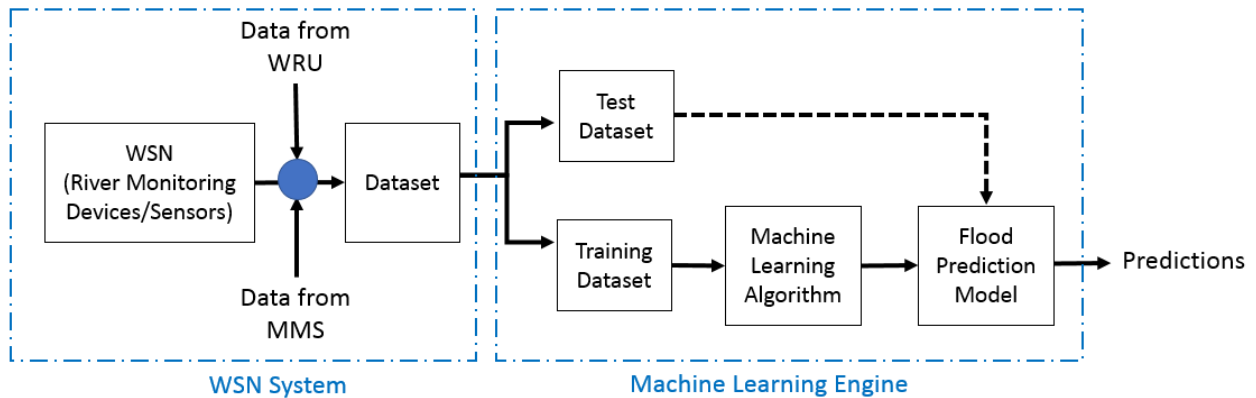


Figure 6.3: Machine Learning Component

To be able to build a neural network the following python library are used:

- Scikit-Learn
  - Import and split dataset into train and test set.
  - Scales values
  - Calculate model accuracy
- TensorFlow
  - Build a neural network/ Create a model
  - Train and run prediction for a model
- Keras
  - A high-level API running on top of TensorFlow to facilitate creation of models

RNN is a class of artificial neural networks where the connection between nodes form a directed graph along a temporal sequence. Unlike ANN, RNN uses their internal state memory for processing sequences. LSTM, is an RNN architecture with feedback connections, which enables it to perform or compute anything that a Turing machine can. A single LSTM unit is composed of a cell, an input gate, an output gate and a forget gate, which the cell uses to remember values for a defined amount of time. The gates control the flow of information in and out of the LSTM cell. LSTM addresses the problem of training over long sequences of data and retaining memory. Hence in flash flood prediction the model should retain previous hours or days weather conditions to make a prediction.

## Implementation of RNN-LSTM

### Data preparation

Importing the dataset and scale all values between 0 and 1.

```
dataset = pd.read_csv('flowrain1hMultiRandomLag1hv2.2.csv')
values = dataset.values
values = values.astype('float32')

scaler = MinMaxScaler(feature_range=(0, 1))
values = scaler.fit_transform(values)
```

Specifying the number of lag hours (3 hours of previous data) and the number of features of the dataset. And convert the sequential dataset into supervised learning RNN input format.

```
# specify the number of lag hours
n_hours = 3
n_features = 4
# frame as supervised learning
reframed = series_to_supervised(values, n_hours, 3)
```

Splitting the dataset into train and test sets.

```
# split into input and outputs
n_obs = n_hours * n_features
train_X, train_y = train[:, :n_obs], train[:, n_features+10]
test_X, test_y = test[:, :n_obs], test[:, n_features+10]

train_X = train_X.reshape((train_X.shape[0], n_hours, n_features))
test_X = test_X.reshape((test_X.shape[0], n_hours, n_features))
```

### Model Architecture

Creation of the model. The first hidden layer consists of 32 LSTM nodes and Selu activation function, followed by a dropout of 10%, followed by another set of 32 LSTM and 10% dropout. The node in the last layer is the output node with a linear activation function. The model is set to user Adam learning rate of 0.0001 and mean absolute error to evaluate the model during training. The early stop function is used to stop the training process when overfitting starts.

```
model = Sequential()
model.add(LSTM(32, input_shape=(train_X.shape[1],train_X.shape[2]), activation='selu', return_sequences=True))
model.add(Dropout(0.1))
model.add(LSTM(32, activation='selu'))
model.add(Dropout(0.1))
model.add(Dense(1, activation='linear'))
```

```

model.compile(Adam(lr=0.0001),loss='mae')
early_stop = callbacks.EarlyStopping(monitor='val_loss', min_delta=0, patience=30
, verbose=1, mode='auto')

```

Below is a summary of the model:

Layer (type)	Output Shape	Param #
lstm_1 (LSTM)	(None, 3, 32)	4736
dropout_1 (Dropout)	(None, 3, 32)	0
lstm_2 (LSTM)	(None, 32)	8320
dropout_2 (Dropout)	(None, 32)	0
dense_1 (Dense)	(None, 1)	33
Total params: 13,089		
Trainable params: 13,089		
Non-trainable params: 0		

### Model Training

The fit function is used to start the training process. Once training completed the model parameter and architecture is saved in a .h5 file for future predictions.

```

history = model.fit(train_X, train_y, batch_size=1000, epochs=2500000, validation
_data=(test_X, test_y), shuffle=False, verbose=0, callbacks=[early_stop])
model.save('model3hRnn.h5')

```

## Prediction

Prediction on the test set. The forecast scaling is then reverted back to its true value.

```
prediction = model.predict(test_X, batch_size=1000, verbose=0)
test_X = test_X.reshape((test_X.shape[0], n_hours*n_features))
# invert scaling for forecast
inv_yhat = concatenate((prediction,test_X[:, :-9]), axis=1)
inv_yhat = scaler.inverse_transform(inv_yhat)
inv_yhat = inv_yhat[:,0]
test_y = test_y.reshape((len(test_y), 1))
inv_y = concatenate((test_y,test_X[:, :-9]), axis=1)
inv_y = scaler.inverse_transform(inv_y)
inv_y = inv_y[:,0]
rmse = sqrt(mean_squared_error(inv_y, inv_yhat))
print('Test RMSE: %.3f' % rmse)
```

## 6.3 Web Application User Interface Implementation

The web application was developed in PHP programming language and deployed on an Apache server for hosting. Bootstrap 4 and jQuery libraries is used for web responsiveness across all types of devices and animate.js library is used to generate live graph.

In the web application there are five different sections, which are described below:

1. Sensors management: This section allows the user to view sensors status whether the sensors are working as intended, offline due to malfunction and power-state of the sensor. It also allows the user to manually enable or disable a sensor.
2. Graph: The user is able to view live prediction each hour, view trending of actual water flow and predicted water flow for the past 9-hours. The graph also indicates the warning level (flooding is possible) and danger level (high risk of flooding) of the river.
3. Information: The user is able to see the actual water flow and rainfall data of the river compared to the +1-hour predicted flow. It also indicated status water flow (safe, warnings, danger).
4. Logs and controls: The user can view the whole system logging information, pulls the raw database from the WSN processing component (raspberry pi) and allows the user to make instant prediction with the latest collected data.
5. Search: The user can search for and manage another system implementation in another river.

Figure 6.2 shows the main screen of the web application. It allows users to view real-time updates and predictions, and select different tasks.

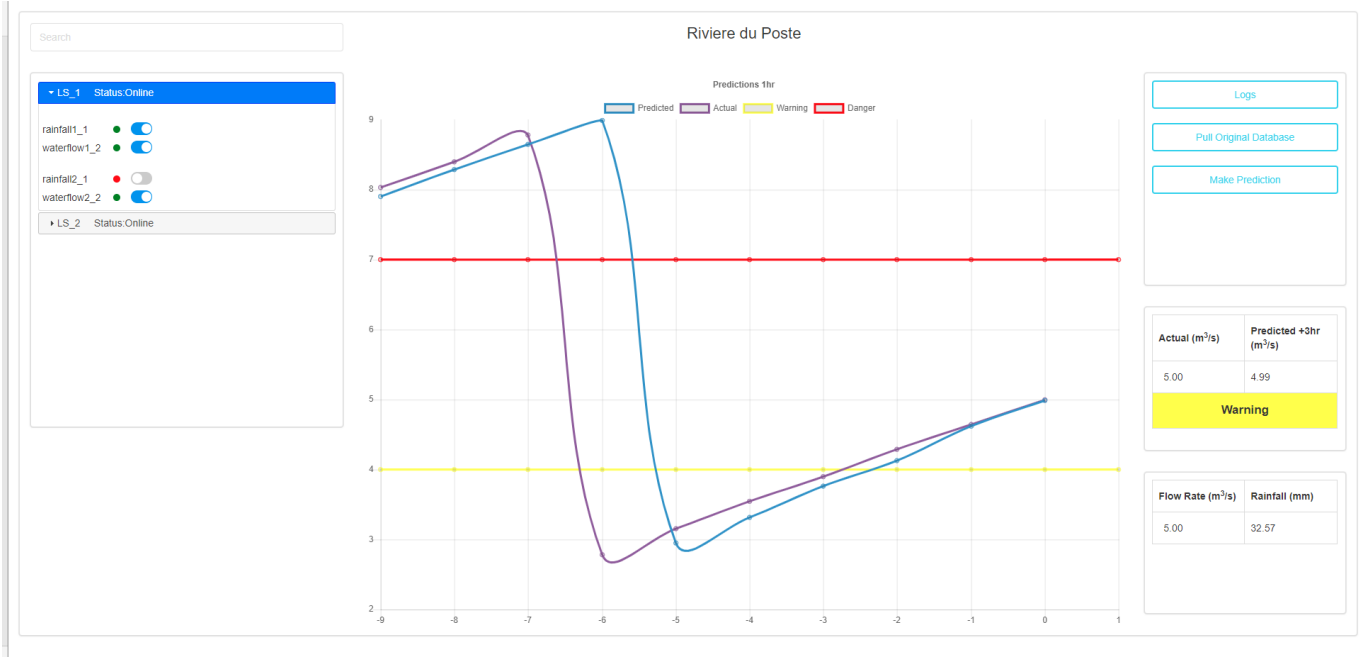


Figure 6.2: Main Screen

Figure 6.3 shows the prediction / real-time water flow data plotted. It also shows the warning limit and dangerous levels of the river water flow per hour. Y-axis represents water flow  $m^3/s$ , X-axis represents hours (1-hour step).

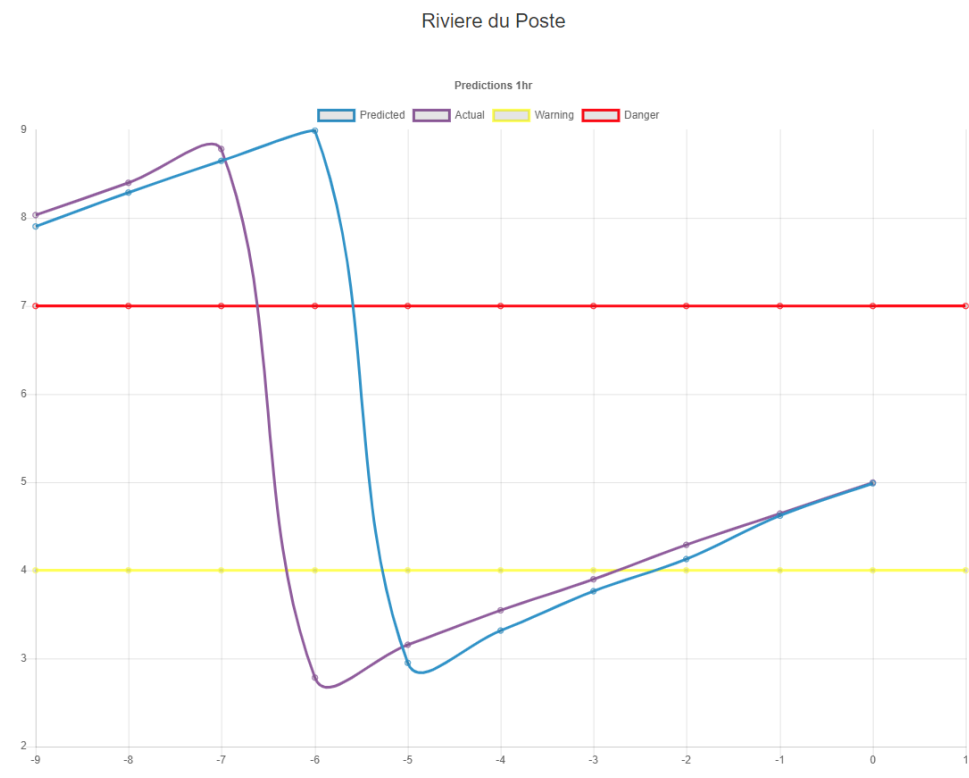


Figure 6.3: Graph

Figure 6.4 shows buttons and logs section

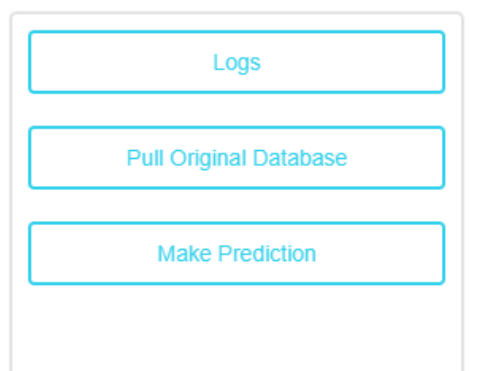


Figure 6.4: Buttons

The Pull Original Database allows the user to get raw collected data directly from the WSN. The data includes collected from all sensors. The log button when clicked, generates an excel document containing user action logs, for example, turning on and off sensors. Errors that occur in the WSN system are also logged in the excel sheet. The user can look at which point of time the malfunction occurred. Figure 6.5 and Figure 6.6 show screenshots of the system log and error log of the WSN, respectively.

	A	B	C	D
1	Timestamp	Action by	Item	Status
2	12/06/2019 13.00	System	LS_1;rainfall2_1	OFF
3	13/06/2019 14.50	User	LS_1;waterflow2_1	OFF
4	13/06/2019 14.51	User	LS_1;rainfall2_1	ON
5	13/06/2019 14.52	System	LS_1;rainfall2_2	OFF
6				

Figure 6.5: System Logs

	A	B	C	D	E
1	Timestamp	Item	PowerState	Status	Action
2	12/06/2019 13.00	LS_1;rainfall2_1	ON	Error occurred. Inconsistent data	Switch Off
3	12/06/2019 13.00	LS_1;rainfall2_1	OFF	OFFLINE	
4					

Figure 6.6: Error Logs

Figure 6.7 shows live river data and predicted water flow. The user is able to see the difference between the actual and the predicted water flow.

Actual (m <sup>3</sup> /s)	Predicted +1 hr (m <sup>3</sup> /s)
5.00	4.99
<b>Warning</b>	

Flow Rate (m <sup>3</sup> /s)	Rainfall (mm)
5.00	32.57

Figure 6.7: Live+Predicted data

#### 6.4 Test Strategies

The functional and non-functional requirements were tested during the development and after the implementation of the developed system. The following table below shows test cases written to evaluate the functionality of the combined approach.

Test Requirement	F1
Passing Criteria	Admin users should be able to view both raw and processed real-time data (data that are being collected) from each node and station
Test	Real-time data can be seen in the main page graph and flow and rainfall data from the right section of the page. The user can click on the Pull Original Database button to download raw collected data from the WSN
Status	PARTIAL

Test Requirement	F2
Passing Criteria	Normal users (mobile version) should be able to view predictions for the next 1-hour real time. Admin users should be able to view predictions with previous predictions trends.
Test	The main page graph shows prediction for each next hour. The graph also shows previous prediction for the past 9 hours
Status	PARTIAL

Test Requirement	F3
Passing Criteria	An option where the user can download the raw dataset
Test	The user can click on the Pull Original Database button to download raw collected data from the WSN
Status	PASS

Test Requirement	F4
Passing Criteria	Automated prediction at 5 minutes interval
Test	Prediction is done and the graph is updated at 5 minutes interval.
Status	PASS

Test Requirement	F5
Passing Criteria	Admin should be able to make predictions instantaneously.
Test	The user can click on the Make Prediction button to make a prediction instantly with the last collected data from the WSN
Status	PASS

Test Requirement	F6
Passing Criteria	Monitor all sensors activities including data transmission and power state
Test	All system logs are sent to the web server and stored in a database
Status	PASS

Test Requirement	F7
Passing Criteria	Collect data from sensors, redundant sensors and analyse the data to detect anomalies.
Test	The system is able to identify if a sensor is transmitting inconsistent data due to a malfunction
Status	PASS

Test Requirement	F8
Passing Criteria	Admin users should be able to see connected sensors status; online, warning, offline.
Test	The admin can see sensors status and power state. The user can click on Logs button to view detailed logs of the WSN
Status	PASS

Test Requirement	F9
Passing Criteria	The system should be able to calculate power usage, battery remaining current capacity and solar time. The system should also provide notification to the admin if a station is about to go offline in case of insufficient solar charging rate.
Test	Not Implemented
Status	FAIL

Test Requirement	F10
Passing Criteria	Admin should be able to turn off redundant sensors in case of low battery alert to preserve power and damaged sensors
Test	The user can switch on or off a sensor. Battery level logs not implemented.
Status	PARTIAL

Test Requirement	F11
Passing Criteria	The search bar will be used to search for a river monitoring and predictions information.
Test	The users can search for a river/ location where the system is deployed and see predictions.
Status	PARTIAL

### 6.5 Chapter Summary

Flash flood occurrences in Mauritius have been very damaging to the infrastructure, economy and human lives. Nevertheless, from an intelligent system perspective, there have been relatively few occurrences of flash floods at national level. Thus, for effective training, more instances are required and as such, the Wireless Sensor Network for data collection has been partly implemented. A simulation approach has been adopted to avoid the delay incurred in purchasing of hardware and the construction of support infrastructures and as well as concrete fixing of different components in specific rivers/canals. More importantly, it helps to avoid unpredictable waiting time for flash flood occurrences (no episodes have been witnessed during the implementation of this project). Therefore, all data to be fed into the system have been simulated based on data available from different Mauritian institutions (namely: The Water Resources Unit and Mauritius Meteorological Services). The Machine Learning Engine has been completely implemented using python and deployed on a web server, from which a system administrator can use the web interface to view the river monitoring details and predictions of the system. Given all assumptions made on the WSN, the system tests performed have been quite successful. A more detailed evaluation is presented in the next section.

## Chapter 7 – Experimental Results & Evaluation

In this chapter, the proposed solution is evaluated using simulation techniques. Since the WSN has been implemented as a prototype, detailed explanation of all simulated datasets is also provided. All experiments in this section refer mainly to the performance and effectiveness of the Machine Learning Engine.

### 7.1 Evaluation Method

Different Machine Learning algorithms and datasets are evaluated to find the most appropriate and effective prediction model. It is to be noted that the same experimental setup described in section 4.5.2 (page 33) has been used, i.e. same computer resources and python libraries. In this section, river flow from the WRU and rainfall data from the MMS are used as the building blocks to generate synthetic datasets. Approximations based on the river 'Rivière du Poste' have been considered, as peaks of water flow from WRU data corresponds to the high rainfall amount which generated flash floods in 2008. As depicted in the diagram below, the data generated by the WSN sensor devices are simulated with the help of data from the WRU and MMS. Once the synthetic dataset is created, its divided into 70% and 30% for training and testing respectively. The training set is used to train the Machine Learning algorithm to produce a flood prediction model (step 2). Following which, in step 3, the test data set is used for making predictions. As per our investigations, it has been noted that very few occurrences of flash flood have been recorded for Mauritius over the last 15 years. As such synthetic datasets which contains enough occurrences has been randomly generated, based on real past data. The sections below describe several experiments which include dataset processing, training and prediction. Different ML techniques have been implemented to find the best approach by minimizing prediction errors.

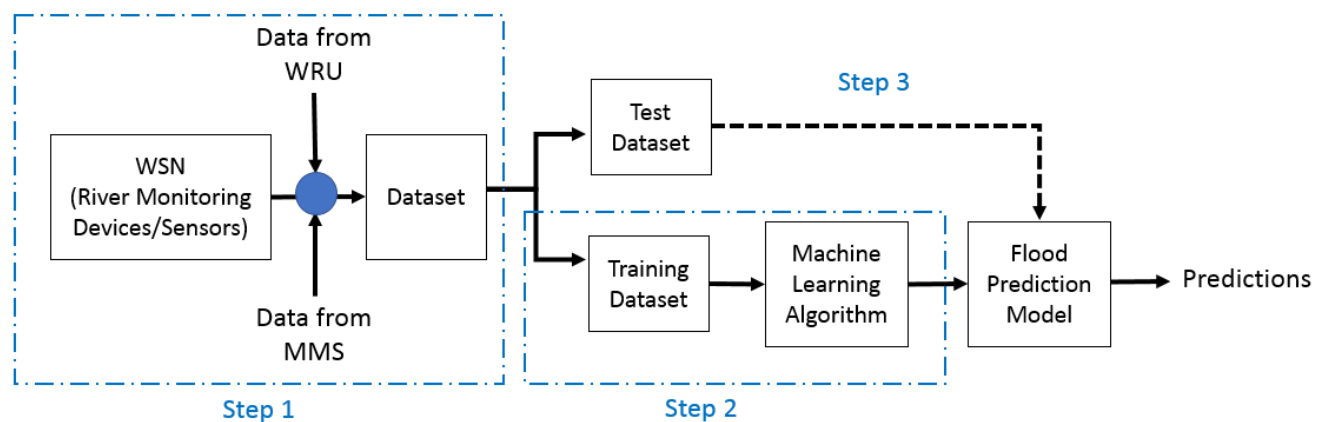


Figure 7.1: Three step approach

#### 7.1.1 Data Set Information

To evaluate the effectiveness of the proposed method, several processed versions of the dataset are used. The description of the time-series datasets used in the experiments analysis is as follows:

- 1) Unprocessed Water Flow Dataset (UWF):** The dataset contains 389 days of water flow data extracted from water flow peaks form year 2006 to 2010.

- 2) **3-Hour Water Flow Dataset (HWF):** The 389 daily records of the UWF dataset is converted to 3-hour intervals records by subtracting the following water-flow value to the previous value, divided by 8. A random percentage of 0-15% is added to each record to give the dataset some randomness
- 3) **Hourly Water Flow Dataset (HWF):** The 389 daily records of the UWF dataset is converted to hourly records by subtracting the following water-flow value to the previous value, divided by 24. A random percentage of 0-15% is added to each record to give the dataset some randomness. The dataset contains 7324 records.
- 4) **Hourly Water Flow-Rainfall Dataset (HWFR):** On February 26<sup>th</sup> 2017, WRU recorded a peak water flow of 31.5 m<sup>3</sup>/s and MMS recorded 200 mm of rainfall. To assess the necessity of MMS data, synthetic rainfall hourly data is created. We assume that 31.5 m<sup>3</sup>/s is equivalent to 200 mm of rainfall, thus all the water flow records are converted proportionally to rainfall by dividing the dataset waterflow peak by 200 mm, multiply by the flow of each record to option the rainfall values. A random percentage of -15 to 15% is added to each for randomness. The dataset contains 7323 records.
- 5) **WSN Hourly Water Flow-Rainfall Dataset (WHWFR):** New water flow and rainfall data are created to simulate collection of data upstream. This simulation involves collection of data with two set of water flow and rainfall sensors places at two different points in the river, upstream and downstream (flooded area). The HWFR data are duplicated and divided by 2 to simulate flow upstream. The dataset contains 7324 records. Figure 7.1 WHWFR shows data represented on a graph.

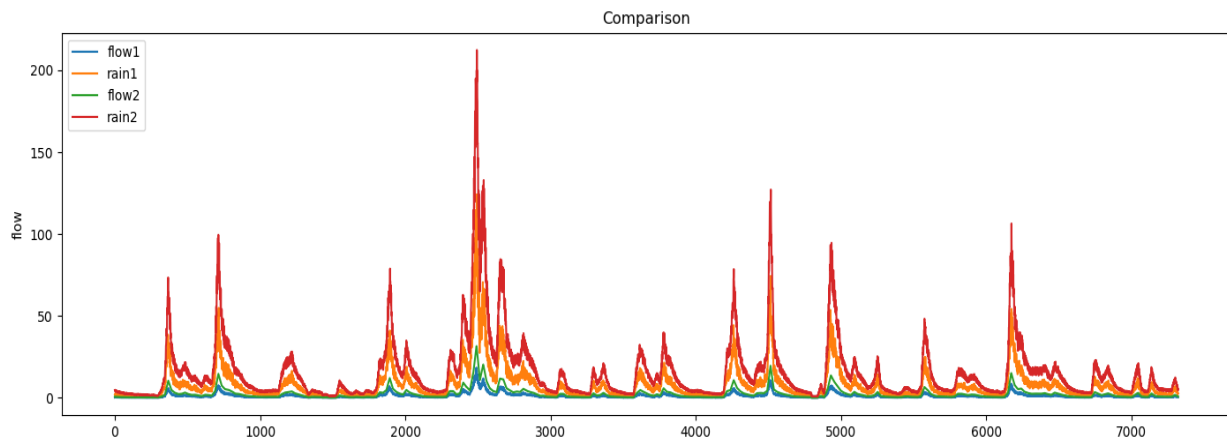


Figure 7.1: WHWFR graph

- 6) **WSN Hourly Water Flow-Rainfall duplicate Dataset (WHWFRD):** Figure 7.1 WHWFR shows that the highest peak at around hour 2700 is unique throughout the whole dataset. To ensure the model learns to predict high peaks, the peak sequence is duplicated randomly 11 times in the dataset as shown in figure WHWFRD. The dataset contains 8148 records. Figure 7.2 shows the WHWFRD data graph.

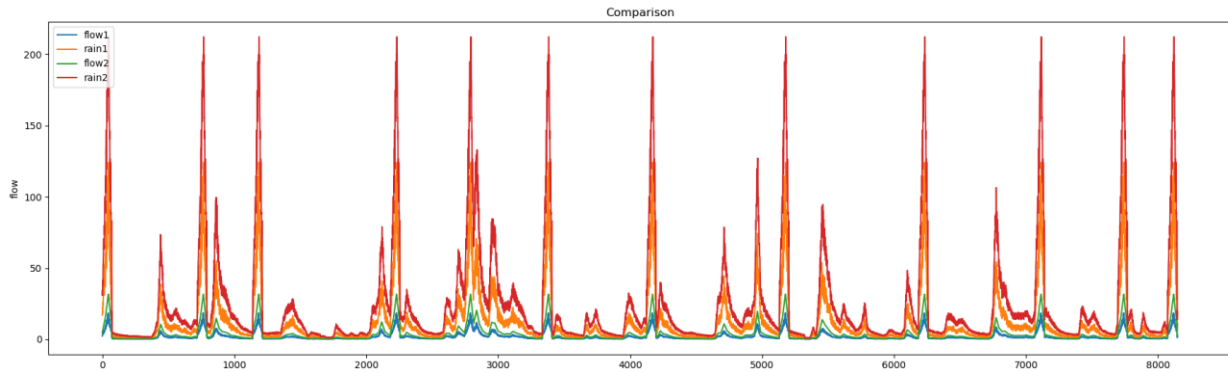


Figure 7.2: WHWFRD graph

**7) High Peak test dataset (HPT):** This dataset contains all the peaks scenarios of the WHWFR dataset. It is used to evaluate all the different prediction methods of the WHWFR and WHWFRD datasets. The dataset contains 1567 records. The HPT dataset is shown in Figure 7.3.

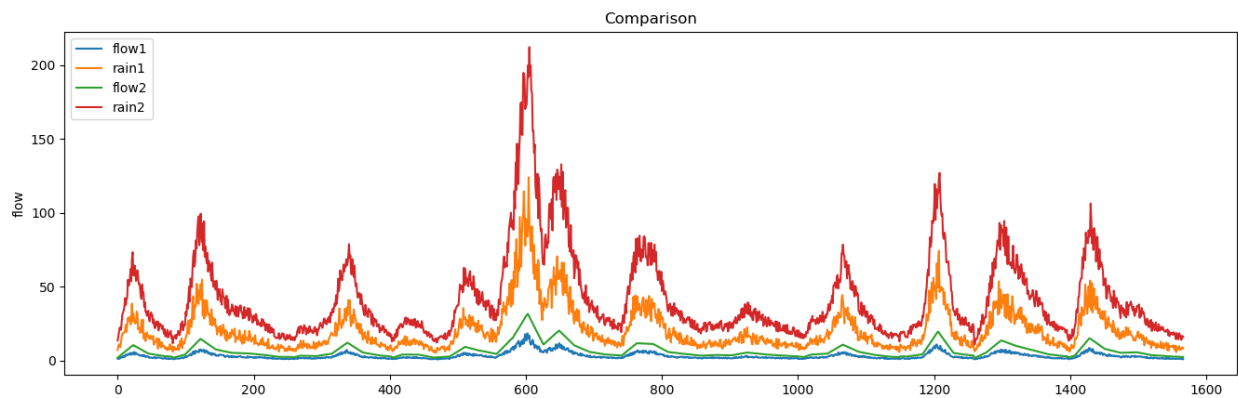


Figure 7.3: HPT graph

### 7.1.2 Experimental results and analysis

To find the most appropriate prediction model, several methods have been trained and compared for dataset WHWFR and WHWFRD. The trained models are then evaluated with the HPT dataset to obtain the RMSE for all water flow and flash flood scenarios.

#### Scenario 1

Table 7 shows the performance comparison of MLP and RNN for the WHWFR dataset. Both model's parameters are configured as closest as possible. RNN scored the lowest error compared MLP but the Training time is more than MLP. While the training and testing time is higher, it is justifiable as RNN uses and keeps sequence of data in memory for the next prediction. Hence the higher dimensionality data costs more in terms of computational power. Figure 7.4 and Figure 7.5 show the predicted values compared to the actual values for MLP and RNN, respectively. Figure 7.5 shows the MLP model causes false negative in all cases, while figure 5 shows that RNN prediction is closer to the actual values but gives

false positive in most cases. As RNN scored the error, in the next experiment GA is used to optimize the RNN model parameters and configure the model network architecture to obtain the best results possible.

TECHNIQUE	MLP	RNN
<b>MODEL PARAMETERS</b>	Dense(32, activation='selu'), Dropout((0.1)), Dense(32, activation='selu'), Dropout((0.1)), Dense((1), activation='linear')	LSTM(32, activation='selu', return_sequences=True), Dropout(0.1), LSTM(32, activation='selu'), Dropout(0.1), Dense(1, activation='linear')
<b>TRAINING TIME (S)</b>	41.52	44.45
<b>TESTING TIME (S)</b>	1.519	4.694
<b>EVALUATION RMSE</b>	5.258	4.874

Table 7: Models Comparison of Scenario 1

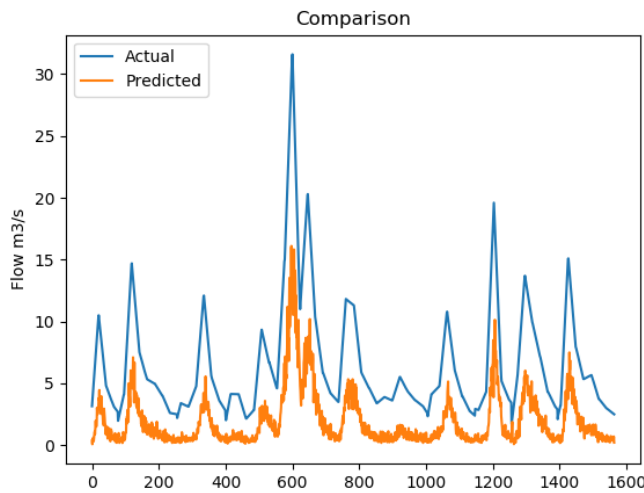


Figure 7.4: MLP result (scenario 1)

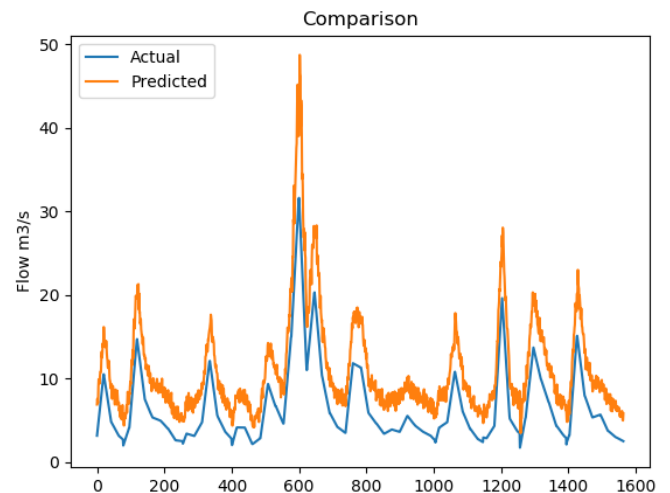


Figure 7.5: RNN result (scenario 1)

### Scenario 2 – GA Optimization

Experiments from scenario 1 shows that RNN is better in terms of RMSE of 4.874. From this experiment the RNN model parameters configuration is optimized with Genetic Algorithm (GA) from a pool of parameters given in Table 8. The performance of RNN-GA is compared to the previous RNN experiment. The result shows that RNN-GA is significantly better in prediction RMSE. RNN-GA is computationally intensive and requires nearly 7 hours to train the model. Also, it takes 1.357 seconds longer for the HPT dataset as the model network is now more complex with 3 layers of 60 neurons. Figure 7.6 show the prediction comparison of RNN-GA. The model is able to make good prediction in most cases, but is unable to capture the highest peak at around hour 600. This is due to the lack of high peak instances in the dataset training. This experiment is able to show that the WHWFR dataset lacks data, to compensate a new dataset is created (WHWFRD), which contains duplicates of high peaks data. In the next experiment, the WHWFRD is used in the regular MLP and RNN models to observe the RMSE of the new dataset compared to Scenario 1.

PARAMETERS	
NUMBER OF NEURONS	4,12,20,32,42,60,70
NUMBER OF LAYERS	2,3,4,5
DROPOUT	0, 0.1, 0.2, 0.3,0.4,0.5
ACTIVATION	relu, elu, tanh, sigmoid, selu, softplus, softsign, hard_sigmoid, linear, softmax
GENERATION	5
POPULATION	15

Table 8: GA parameters (scenario 2)

TECHNIQUE	RNN	RNN-GA
MODEL PARAMETERS SELECTED PARAMETERS (RNN-GA)	LSTM(32, activation='selu', return_sequences=True), Dropout(0.1), LSTM(32, activation='selu', Dropout(0.1), Dense(1, activation='linear')	LSTM(60, activation='softsign', return_sequences=True), LSTM(60, activation='softsign'), LSTM(60, activation='softsign'), Dropout(0.1), Dense(1, activation='linear')
TRAINING TIME (S)	98.45	24582
TESTING TIME (S)	4.694	6.051
EVALUATION RMSE	4.874	0.973

Table 9: Models Comparison of Scenario 2

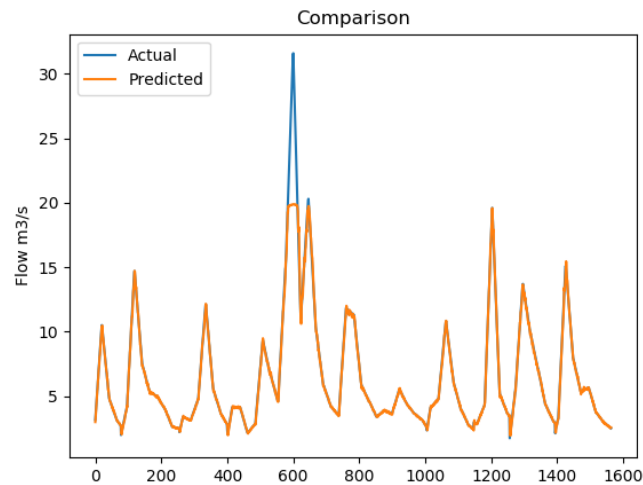


Figure 7.6: RNN-GA results (scenario 2)

Scenario 3

Table10 shows the performance comparison of MLP and RNN for the WHWFRD dataset. Both model's parameters are configured as closest as possible. RNN scored the lowest error compared MLP with nearly half the RMSE. Figure 7.7 and Figure 7.8 show the predicted values compared to the actual values for MLP and RNN, respectively. Figure 7.7 shows the MLP model now overshoots the target compared to MLP experiment in scenario 1 causing false positive in most cases. Figure 8 shows a substantial improvement compared to RNN experiment from scenario 1. However, the prediction is rather spiky, which may confuse the end user about the water flow trends. Also, the RNN RMSE is more than twice lower than RNN scenario 1 and this indicates that having more high peaks data improves the prediction error. To further lower the error GA is added to the model in next experiment.

TECHNIQUE	MLP	RNN
<b>MODEL PARAMETERS</b>	Dense(32, activation='selu'), Dropout((0.1)), Dense(32, activation='selu'), Dropout((0.1)), Dense((1), activation='linear')	LSTM(32, activation='selu', return_sequences=True), Dropout(0.1), LSTM(32, activation='selu'), Dropout(0.1), Dense(1, activation='linear')
<b>TRAINING TIME (S)</b>	41.52	57.52
<b>TESTING TIME (S)</b>	1.554	4.83
<b>EVALUATION RMSE</b>	4.409	2.129

Table10: Models Comparison of Scenario 3

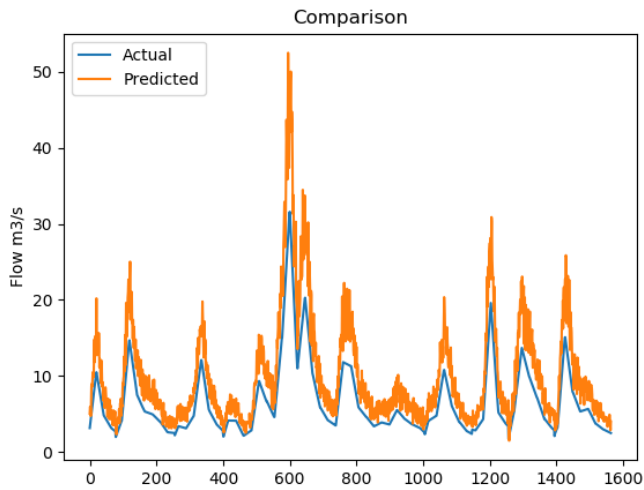


Figure 7.7: MLP result (scenario 3)

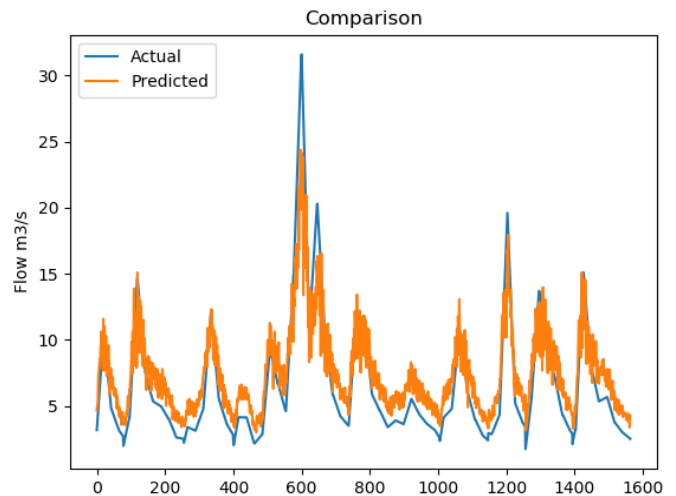


Figure 7.8: RNN result (scenario 3)

*Scenario 4 – GA Optimization*

In this experiment the RNN model parameters configuration is optimized by Genetic Algorithm (GA) from a pool of parameters given in Table 11. The performance of RNN-GA is compared to the previous RNN-GA experiment from scenario 2. The result shows that new RNN-GA is significantly better in prediction RMSE, and is able to predict highest water flow peak at hour 600 with low error margin. The new RNN-GA takes 1.989 seconds longer than the previous model as the network is more complex with 4 layers of 42 neurons. Figure 7.9 shows the prediction comparison of RNN-GA. The RNN-GA model with the WHWFRD dataset is able to predict all cases of floods cases with low RMSE of the HPT dataset.

PARAMETERS	
NUMBER OF NEURONS	4,12,20,32,42,60,70
NUMBER OF LAYERS	2,3,4,5
DROPOUT	0, 0.1, 0.2, 0.3,0.4,0.5
ACTIVATION	relu, elu, tanh, sigmoid, selu, softplus, softsign, hard_sigmoid, linear, softmax
GENERATION	5
POPULATION	15

Table 11: GA parameters (scenario 4)

TECHNIQUE	RNN-GA (SCENARIO 2)	RNN-GA (SCENARIO 4)
MODEL PARAMETERS SELECTED PARAMETERS (RNN-GA)	LSTM(60, activation='softsign', return_sequences=True), LSTM(60, activation='softsign'), LSTM(60, activation='softsign'), Dropout(0.1), Dense(1, activation='linear')	LSTM(42, activation='softsign', return_sequences=True), LSTM(42, activation='softsign'), LSTM(42, activation='softsign'), LSTM(42, activation='softsign'), Dropout(0.1), Dense(1, activation='linear')
TRAINING TIME (S)	24582	24582
TESTING TIME (S)	6.051	8.04
EVALUATION RMSE	0.227	0.973

Table 12: Models Comparison of Scenario 4

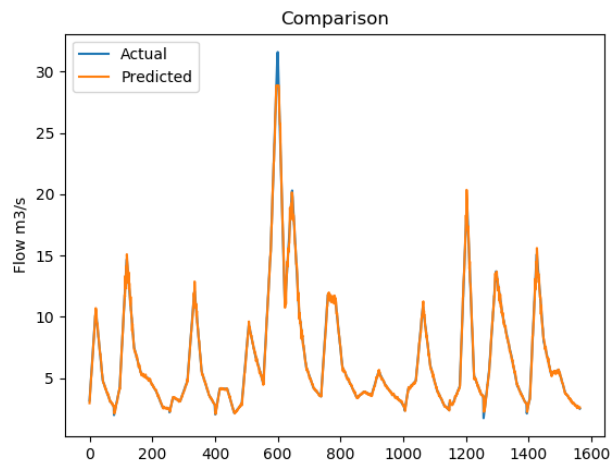


Figure 7.9: RNN-GA result (scenario 4)

### 7.1.3 Performance Analysis

The comparison result in terms of the RMSE is shown in Table 13. It can be seen that RNN-GA outperforms all approaches on both types of dataset. For example, RNN-GA with WHWFRD train dataset and HPT test dataset obtain the lowest RMSE of 0.227. For dataset WHWFR, Higher RMSE are seen across all prediction methods compared to WHWFRD dataset. While RNN-GA obtained the best results in RMSE, we observed that the training time has increased by more than 550 times or around 6.8 hours. We also observed an increase of the test time for RNN-GA, and this is due to the increase of complexity of the network architecture as the network has nearly twice more nodes and twice the number of layers compared to MLP and RNN alone.

	RMSE (m <sup>3</sup> /s)	Training Time (s)	Test set prediction time (s)
<b>MLP (scenario 1)</b>	5.258	41.52	1.519
<b>RNN (scenario 1)</b>	4.874	44.45	4.694
<b>RNN-GA (scenario 2)</b>	0.973	24582	6.051
<b>MLP (scenario 3)</b>	4.409	41.52	1.554
<b>RNN (scenario 3)</b>	2.129	57.52	4.83
<b>RNN-GA (scenario 4)</b>	0.227	24582	8.04

Table 13: Performance Comparison of Experiments

In this section, three prediction techniques have been tested and evaluated in four scenarios along with seven datasets. From these created datasets, two are used to train the models and one is used as test set to evaluate the trained model ability to predict water flow. The two datasets used for training are the WHWFR which represents water flow and rainfall from the period of year 2006 to 2010, processed to reflect the proposed WSN design data collection and WHWFRD which is the same as WHWFR but contains duplicates of the highest water flow and rainfall peaks. The best results with lowest error are obtained with RNN and RNN-GA from scenario 3 and 4 with a RMSE of 2.129 and 0.227, respectively. While RNN-GA has the lowest error, it requires nearly 7 hours to find the best network architecture to train the model compared to less than 1-minute training time of RNN and MLP alone. From the conducted experiments, RNN-GA is considered as the best solution to predict flash flood as high accuracy is critical in nowcasting events of flash floods. The low RMSE on RNN-GA outweigh the high training time as frequent model training is not required, training the model with new data after events of flooding does not stop the previous model from working during the training time. The newly trained model RMSE is compared to the previous model and the new trained model is applied to the nowcasting system only if the model has lower RMSE.

## 7.2 RNN-GA Evaluation

In this section, the trained RNN-GA model is evaluated over normal conditions, low rainfall conditions and very heavy rainfall conditions. The evaluation is presented using seven regression metrics for better understanding. The three scenarios are devised based on four years of data and are as follows: Firstly, a dataset containing normal occurrences of flash floods. Secondly, a dataset containing no flash flood occurrences. Lastly, a dataset containing an excessive number of flash flood occurrences. The outcome of this evaluation is to deduce if the trained nowcasting model is able to provide accurate prediction depending on several weather conditions and if whether frequent training is required.

### 7.2.1 Dataset Creation

In this section, three different datasets are created. The first dataset contains rainfall and waterflow frequency and intensity based on the WRU data from 2006-2010. As seen in Figure 7.10, this dataset contains a few episodes of flash flood as experienced by Mauritius till 2010. The second dataset (as seen in Figure 7.11) simulated over four years contains no occurrence of flash flood depicting mainly long periods of drought. As seen in Figure 7.12, the third dataset simulates an increased number of heavy rainfall and flash flood occurrences for a period of four years.

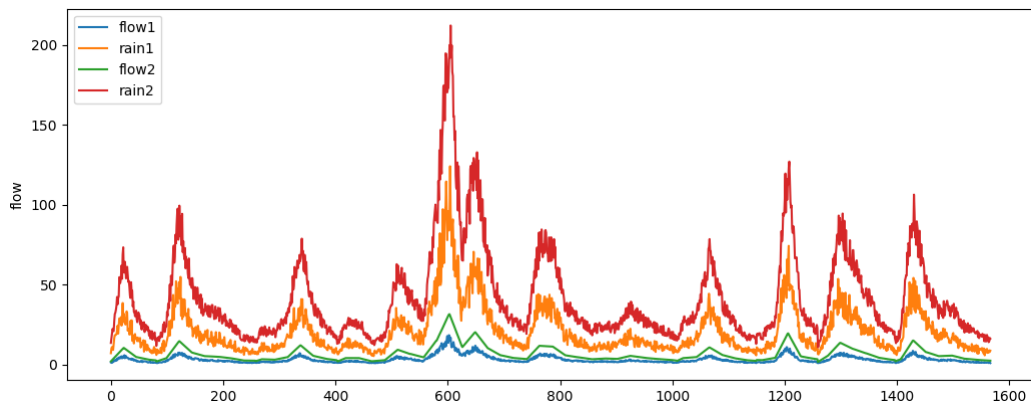


Figure 7.10: Normal

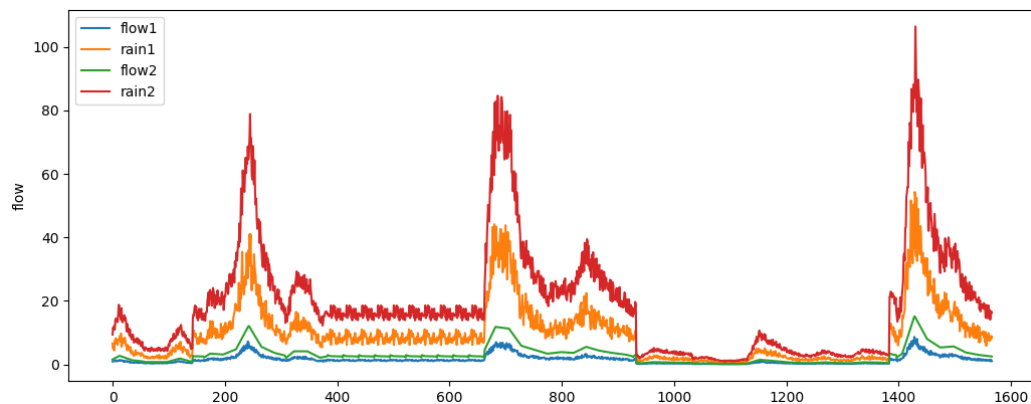


Figure 7.11: Drought

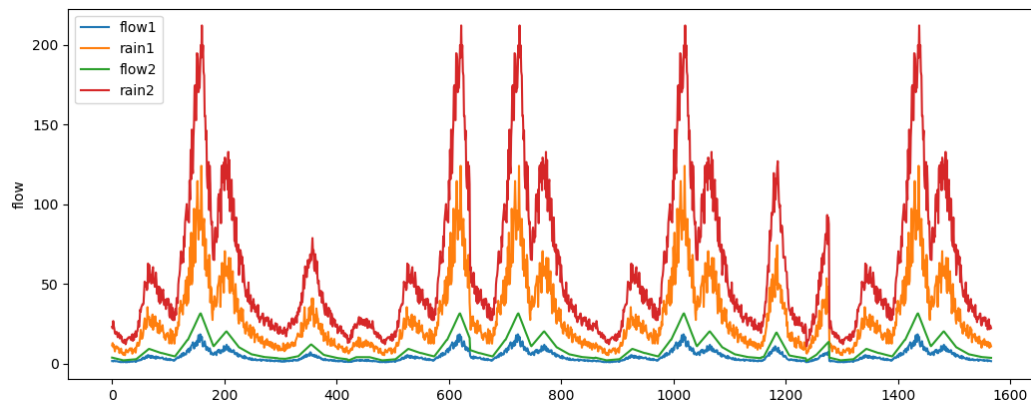


Figure 7.12: Extreme

### 7.2.2 Simulation results

The trained RNN-GA model from Chapter 6, Scenario 4, is evaluated against 3 different dataset scenarios. The conducted experiments are simulations of scenarios that may occur in the following next years. The experiments are evaluated with the following metrics; Mean Squared Error (MSE), Root Mean Squared Error (RMSE), Explained Variance Score (EVS), Mean Absolute Error (MAE), Mean Squared Log Error (MSLE), Median Absolute Error (MeAE), R2 Score (R2). Table 14 below shows the evaluation of the simulations using the mentioned metrics for three main scenarios.

	<b>Normal</b>	<b>Drought</b>	<b>Extreme Flooding</b>
MSE	0.057	0.037	0.235
RMSE	0.227	0.191	0.485
EVS	0.998	0.995	0.995
MAE	0.122	0.073	0.119
MSLE	0.001	0.003	0.002
MEAE	0.066	0.032	0.087
R2	0.998	0.995	0.995

Table 14: Evaluation

After evaluation has been carried out on the 3 scenarios, it is determined that prediction on drought scenario provides the lowest error and results are as expected. Hence, future training on drought or low rainfall should be avoided and filtered out as there are no additional gains in the prediction flash flood. Extreme Flooding has the highest error. Most of the errors occurs at the peak of flash floods occurrences. A model training is therefore required upon each flash flood occurrences and specially if the flooding has exceeded previous records.

### 7.3 General Discussion

The experiments have been conducted using a systematic approach, as most of the rainfall and water flow data have been simulated from information gathered by WRU and MMS. In a first instance, the Machine Learning approach was evaluated, and we conclude that the Recurrent Neural Network with Genetic Algorithm (RNN-GA) provides the highest prediction accuracy with a root mean squared error of 0.227, but at the expense of a relatively high training time of about 6.9 hours. From an operational perspective, this high training time does not necessary affect the proposed solution, as it is expected that subsequent training sessions can be performed in batch. Training eventually takes place before first time usage of the prediction system and is further required after a batch of flash flood occurrences. Since the machine learning technique demonstrates a relative high degree of accurate predictions, a second set of experiments have been conducted to further evaluate the approach in three specific scenarios, i.e. with normal conditions (normal flood conditions), followed by very low rainfall (no flood conditions) and very heavy rainfall (extreme flood conditions). All the simulated data have been approximated from data collected by the WRU from 2006 to 2010. The results demonstrate that the machine learning model performs relatively well in the first two conditions, showing higher degree of accuracy. As for the last case

which contains extreme conditions which have not been experienced by Mauritius, the prediction model requires more training to better account for these new values. As extreme conditions were not part of the initial training set, the third scenario demonstrates that the model must be trained frequently only if patterns of rainfall and water flow leading to flash floods changes drastically. It is nevertheless expected that the model is trained after a few sets of new flash flood events even when there are no, or few changes in patterns.

All the conducted experiments demonstrate that a machine learning approach for the nowcasting of flash flood based on river monitoring is achievable. Nevertheless, the application of the solution requires specific training set data collected over different weather and topological conditions in different parts of the island over several years with flash flood occurrences. This chapter (and the study) is limited by the lack of such data sets. It can be enhanced with the setting up of the proposed wireless sensor network for real time data collection. Furthermore, all experiments have been conducted on a specific simulated river with a specific set of characteristics. The prediction results therefore, cannot be directly applied to all rivers/canals around the island. Extended research from a hydrological perspective is required to further assess the system in various different real-world conditions.

## Chapter 8 – Conclusion & Future Works

In this chapter, a detailed summary of every phases of the research study is presented. The summary covers the initial part of the research study, starting with the literature review till the design and development of the system and the evaluation of Machine Learning Engine.

### 8.1 Research Summary

This research study investigates the possibility of predicting flash flood occurrences in Mauritius using an intelligent automated system. As flash floods are a relatively new phenomenon in Mauritius, not enough work is available at national level towards its prediction. The topology of the island indicates a relative steep slope towards sea level which when combined with heavy rainfall events causes rapid water flow in large volumes which can be dangerous specially with flow obstructions at bridges and high soil saturation levels. Increased urbanisation also contributes to the increased risk and occurrences of flash floods.

Different types of ICT based systems exist or have been proposed for the prediction of floods around the world. They mainly involve the use of sensors or satellite images to capture data. The core of these systems consists mainly of a statistical prediction model, and very few implementations are based on modern machine learning techniques, although their rate of success is satisfactory. Deep Learning is a recent ML technique which has proved to be very effective in various domains.

While modern ML techniques might be producing interesting prediction results, there is a need for specific data to be collected and fed into the system. It is a sine qua non for successful results from modern machine learning techniques. Rainfall, water level, temperature, soil moisture, land topology, humidity and wind speed are some of the data used in flood prediction systems. Moreover, some systems use satellite and radar images. Data availability is limited to the Mauritius Meteorological Services (MMS) and the Water Resources Unit (WRU) in the Mauritian context. As at now, the MMS can provide near real time data, with a window of 3 hours, for all recorded parameters from its two main stations located in the central part of the island, the Vacoas Station and in the South East, Plaisance Station although there are various other stations around the island. Its only during special situations, that data are collected and analysed on an hourly basis. The Water Resources Unit is responsible for the assessment, mobilisation, control, development, management and conservation of water resources in Mauritius. It is understood that they use around 150 gauging stations around the island to collect water flow and level in canals and rivers. This data is available from 2006 to 2010 and contains only certain canal/rivers. Reconciling the data between these two institutions have been one of the major difficulties experienced by this study.

A system which focuses on three main aspects has been proposed and designed. The first element of the system is a Wireless Sensor Network (WSN) for monitoring water flow at natural and man-made canals/rivers. This wireless network of nodes can transfer data in real time to a main station, which feeds the data into the second element of the system, the Machine Learning Engine. The data needs to be divided into a training and testing set. The Machine Learning algorithm requires training on various scenarios (from normal to extreme conditions, with parameters such as velocity of water flow, height of water level, temperature, etc) which is not available. Therefore, a combination of existing data has been used to simulate the output of WSN. Once simulated the data is fed into the system to train a Machine Learning algorithm which generates a prediction model. The latter can further flag for possible occurrences of possible flash flood events in real-time based on amount of rainfall. The design also caters for a web interface design which provides notifications to users.

During implementation of the system, it has been decided to simulate the WSN system as it involves setting up various infrastructures in canals/ivers from which data can be collected. Also, in the first instant, such an infrastructure will not be effective for training the model. Therefore, a laboratory simulation was devised to determine the feasibility of the WSN System. An extended version of the existing data available from the MMS and WRU has been used to further generate data for training the machine learning model, using a Recurrent Neural Network approach. A Web Interface was successfully implemented which shows the current values and the model's predictions.

Since most of the data used in the system have been generated by simulation, our evaluation focused on the efficiency of the prediction model. Several experiments with different datasets and machine learning algorithms have been conducted and the Recurrent Neural Network (RNN) optimised with Genetic Algorithm (GA) showed the lowest error in prediction when compared with other approaches. We further evaluated the trained model with different sets of data in order to distinguish from, and avoid overfitting. These experiments show that data corresponding to past weather conditions in Mauritius provides a better result when compared to the extreme conditions. Results demonstrate a root mean squared error of only 0.227 m<sup>3</sup>/s for the prediction of flash flood. As global warming is creating new patterns of weather conditions, it is important that the model is trained after every new flash flood occurrence. This will contribute to maintain and further increase its accuracy.

## 8.2 Research Limitations

The main challenge of this research work is two-fold. Firstly, it is limited to the type of data available. Data currently available can hardly be used for real time nowcasting of flash floods as most of the institutions work in isolation. For example, with features such as rainfall, temperature (Maximum, minimum, dry bulb, wet bulb and dew point) and relative humidity are not effective for the prediction of flash floods. As for river monitoring data, it is not available for all rivers of the island and for specific time periods. Given all these constraints, we made some reconstructions based on specific dates of events, using water flow for one specific river and the amount of rainfall. Eventually, more parameters can provide better insights. Different data capture techniques, concepts, tools and frequency of monitoring must be considered. The second major issue experienced is the setting up of the proposed WSN infrastructure, which requires much more resources as initially expected. Therefore, results from the study must be taken with caution and avoid generalisation without performing more realistic (out of laboratory) experiments.

## 8.3 Future Works

In an attempt to further enhance the Flash Flood Nowcasting system, the Wireless Sensor Network needs to be setup in a real world setting for data collection. Various sensors have been identified during the research work, but they need to be tested in the context of our local rivers/canals to identify their effectiveness, lifetime and limitations. In the meantime, since data is limited, we believe that more datasets with various features need to be simulated in various topologies and river configurations to better assess the generalisation of the results.

## References

- Abdul-Kader, H. et al., 2018. Forecasting Rainfall based on Computational Intelligent Techniques. *International Journal of Computer Applications*, 180(23), pp. 33-36.
- Artigue, G., Johannet, A., Borrell, V. & Pistre, S., 2011. Flash floods forecasting without rainfalls forecasts by recurrent neural networks. Case study on the Mialet basin (Southern France). *Nature and Biologically Inspired Computing (NaBIC), 2011 Third World Congress on*, pp. 303-310.
- Basha, E., Ravela, S. & Rus, D., 2008. *Model-based monitoring for early warning flood detection*. s.l., ACM, pp. 295-308.
- Birkmann, J., Garschagen, M., Mucke, P., Schauder, A., Seibert, T., Welle, T., Rhyner, J., Kohler, S., Loster, T., Reinhard, D. and Matuschke, I., 2014. *World Risk Report*, s.l.: s.n.
- Blöschl, G., Reszler, C. & Komma, J., 2007. A Spatially distributed flash flood forecasting model. *Environmental Modelling & Software*, pp. 464-478.
- Blöschl, G., Reszler, C. & Komma, J., 2008. A spatially distributed flash flood forecasting model. *Environmental Modelling & Software*, 23(4), pp. 464-478.
- Boukharouba, K., Roussel, P., Dreyfus, G. & Johannet, A., 2013. Flash flood forecasting using Support Vector Regression: An event clustering based approach. *Machine Learning for Signal Processing (MLSP)*, pp. 1-6.
- Cabinet Decision, 2008. *Cabinet Decision*. [Online]  
Available at: <http://pmo.govmu.org/English/Pages/Cabinet-Decisions-taken-on-28--March-2008.aspx>  
[Accessed 30 11 2016].
- Caicedo-Ortiz, J. et al., 2018. Monitoring system for agronomic variables based in WSN technology on cassava crops. *Computers and Electronics in Agriculture*, Volume 145, pp. 275-281.
- Chang, F., Chang, L. & Huang, H., 2002. Real-time recurrent learning neural network for stream-flow forecasting. *Hydrological processes*, 16(13), pp. 2577-2588.
- Chang, F. et al., 2014. Watershed rainfall forecasting using neuro-fuzzy networks with the assimilation of multi-sensor information. *Journal of hydrology*, Volume 588, pp. 374-384.
- Chiang, Y.-M. et al., 2007. Merging multiple precipitation sources for flash flood. *Journal of Hydrology*, pp. 183-196.
- Climate NASA, 2018. *Global Climate Change: Vital Signs of the Planet*. [Online]  
Available at: <https://climate.nasa.gov/>  
[Accessed 20 January 2018].
- Collier, C., 2007. Flash flood forecasting: What are the limits of predictability?. *Quarterly Journal of the royal meteorological society*, 133(622), pp. 3-23.
- De Roo, A. et al., 2003. Development of a European flood forecasting system. *International Journal of River Basin Management*, 1(1), pp. 49-59.

De Roo, A. et al., 2001. Assessing the effects of land use changes on floods in the Meuse and Oder catchment. *Physics and Chemistry of the Earth, Part B: Hydrology, Oceans and Atmosphere*, 26(7-8), pp. 539-599.

De Roo, A., Wesseling, C. & Van Deursen, W., 2000. Physically based river basin modelling within a GIS: the LISFLOOD model. *Hydrological Processes*, 14(11-12), pp. 1981-1992.

Defi Media Group, 2013. *Floods: What Economic Impact*. [Online]  
Available at: <https://business.mega.mu/2013/04/04/floods-what-economic-impact/>  
[Accessed February 2018].

DesInventar, n.d. *DesInventar*. [Online]  
Available at: <https://www.desinventar.net/DesInventar/profiletab.jsp>  
[Accessed 18 03 2018].

Dolcine, L., Andrieu, H., Sempere-Torres, D. & Creutin, D., 2001. Flash flood forecasting with coupled precipitation model in mountainous Mediterranean basin. *Journal of Hydrologic Engineering*, 6(1), pp. 1-10.

Doocy, S. et al., 2013. *The human impact of earthquakes: a historical review of events 1980-2009 and systematic literature review*, s.l.: PLoS currents.

Doswell III, C., Brooks, H. & Maddox, R., 1996. Flash flood forecasting: An ingredients-based methodology. *Weather and Forecasting*, 11(4), pp. 560-581.

Elnaggar, O., Ramadan, R. & Fayek, M., 2015. WSN in monitoring oil pipelines using ACO and GA. *Procedia Computer Science*, Volume 52, pp. 1198-1205.

Furquim, G. et al., 2014. *Combining wireless sensor networks and machine learning for flash flood nowcasting*. s.l., IEEE, pp. 67-72.

Grillakis, M., Tsanis, I. & Koutroulis, A., 2010. Application of the HBV hydrological model in a flash flood case in Slovenia. *Natural Hazards and Earth System Sciences*, 10(12), p. 2713.

Guesmi, H., 2017. Wireless Smart Sensor Networks for Real-Time Warning System of Flash Floods and Torrents in KSA. *International Journal of Computer Applications*, 165(6), pp. 14-21.

Hapuarachchi, H., Wang, Q. & Pagano, T., 2011. A review of advances in flash flood forecasting. *Hydrological Processes*, 25(18), pp. 2771-2784.

Honga, Y., Hsub, K.-L., Sorooshian, S. & Gao, X., 2004. Precipitation Estimation from Remotely Sensed Imagery Using an Artificial Neural Network Cloud Classification System. *Journal of Applied Meteorology*, 43(12), pp. 1834-1852.

INDC, 2015. *Intended Nationally Determined Contribution For The Republic of Mauritius*, s.l.: s.n.

Junie, P. et al., 2012. A WSN based monitoring system for oil and gas transportation through pipelines. *IFAC Proceedings Volumes*, 45(6), pp. 1796-1801.

Mauritius Meteorological Services, 2017. *Météo: la saison cyclonique étalée du 1er novembre au 15 mai*. [Online]

Available at: <https://www.lexpress.mu/article/319734/audio-meteo-saison-cyclonique-etalee-1er-novembre-au-15-mai>

Mauritius Meteorological Services, 2017. *Météo: la saison cyclonique étalée du 1er novembre au 15 mai*. [Online] Available at: <https://www.lexpress.mu/article/319734/audio-meteo-saison-cyclonique-etalee-1er-novembre-au-15-mai> [Accessed 07 November 2017].

Mauritius Meteorological Services, 2018. *Torrential Rain Warning System*. [Online] Available at: <http://metservice.intnet.mu/torrential-rain/torrential-rain-warning-system.php> [Accessed 30 January 2018].

Ministry of Environment and Sustainable Development Division, 2015. *Climate Change Information Centre*. [Online] Available at: [http://environment.govmu.org/English/Climate\\_Change/Pages/CCIC.aspx](http://environment.govmu.org/English/Climate_Change/Pages/CCIC.aspx) [Accessed February 2018].

NDRRMC, 2017. *List of Known Flood Prone Areas*, Mauritius: Ministry of Civil Service and Administrative Reforms.

Ng, E., 2013. *Eric Ng: "Rs 400-500 Millions Damage Caused by Floods"*. [Online] Available at: <https://business.mega.mu/2013/04/04/eric-ng-rs-400-500-millions-damage-caused-floods/>

Office of the Director of Public Prosecutions, 2015. *DPP Press Release*, s.l.: Office of the Director of Public Prosecutions.

PQ Written Answers, 2013. *PQ Written Answers*. [Online] Available at: <http://mauritiusassembly.govmu.org/English/Pages/Answers/PQ-Written/2013/pqanswritten16april2013.pdf> [Accessed 30 11 2016].

Sharif, H., Yates, D., Roberts, R. & Mueller, C., 2006. The use of an automated nowcasting system to forecast flash floods in an urban watershed. *Journal of Hydrometeorology*, 7(1), pp. 190-202.

Trenberth, K. E., 2011. Changes in precipitation with climate change. *Climate Research*, 47(1/2), pp. 123-138.

U.S Global Change Research Program, 2014. *Extreme Weather*. [Online] Available at: <https://nca2014.globalchange.gov/highlights/report-findings/extreme-weather> [Accessed February 2018].

Wang, Y., Haiden, T. & Kann, A., 2006. The operational limited area modelling system at ZAMG: ALADIN-AUSTRIA. *Zentralanstalt für Meteorologie und Geodynamik*.

Wu, C. & Chau, K., 2006. *Evaluation of several algorithms in forecasting flood*. Berlin, Heidelberg, International Conference on Industrial, Engineering and Other Applications of Applied Intelligent Systems. Springer, pp. 111-116.

Yang, H. & Su, C., 2015. Real-time river bed scour monitoring and synchronous maximum depth data collected during Typhoon Soulik in 2013. *Hydrological processes*, 29(6), pp. 1056-1068.

## Appendix A

### List of Known Flood Prone Areas



**MINISTRY OF CIVIL SERVICE AND ADMINISTRATIVE REFORMS  
MAURITIUS**

20 November 2017

**Ministry of Civil Service and Administrative Reforms  
Circular Note No. 30 of 2017  
E/60/30/01 V4**

**From: Secretary for Public Service**

**To: Supervising Officers in-Charge of Ministries/Departments  
Island Chief Executive, Rodrigues Regional Assembly**

**Protocol on Heavy Rainfall for the Public Sector – List of Known Flood Prone Areas**

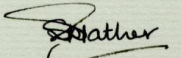
Reference is made to the Protocol on Heavy Rainfall for the Public Sector which was issued on 03 April 2017 and wherein, at paragraph 4 (iv), it has been stated that “an updated list of flood prone areas be kept readily available” for the proper implementation of the Protocol.

2. At the 8<sup>th</sup> National Disaster Risk Reduction and Management Council’s Meeting, it has been agreed that the list of known flood prone areas be included in the Protocol. Accordingly, the Ministry of Social Security, National Solidarity and Environment and Sustainable Development (Environment and Sustainable Development Division) has submitted the relevant list (a copy is herewith enclosed) for incorporation in the Protocol.

3. It is to be noted that the attached list indicates the known flood prone areas as at 24 October 2017. Attention is also being drawn to the disclaimer note placed therein by the National Disaster Risk Reduction and Management Centre to the effect that:

*“This list has been produced solely for the purpose of the Protocol on Heavy Rainfall for the Public Sector and is not meant to be relied on or used by entities or individuals other than those involved in the implementation of the Protocol on Heavy Rainfall for the Public Sector. Although reasonable care and skill has been taken to include in the above list all flood prone Sites in Mauritius, the above list is only meant to be an indicative and non – exhaustive list of the flood – prone areas in Mauritius. Thus, sites which due to unforeseen circumstances, become flooded, may not have been included in the above list. Further, the list may be amended from time to time to include or exclude further flood – prone areas depending on changing circumstances. The National Disaster Risk Reduction and Management Centre shall not bear any liability, legal or otherwise, with respect to any information provided in the above list and / or any use made of and/ or reliance placed on the list and/ or any other matter associated with this list.”*

4. The list of known flood prone areas as at 24 October 2017 is sent to you for inclusion in the Protocol; and I should appreciate if you could cause needful to be done.

  
**S. K. Pather**  
Secretary for Public Service

Copy to: Secretary to Cabinet and Head of the Civil Service

SICOM Building 2, Cnr Chevreau & Rev. Jean Lebrun Streets, Port Louis  
Tel No: 405 4100 Email: civser@govmu.org

**Permanent Secretary, Ministry of Social Security, National Solidarity, and Environment  
and Sustainable Development  
(Environment and Sustainable Development Division)**

**National Disaster Risk Reduction and Management Centre**

**List of Known Flood Prone Areas  
(24 October 2017)**

<b>SN</b>	<b>Location</b>	<b>Nature</b>
<b>Port Louis</b>		
1	Canal Dayot	Flooding of residential area at Canal Dayot and Riviere St Louis
2	Sable Noir	Flooding of residential area near old bridge
3	Bell Village	Flooding of M1 road
4	Port Louis	Flooding along Le Pouce stream
5	Port Louis	Flooding along Ruisseau des Creoles
6	Port Louis	Flooding in front Jeetoo Hospital
7	Port Louis	Flooding at Camp Mana, Tranquebar
8	Port Louis	Flooding at Le Cornu residential area
9	Port Louis	Flooding along La Poudriere Street including Cine City and Jardin Campanie
10	Cite La Cure	Flooding at Pont Marjolin and Pont Sophia
11	Saint Croix	Flooding of residential area at Captain Pontre
<b>Pamplemousses</b>		
12	Fond du Sac	Flooding at Government School, football playground, Subash Chandra Bose Street, Shakespeare Street, Filling station and State Bank of Mauritius, Shivala Lane, Tagore Lane, Mahatma Gandhi Road, Kallee Lane
13	Pamplemousses	Flooding at Belle Eau (Behind Botanical Garden), Bois Rouge near Football ground, Morcellement Ripailles, Belle source, Derby Lane
14	Terre Rouge	Flooding on main road near RDA
15	Riche Terre	Flooding at Cite Roma and Jumbo round about
16	Bois Marchand	Flooding behind PADCO Warehouse
<b>Rivière du Rempart</b>		
17	Mapou	Flooding at Mapou round about
18	Gokoola	Flooding

19	Barlow	Flooding at entrance of Barlow to Amaury
20	Cottage	Flooding at Cite CHA and John Kennedy Street
21	Grand Baie	Flooding at Camp Carol due to wetland
22	Riviere du Rempart	Flooding at Schoenfeld Road, Riverside Bridge and Cite Riverside near Riverside Commercial Centre
23	Roche Noire	Flooding at link road Roche Noire/Poste La Fayette
24	Pereybere	Flooding at Beach Lane due to wetland
25	Beau Sejour	Flooding from Mont Piton on main road at Beau Sejour
<b>Flacq</b>		
26	Clemencia	Flooding of main road at bridges
27	Centre de Flacq	Flooding of Eastern College Lane, Cite Hibiscus
28	Argy	Flooding at Argy Bridge and Cite Argy
29	Sebastopol	Flooding of Lesur main road
30	Poste de Flacq	Flood at Camp Poorun and Cite Debarcadere
<b>Grand Port</b>		
31	Camp Carol, Le Bouchon	Flooding at Courteau Lane Le Bouchon
32	Carreau Accacia	Flooding at Rishi Dayanand Road
33	Bambous Virieux	Flooding near Football playground, bridge on main road
34	Anse Jonchee	Flooding at Anse Jonchee bridge
35	Mare Tabac	Flooding at School Lane, NHDC near Naiko house
36	Petit Bel Air	Flooding at Rishi Dayanand Road, Pandit Kistoe Street
37	Trois Boutiques	Flooding at Pillay Lane, near Pre-primary school. Main Road near Community Centre, Gooranah Lane, Bombay Street
38	Plaine Magnien	Flooding at Cite L'Anglois
<b>Savanne</b>		
39	Souillac	Flooding at Morcellement Brise de Mer
40	Surinam	Flooding at Virahsawmy Lane

41	Bel Ombre	Flooding of residential area (Cite Bel Ombre), Jumbo, Berry Lane. Flooding of St Martin bridge
42	Riviere du Poste	Flooding near round about, Traffic centre, Camp Rabeau and bridge on main road
43	Camp Diable	Flooding at St Armand Bridge, near Tookay Kovil
44	Grand Bois	Flooding at Camp Bananes, Royal Road near CAB
45	L'Escalier	Flooding at Morcellement Camp Tagore, Chattergoon Road, VRS 2
46	La Flora	Flooding at Matoo Street, Baruthsing opposite sub hall
<b>Black River</b>		
47	Case Noyale	Flooding of bridge and road adjoining mangrove site and near church
48	Chamarel	Flooding of Pere D'Arifat bridge
49	Riviere Noire	Flooding of road at La Balise
50	Flic en Flac	Flooding of low lying residential area in Morcellement De Chazal
51	Bambous	Flooding at Avenue Folles Herbes, Cite La Ferme and Geoffroy Road
52	Albion	Flood at bridge near Albion Fisheries Research Centre
<b>Beau Bassin Rose Hill</b>		
53	Berthaud Corp de Garde/Boundary, Stanley Rose Hill	Flooding
54	Coromandel	Flood at Champman View, Royal Road, Emmaus Street, Pave D'amour road
55	Riche Lieu	Flooding at branch road
<b>Quatre Bornes</b>		
56	Quatres Bornes	Flooding at Ave Ollier, Coodien Lane, La Source, Avenue Berthaud (Corps de Garde)
<b>Vacoas Phoenix</b>		
57	Vacoas	Flood at Chasteau Street, Allyman lane La Caverne
58	Henrietta	Flooding at Camp Belin

59	La Marie	Flooding at Malakoff and Accacia No. 5
60	St Paul	Flooding of residential areas at St Paul junction, residential area adjoining Promenade Pere Laval
61	Belle Terre	Flooding of residential area
<b>Curepipe</b>		
62	Curepipe	Flooding at Gold Crest Lane, Cite St Luc, Couvent Lorette Street
<b>Moka</b>		
63	Montagne Ory	Flooding of M1
64	Lesperance	Flooding of Riviere Francoise
65	Montagne Blanche	Flooding at Morcellement Sans Souci

**Disclaimer:**

*This list has been produced solely for the purpose of the Protocol on Heavy Rainfall for the Public Sector and is not meant to be relied on or used by entities or individuals other than those involved in the implementation of the Protocol on Heavy Rainfall for the Public Sector. Although reasonable care and skill has been taken to include in the above list all flood-prone Sites in Mauritius, the above list is only meant to be an indicative and non-exhaustive list of the flood-prone areas in Mauritius. Thus, sites which due to unforeseen circumstances, become flooded, may not have been included in the above list. Further, the list may be amended from time to time to include or exclude further flood-prone areas depending on changing circumstances. The National Disaster Risk Reduction and Management Centre shall not bear any liability, legal or otherwise, with respect to any information provided in the above list and/or any use made of and/or reliance placed on the list and/or any other matter associated with this list.*

NDRRMC, 24 October 2017

**PRESS RELEASE**

**Judicial Enquiry into the cause of death of Jeffrey Allan Wright, Sylvia Wright (born Fokeer), Toolsee Ram Ramdhari, Pravin Kumar Khoosye, Karmish Saligram Tewary, Dhanraj Saligram Tewary, Retnon Sithanen, Rabindranath Bhubany, Fan Lan Wong Tat Chong Lai Kim and Stevenson Henriette who died during the floods of 30<sup>th</sup> March 2013.**

Following the enquiry carried out by the police into the cause of death of 1) Jeffrey Allan Wright; 2) Sylvia Wright (born Fokeer); 3) Toolsee Ram Ramdhari; 4) Pravin Kumar Khoosye; 5) Karmish Saligram Tewary; 6) Dhanraj Saligram Tewary; 7) Retnon Sithanen; 8) Rabindranath Bhubany; 9) Fan Lan Wong Tat Chong

Lai Kim and 10) Stevenson Henriette, the Office of the Director of Public Prosecutions instituted a Judicial Enquiry before the District Court of Port Louis on the 4<sup>th</sup> March 2014 pursuant to sections 111 and 112 of the District and Intermediate Courts (Criminal Jurisdiction) Act.

The proceedings started before the Learned Magistrate Mrs Ida Dookhy-Rambarun, on the 21<sup>st</sup> April 2014 and 97 witnesses including the relatives of the deceased, representatives of the Police Force, Fire Services, Mauritius Meteorological Services, Rapid Security Services, Caudan Security Services, Prime Minister's Office, National Disaster Risk Reduction and Management Centre, the National Development Unit, the Ministry of Public Infrastructure and the Ministry of Housing and Lands were heard. CCTV footages of the events were also viewed. The proceedings were completed on the 15<sup>th</sup> July 2014. On the 29<sup>th</sup> December 2014, the findings of the Learned Magistrate were communicated to the Director of Public Prosecutions.

**A. Background facts**

The learned Magistrate found established the following background facts:

- (a) On the 30<sup>th</sup> March 2013, following the heavy flooding in Port-Louis, ten persons lost their lives. The bodies of six persons namely Jeffrey Allan Wright, Sylvia Wright (born Fokeer), Toolsee Ram Ramdhari, Pravin Kumar Khoosye, Karmish Saligram Tewary and Dhanraj Saligram Tewary were retrieved from the Caudan underpass. The bodies of Rabindranath Bhubany and Fan Lan Wong Tat Chong Lai Kim were retrieved from the underground parking of Harbourfront Building. The body of Retnon Sithanen was found in Company Garden while the body of Stevenson Henriette was found near KFC of Chaussée Street.
- (b) More than 136mm of rain fell within two hours i.e. between 13h00 and 16h00. Members of the public were taken by surprise by the sudden downpour.

- (c) The city centre is surrounded inland by a mountain range and because of the steep mountain slopes, the storm water generated reaches the foot of the mountain very quickly. The water crosses the city area in a very short time through the existing water courses to reach the sea.
- (d) The Port Louis area between the Caudan Flyover and the Place D'Armes is drained by four main water courses namely the Deviation Canal which runs along Signal Mountain Road, the drain along Volcy Pougnet Street, Le Pouce Stream which passes behind Cinema Majestic and Le Pouce Canal which passes in front of the Museum and Shoprite Supermarket. These main water courses were completely flooded.
- (e) After the flooding some 300 tons of debris and garbage were removed from the drains. The debris included mattresses, old fridge, iron sheets, plastic bags, bottles and vegetation.
- (f) The cumulative effect of the deficient drainage system and the surface run-off generated with the urban area has contributed to the flooding.

## **B. Assessment of the role of various government Agencies**

The Learned Magistrate commended the assistance provided by officers of the Special Supporting Unit, the National Coast Guard, the Special Mobile Force, the Helicopter Squadron, the GIPM and the Fire Services. Based on the evidence in front of her, she identified a number of disturbing institutional failures:

### **(a) The Mauritius Meteorological Services (MMS)**

The special bulletin of the MMS came relatively late when several places were already flooded so that there was little room for precautionary measures.

The absence of a weather radar presented a serious shortcoming in the weather monitoring system. The forecasters did not resort to other resources which were available such as the weather forecast of Reunion Island.

The MMS cannot vouch about the amount of rainfall that fell on Signal Mountain. An automatic Weather Station and a weather radar would have helped the MMS to give a more precise forecast.

The MMS is not equipped in terms of knowledge and skills to predict flash floods. The MMS alone with its data cannot forecast flash floods. Other Stakeholders like the Water Resources Unit, the Ministry of Public Infrastructure and Local Authorities need to provide their input.

**(b) The Water Resources Unit (WRU)**

Whilst the Water Resources Unit should be a major stakeholder for the forecasting of floods, it lacks required expertise in flooding.

**(c) The National Disaster Operations and Coordination Centre (NDOCC)**

The NDOCC was not equipped to deal with the flash floods of the 30<sup>th</sup> March 2013. The Cyclone and Other Natural Disaster Scheme 2012-2013 did not make any provision for flash floods.

**(d) Police and Fire Services**

The Police as well as the Fire Services faced communication problems on the 30<sup>th</sup> March 2013. The telephone network was clogged and people could not reach the Fire Services. The Fire Services did not have sufficient manpower to deal with the situation.

**(e) The Municipal Council of Port-Louis, the Ministry of Public Infrastructure (MPI), the Ministry of Environment and Sustainable Development and the National Development Unit**

There was lack of coordination between the relevant Authorities as to the maintenance of several major drains. Due to lack of maintenance, some major cut-off drains have been reduced to a poor state and this has contributed to the major flood in Port-Louis.

Furthermore, in some places the drains were unlined. In other places the drains have undergone physical damage and have not been repaired. The capacity of drains has been reduced due to pavement structure or vegetation growth. There are illegal constructions by the citizens on drains or by the side of existing drains.

A number of properties dispose of their roof and yard storm water on the road immediately in front of their premises.

**C. Constructions and other obstructions in Le Pouce Stream and Le Pouce Canal**

Structures on Le Pouce Stream and Le Pouce Canal which have been allowed by the Authorities have reduced the cross sectional area of the canals, for instance the construction of KFC building on Chaussée Street on Le Pouce Canal. The foundation of the building is on the drain and it creates an obstacle for the water flow. Similarly, in respect of the covered spaces of Air Mauritius Parking, Rogers Parking, Hawkers palace and Garden Tower, columns have been casted on the river course. The metal gate which has been placed on Le Pouce Canal near the museum hindered the flow of water. Pipelines of the Central Water Authority, Waste Water Management Authority and of the Mauritius Telecom were found running across the water channels.

**D. Causes leading to the death of the deceased persons**

(a) Retnon Sithanen accidentally fell in Ruisseau Le Pouce and got swept away.

- (b) Stevenson Henriette was carried away by the flood water and his body was stuck next to KFC Building of La Chaussée Street.
- (c) In respect of the two casualties inside the Harbour front parking, there was heavy flow of water entering the parking and metal barrier had collapsed with the water pressure. Only one of the three accesses to the parking had been blocked by the security officers. The cameras inside the parking were not working. The water pumps were in working condition but were insufficient. The security officers had been taken by surprise and were not prepared for the situation.
- (d) In respect of the six casualties inside the Caudan Underpass which was completely flooded, the Court highlighted that nobody expected the underpass to be submerged completely. The camera was defective. The water pumps were inadequate. The measure of having a security officer inside the underpass on a permanent basis for the security of the tenants and users was ineffective. The security officers failed to close the gates of the underpass in order to prevent people from acceding to it. The underpass was not equipped for flooding water.

#### **E. Pertinent Observations by the Learned Magistrate**

- (a) There must be in place a weather radar in Mauritius as well as an Automatic Weather Station in the region where the rain fell on the 30<sup>th</sup> March 2013.
- (b) The practice of the MMS must be revisited so that there is more proactive response if such situations arise in the future.
- (c) The MMS should make maximum use of the data available from the weather radar from Reunion Island as well as other data which may be accessible on the internet, pending the availability of a weather radar. Forecasters should also bear in mind the general effects and consequences of climatic change worldwide.
- (d) The MMS and the WRU must collaborate fully so that information is disseminated efficiently and in time to the National Disaster Risk Reduction and Management Centre.
- (e) Mauritius must make appropriate investments in capacity building, technology development, social infrastructure and sustainability so as to be better prepared to face the phenomenon.
- (f) There should be better maintenance of drains and better coordination between the relevant authorities in relation to the maintenance of drains.
- (g) As per the recommendations of the consultants, all structures over the waterways must be removed to facilitate water flow.

- (h) There must be an overall strategy to address the problem of flooding and there is a need for appropriate infrastructure for drains in Port-Louis.
- (i) Awareness must be created amongst the public and the communication network must be strengthened. There should be an alarm system so that the public can be warned in a timely manner. The PIOR (Police Information Room) should be used to enhance timely coordination between all relevant bodies.
- (j) Persons in charge of the security of the public should be given adequate training so that they are fully equipped to face the crisis. The framework within which companies offering security services operate must be revisited.

**Office of the Director of Public Prosecutions 6<sup>th</sup> January 2015**

## Flood Damages



Figure A.1: Canal Dayot



Figure A.2: Poste-de-Flacq



Figure A.3: Montagne Blanche



Figure A.4: Music Instruments Shop, La Louise, Quatre-Bornes



Figure A.5: La Louise, Quatre-Bornes



Figure A.6: Albion



Figure A.7: Baie-du-Tombeau



Figure A.8: River in Vacoas

## Flash Flood Forecasting/Nowcasting Algorithms

### A.4.1 Basha (2008) flood prediction linear regression algorithm.

The forecasting algorithm below is a multiple linear regression model. Inputs of past flow ( $\phi$ ), air temperature ( $\theta$ ), and rainfall ( $\rho$ ), defining their orders as N, P, and Q respectively, and a single output, predicted river flow ( $Y$ ) By weighting the past N observations of all relevant input variables taken at time  $t$  to produce a prediction of the output variable at time  $t + T_L$ . To determine the weighting factors, some amount of data is designated as the training set for the model, defined here as the data seen in time  $T_T$  (an application-defined parameter), and a simple inversion-multiply operation provides the coefficients from this data, which is the prediction model until recalibration occurs, defined as a time window of length  $T_R$ . The model self-calibrates, can use very little training data (on the order of weeks).

---

**Algorithm 1** Flood Prediction Algorithm

---

```
1:  $\phi$  : past flow
2:  $\theta$  : air temperature
3:  $\rho$  : rainfall
4:  $N$  : # past flow values used
5:  $Q$  : # rainfall values used
6:  $P$  : # air temperature values used
7:  $Y$  : predicted flow
8:  $e$  : prediction error
9:  $T_T$  : training time window
10:  $T_L$  : prediction lead time
11:  $T_R$  : recalibration time window
12:
13:  $T_{TL} = T_T - T_L$ ;
14:      $\triangleright$  Compute initial coefficients and prediction
15:  $\phi_N \leftarrow [\phi(1 : T_{TL} - N), \dots, \phi(1 + N : T_{TL})]$ 
16:  $\theta_P \leftarrow [\theta(1 : T_{TL} - P), \dots, \theta(1 + P : T_{TL})]$ 
17:  $\rho_Q \leftarrow [\rho(1 : T_{TL} - Q), \dots, \rho(1 + Q : T_{TL})]$ 
18:  $X \leftarrow [\phi_N, \theta_P, \rho_Q]$ 
19:  $C = ((X * X^T)^{-1} * X^T) * Y(1 + T_L : T_T)$ 
20:  $Y(1 + T_L : T_T) = X * C$ 
21:      $\triangleright$  Recompute using prediction error
22:  $e = Y(1 + T_L : T_T) - \phi(1 : T_T - T_L)$ 
23:  $X \leftarrow [\phi_N, e, \theta_P, \rho_Q]$ 
24:  $C = ((X * X^T)^{-1} * X^T) * Y(1 + T_L : T_T)$ 
25:  $Y(1 + T_L : T_T) = X * C$ 
26:
27: for  $t = T_T + 1$  to ... do            $\triangleright$  Forecast
28:     if  $(t \% T_R) == 0$  then
29:          $\triangleright$  Recalibrate coefficients
30:          $e = Y(t - T_T : t) - \phi(t - T_T - T_L : t - T_L)$ 
31:          $\phi_N \leftarrow [\phi(t - T_{TL} : t - N), \dots, \phi(t - T_{TL} + N : t)]$ 
32:          $\theta_P \leftarrow [\theta(t - T_{TL} : t - P), \dots, \theta(t - T_{TL} + P : t)]$ 
33:          $\rho_Q \leftarrow [\rho(t - T_{TL} : t - Q), \dots, \rho(t - T_{TL} + Q : t)]$ 
34:          $X \leftarrow [\phi_N, e, \theta_P, \rho_Q]$ 
35:          $C = ((X * X^T)^{-1} * X^T) * Y(t - T_T : t)$ 
36:     end if
37:          $\triangleright$  Compute Forecast
38:      $e = Y(t) - \phi(t - T_L)$ 
39:      $\phi_N \leftarrow [\phi(t - N), \dots, \phi(t)]$ 
40:      $\theta_P \leftarrow [\theta(t - P), \dots, \theta(t)]$ 
41:      $\rho_Q \leftarrow [\rho(t - Q), \dots, \rho(t)]$ 
42:      $X \leftarrow [\phi_N, e, \theta_P, \rho_Q]$ 
43:      $Y(t + T_L) = X * C$ 
44: end for
```

---

Equation 1: Basha Linear Regression Algorithm

#### A.4.2 Wu & Chau (2006) Artificial Intelligence flood forecasting algorithms

##### **Genetic Algorithm-Based Artificial Neural Network (ANN-GA)**

GA is used to optimize initial parameters of ANN before trained by conventional ANN. In the GA sub-model, the objective function used for initializing weights and biases is represented as follows:

$$\min J(W, \theta) = \sum_{i=1}^P |Y_i - f(X_i, W, \theta)|$$

Equation 2: Genetic optimisation Algorithm

where  $W$  is the weight,  $\theta$  is the bias or threshold value,  $i$  is the data sequence,  $\rho$  is the total number of training data pairs,  $X_i$  is the  $i^{\text{th}}$  input data,  $Y_i$  is the  $i^{\text{th}}$  measured data, and  $f(X_i, W, \theta)$  represents simulated output. The main objective of the sub-model is to determine optimal parameters with minimal accumulative errors between the measured data and simulated data.

### Adaptive-Network-Based Fuzzy Inference System (ANFIS)

Each input variable ( $x$ ,  $y$ , and  $z$ ) is divided into three categories. Equally spaced triangular membership functions are assigned. The categories are assigned: “low,” “medium,” and “high.” The number of rules in a fuzzy rule base is  $C^n$ , where  $C$  is the number of categories per variable and  $n$  the number of variables. The format of the rule set contains an output  $O_{i,j,k}$ , for a combination of category  $i$  of input variable  $x$ , category  $j$  of input  $y$ , and category  $k$  of input variable  $z$ , respectively. If a rule is triggered, the corresponding memberships of  $x$ ,  $y$ , and  $z$  will be computed. The weight  $W_{i,j,k}$ , to be assigned to the corresponding output  $O_{i,j,k}$ , will be furnished by the result of a specific T-norm operation. Multiplication operation is adopted here. A single weighted average output will then be acquired by combining the outputs from all triggered rules as follows:

$$O = \frac{\sum W_{i,j,k} \cdot O_{i,j,k}}{\sum W_{i,j,k}}$$

Equation 3: ANFIS

### A.4.3 Chiang et al. (2007) Recurrent Neural Network QPE and QPF

Chiang et al. (2007) recurrent neural network (RNN) model for quantitative precipitation estimation (QPE) and quantitative precipitation forecasting (QPF) by utilizing the meteorological radar data. The model uses gauge observations and satellite-derived precipitation. The learning algorithm that was used to calibrate

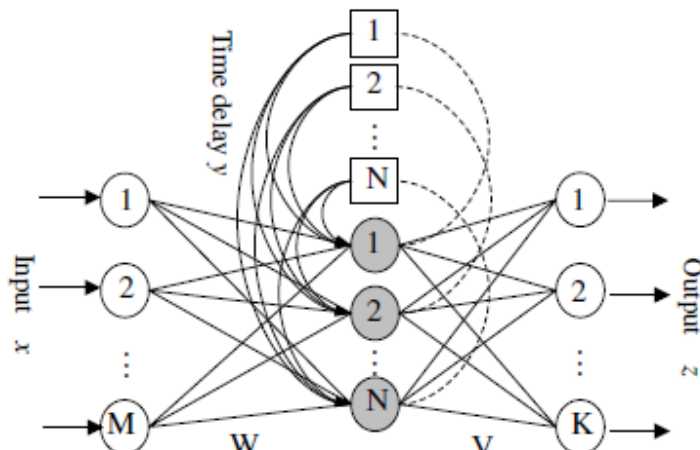


Figure A.9: RNN architecture

the RNN is referred to as real-time recurrent learning (RTRL) (Chang, et al., 2002). Consider a three-layer fully interconnected RNN as shown in Figure A.9 which includes  $M$  external inputs,  $N$  hidden neurons and  $K$  outputs. Let  $V$  and  $W$  denote the  $N \times K$  weight matrix and  $N \times (M + N)$  recurrent weight matrix, respectively.

The network activity of neuron  $j$ , for  $j \in B$ , is computed by

$A$  denotes the set of indices  $i$  for which  $X_i$  is an external input, and  $B$  denotes the set of indices  $i$  for which  $y_i$  is the output of the processing layer. The output of neuron  $j$  in the processing layer is given by passing  $\text{net}_j$  through the nonlinear transfer function  $f(\cdot)$ , yielding

$$y_j = f(\text{net}_j)$$

The output of neuron  $k$  in the output layer is computed by

$$\text{net}_k = \sum v_{kj} y_j$$

The output of network ( $Z_k$ ) is given by passing  $\text{net}_k$  through the nonlinear transfer function  $f(\cdot)$ , yielding

$$z_k = f(\text{net}_k)$$

To minimize the objective function ( $E_{\text{total}}$ ), the steepest descent method is applied to adjust the weights ( $V$  and  $W$ ) along the negative of  $\nabla E_{\text{total}}$ . The objective function is obtained by summing instantaneous network error ( $E(t)$ ) over all time  $T$  and  $E(t)$  can be defined as follows:

$$E_{\text{total}} = \sum_{t=1}^T E(t) \quad \begin{array}{l} \in A \\ \in B \end{array}$$

$$E(t) = \frac{1}{2} \sum_{k=1}^K [T_k(t) - z_k(t)]^2$$

where  $T_k(t)$  is the target value of neuron  $k$  at time  $t$ , and  $Z_k(t)$  is the network output of neuron  $k$  at time  $t$ . The weight change for any particular weight  $V_{kj}$  can thus be written as

$$\Delta v_{kj} = -\eta_1 \frac{\partial E}{\partial v_{kj}}$$

By using the chain rule, the partial derivative of  $V_{kj}$  can be obtained as follows:

$$\Delta v_{kj} = \eta_1 \sum_{k=1}^K e_k f'(\text{net}_k) y_j$$

The same method is also implemented for weight  $W_{mn}$ . Then the weight changes can be computed as

$$\Delta w_{mn} = \eta_2 \left( \sum_{k=1}^K e_k f'(\text{net}_k) v_{kj} \right) \pi_{mn}^j$$

Where  $\pi_{mn}^j(t+1) = f'(\text{net}_j) (\sum_{i \in B} w_{ji} \pi_{mn}^i(t) + \delta_{mj} u_n)$   $\eta_1$  and  $\eta_2$  are learning rate parameters.

A.4.4 Abdul-Kader et al. (2018) Forecasting Rainfall based on Computational Intelligent Techniques

**Radial Basis Function (RBF)**

The weights from the input to hidden layer is determined by computing the distance ( $d_i$ ) between the input vector  $x$  and the center of basis function  $c_i$  as shown in equations below.

$$\varphi_i = \exp\left(-\frac{d_i}{2\sigma^2}\right)$$

Where  $\varphi_i$  is Gaussian function for each node at hidden layer,  $\sigma$  is spread or width for each node in hidden layer.

$$y_{ik} = \sum_{i=1}^n w_{ik}\varphi_i$$

Where  $y_{ik}$  is output,  $w_{ik}$  is weights between hidden layer and output layer.

## Particle Swarm Optimization (PSO)

In PSO each particle in population is reckoned as a solution that algorithm works on finding optimal values to find the global minimum. Each particle changes its velocity and its position according to equations below:

$$V_i(t + 1) = WV_i(t) + c_1r_1(P_i(t) - X_i(t)) + c_2r_2(P_g(t) - X_i(t)) \quad (4)$$

Where  $W$  represent inertia weight,  $V_i(t+1)$  represent new velocity of particle  $i$  in next iteration,  $V_i$  represents velocity of particle  $i$ ,  $t$  represents an iteration number  $c_1, c_2$ , represent the learning rate for individual (local) and group (Global)  $r_1, r_2$  are random values have values between  $[0-1]$ ,  $x_i$  represents the current position of particle  $i$ ,  $P_i$  symbolize the local best for particle  $i$ , and  $P_g$  represent the global best for the swarm.

$$X_i(t + 1) = X_i(t) + V_i(t + 1)$$

Where  $X_i(t+1)$  represent the new position at next iteration. On each iteration of the algorithm the current position considers as solution and if that position better than the previous according to its value of fitness function which has a minimum value (minimize problem), that position considers  $P_{best}$ . The flowchart below *Figure A.10* describes the steps of the proposed model.

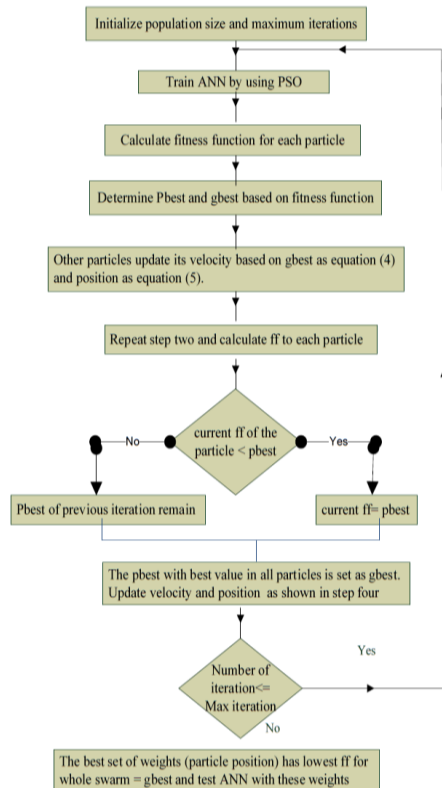


Figure A.10: ANN flowchart

Reference	Hardware	Description	Use	Price
Basha, et al.	ARM7TDMI-S (LPC2148 processor)	Microcontroller (base board)	Used for all nodes. Provides necessary computation power.	\$15.15 (ebay)
Basha, et al.	Xilinx CoolRunner-II CPLD	Physical serial port module (daughter board)	Connect to microcontroller to extend serial ports by 8. Provides IO operations and mini-SD card and FRAM to supply data and configuration storage.	\$3.02 (ebay)
Guesmi	CompactRIO Chassis	Base board for collection of I/O modules	Acts as the network coordinator, responsible for configuring all distributed nodes and collecting measured data from all of them.	Starting from \$ 748.00 (ni.com) Shipping to Mauritius N/A

Table A.1: Base System

Reference	Hardware	Description	Use	Price
Basha, et al.	AC4790	900 MHz wireless module. Operates at a fixed data rate, optimally 76.5 kb/s but dropping to approximately 500 b/s once the internal Aerocomm messaging overhead is considered.	Used by all nodes. Provides RF, interface, protocols, handling issues such as retries, error detection, and peer-to-peer communication.	\$39.99 + \$47.00 Shipping. USED (ebay)
Basha, et al.	Kenwood TM271A	144 MHz voice communication VHF radio	Used by small subset of nodes. Allows cheap long-range communication.	\$219.99 + \$5.00 Shipping (ebay)
Basha, et al.	MX614 Bell 202	Convert 1200 baud serial signal to FSK	Modem to allow data communication to Kenwood TM271A.	\$5.66 + \$4.00 Shipping (ebay)

		signal for radio transmission.		
Guesmi	WSN-3202	Analog Input Node for WSN	Measures analog input signals and performs digital I/O at an outdoor range up to 300 m.	Starting from \$ 734.00 (ni.com) Shipping to Mauritius N/A
Guesmi	WSN-3230	Serial Interface Node for WSN	Provides one RS232 port to interface with serial sensors, instruments, and control boards.	Starting from \$ 718.00 (ni.com) Shipping to Mauritius N/A
Guesmi	NI-9795	Wireless Gateway Module	Connects to the CompactRIO chassis. Collects data from WSN nodes.	Starting from \$ 568.00 (ni.com) Shipping to Mauritius N/A

Table 15: Communication Hardware

Reference	Hardware	Description	Use	Price
Basha, et al.	RS485 and RS232 circuits	Communication	For external communication to sensors if complicated interface is required.	\$2.10 and \$1.22(ebay)
Basha, et al.	Reed magnetic switches	Rainfall sensor. Measure by causing an interrupt after every 1 mm of rainfall.	Measure rainfall.	\$0.99 (ebay) + Rain bucket
Basha, et al.	Resistive Temperature sensor		Measure temperature.	\$1.95 (ebay)
Basha, et al.	Honeywell 24PCDFA6A	Water pressure sensor.	Measure water level.	\$12.99. Shipping not specified (ebay)
Guesmi	WSN-3212	Thermocouple Input Node for WSN	Telemetered sensors.	Starting from \$ 718.00 (ni.com) Shipping to Mauritius N/A

Table A.3: Sensing Nodes

link	Hardware	Description	Use	Price
<a href="#">Arduino UNO</a>	Arduino UNO	Microcontroller (base board)	Operate sensors I/O. Do basic computation. 1 for each sensors' nodes	\$4.15
<a href="#">Arduino MEGA</a>	Arduino MEGA	Microcontroller (base board) Have more I/O ports than Arduino UNO	Operate sensors I/O. Do basic computation. 1 for each sensors' nodes	\$8.33
<a href="#">Raspberry Pi3B</a>	Raspberry Pi 3B	Low cost, credit-card sized computer. Can connect to the internet, do complex computation. Have sensors I/O ports.	Acts as the network coordinator, responsible for configuring all distributed nodes, collecting measured data from all of them and sending the data to an online server.	\$42.75

Table 16: Base Station

Link	Hardware	Description	Use	Price
<a href="#">WIFI Transceiver module</a>	ESP8266 ESP-01 Serial WIFI Wireless Transceiver Module	802.11 b/g/n. Standby power consumption of < 1.0mW. Range: 300m line-of-sight.	Can be used by all close-range sensor nodes. Provides and peer-to-peer communication.	\$1.98
<a href="#">2.4G Wireless Transceiver module</a>	NRF24L01+PA+LNA SMA Antenna Wireless Transceiver module	2.4GHz band frequency. Max Current: 115mA. Range: 1000m line-of-sight, 270m in forest.	Can be used to transfer data from 1 nodes to another. Provides and peer-to-peer communication.	\$2.53
<a href="#">433Mhz HC-12</a>	HC-12 Wireless Serial Port Module	433MHz band. Transmitting power: 0.79-100mW.	Can be used to transfer data from 1 nodes to another close or long range. Provides and peer-to-peer communication.	\$3.55

		Max range: 600-1800m		
<a href="#">GSM module</a>	SIM900 850/900/1800/1900 MHz GPRS/GSM	Class 4 (2 W @ 850 / 900 MHz)  Class 1 (1 W @ 1800 / 1900MHz)  Low power consumption - 1.5mA(sleep mode)  Embedded TCP/UDP stack - allows you to upload data to a web server.	Can be used to allow communication between very far apart nodes. Upload sensed data to server.	\$13.70
<a href="#">4G module</a>	SIM7000E 2G 3G 4G GSM GPRS Module	Output power - GSM900: 2W - DCS1800: 1W	Can be used to allow communication between very far apart nodes. Upload sensed data to server.	\$47.83

Table 17: Communication Hardware

link	Hardware	Description	Use	Price
<a href="#">Pressure sensor</a>	Gravity: Analog Water Pressure Sensor	Water pressure is converted into water level.	Measure river water level	\$12.90
<a href="#">Barometric Pressure sensor</a>	Barometric Pressure Sensor Module	Measure water level by measuring air pressure in a tube with one end in the river and the other end connected to the sensor.	Measure river water level	\$4.29
<a href="#">Water pressure sensor</a>	MS554 MS5540-CM	Water pressure is converted into water level.	Measure river water level	\$19.87

<a href="#">Barometric pressure sensor</a>	GY68 BMP180	Measure water level by measuring air pressure in pipe submerged in water with the sensor in.	Measure river water level	\$1.22
<a href="#">Ultrasonic sensor</a>	HC-SR04 Distance Sensor	Measure the distance between the sensor and the water surface.	Measure river water level	\$0.99
<a href="#">DHT22</a>	DHT22	<p>Temperature and Humidity Sensor</p> <p>Accuracy resolution:0.1.</p> <p>Humidity range:0-100%RH.</p> <p>Temperature range:-40~80°C.</p> <p>Humidity measurement precision:±2%RH.</p> <p>Temperature measurement precision:±0.5°C</p>	Temperature and Humidity	\$3.16
<a href="#">AcuRite</a>	AcuRite 06014 PRO	5-in-1 Weather Sensor with Rain Gauge, Wind Speed, Wind Direction, Temperature and Humidity	Rain Gauge, Wind Speed, Wind Direction, Temperature and Humidity	\$85.87

Table 18: Sensors

## Installation Procedures

The steps below show how to install TensorFlow with GPU support (NVIDIA GPU only), Keras API and prerequisites for Windows 10 operating system.

### Step 1: Requirements to run TensorFlow with GPU support

The following NVIDIA software must be installed on your system:

- CUDA® Toolkit 9.0. For details, see [NVIDIA's documentation](#). Ensure that you append the relevant Cuda pathnames to the %PATH% environment variable as described in the NVIDIA documentation.
- The NVIDIA drivers associated with CUDA Toolkit 9.0.
- cuDNN v7.0. For details, see [NVIDIA's documentation](#). Note that cuDNN is typically installed in a different location from the other CUDA DLLs. Ensure that you add the directory where you installed the cuDNN DLL to your %PATH% environment variable.
- GPU card with CUDA Compute Capability 3.0 or higher for building from source and 3.5 or higher for our binaries. See [NVIDIA documentation](#) for a list of supported GPU cards.

### Step 2: Install python 3

TensorFlow supports Python 3.5.x and 3.6.x on Windows.

[Python 3.6.x 64-bit from python.org](#)

### Step 3: Install tensorflow-gpu

To install TensorFlow with GPU support, run Command Prompt as administrator and enter the following command:

```
C:\WINDOWS\system32> cd C:/  
C:\> pip3 install --upgrade tensorflow-gpu
```

### Step 4: Install Keras

To install Keras API, run Command Prompt as administrator and enter the following command:

```
C:\WINDOWS\system32> cd C:/  
C:\> pip install keras
```

### Step 5: Prerequisites

Install Scikit-Learn python package:

```
C:\> pip install -U sklearn
```

Install Pandas python package:

```
C:\> pip install pandas
```

Install matplotlib python package:

```
C:\> pip install matplotlib
```

Install numpy python package:

```
C:\> pip install numpy
```